UC Riverside

UC Riverside Electronic Theses and Dissertations

Title

Functions of Leucine Rich Repeat Receptor-Like Kinases (LRR-RLKs) in Arabidopsis Sexual Reproduction

Permalink

https://escholarship.org/uc/item/31v3t5pg

Author

Khamsuk, Ornusa

Publication Date

2011

Peer reviewed|Thesis/dissertation

eScholarship.org Powered by the California Digital Library
University of California

UNIVERSITY OF CALIFORNIA
RIVERSIDE

Functions of Leucine Rich Repeat Receptor-Like Kinases (LRR-RLKs) in Arabidopsis Sexual Reproduction

A Dissertation submitted in partial satisfaction
of the requirements for the degree of

Doctor of Philosophy

in

Plant Biology

by

Ornusa Khamsuk

December 2011

Dissertation Committee:
Dr. Zhenbiao Yang, Chairperson
Dr. Natasha Raikhel
Dr. Venugopala Gohenal Reddy

Copyright by
Ornusa Khamsuk
2011

The Dissertation of Ornusa Khamsuk is approved:

_____

_____

_____

Committee Chairperson

University of California, Riverside

ACKNOWLEDGEMENTS

I would like to express my appreciation to my major professor, Dr. Zhenbiao Yang for mentoring and challenging me to be an independent researcher. I acknowledge my former major professor, Dr. Elizabeth Lord for her venerable support and encouragements throughout my academic program.

I acknowledge my dissertation committee members, Dr. Natasha Raikhel and Dr. Venugopala Gohenal Reddy for their comments regarding my research.

I acknowledge help from Dr. Yong-Jik Lee and Dr. Stephen Karr for lab techniques and various suggestions. My thanks also go to members of Lord and Yang labs for their help and friendship.

I would like to thank Dr. Ravi Palanivelu and Dr. Yuan Qin (University of Arizona, Tucson) for LAT52p-GUS seeds and advice regarding semi-*in vivo* technique. I also acknowledge Dr. Venkatesan Sundaresan (University of California, Davis) for providing us with female gametophyte cell-specific markers.

I acknowledge Royal Thai Government for financial support throughout my academic program. This work was also supported by National Science Foundation grants to Dr. Elizabeth Lord and Dr. Zhenbiao Yang.

Last but not least, I would like to express my deepest thanks to my family for their caring words and warm support.

DEDICATION

In memory of my beloved father, Udom Khamsuk

ABSTRACT OF THE DISSERTATION

Functions of Leucine Rich Repeat Receptor-Like Kinases (LRR-RLKs)
in Arabidopsis Sexual Reproduction

by

Ornusa Khamsuk

Doctor of Philosophy, Graduate Program in Plant Biology
University of California, Riverside, December 2011
Dr. Zhenbiao Yang, Chairperson

ABSTRACT

Sexual reproduction is a critical process in the life cycle of flowering plants. To achieve successful reproduction, some important steps are required including gametogenesis, pollination, and fertilization. Gametogenesis refers to the development of haploid gametes (egg and sperm) whereas pollination requires pollen-pistil recognition to promote pollen tube growth toward the ovule. During fertilization, the reproductive gametes fuse to each other and an embryo is produced. In this study, different approaches were used to clarify the biological functions of three leucin rich repeat receptor-like kinases (LRR-RLKs); RLK B, RLK C, and RLK D, during sexual reproduction in Arabidopsis. RLK B, RLK C and RLK D belong to LRR VI, LRR III, and LRR VIII-type of the LRR-RLK subfamily, respectively. According to the phenotypic characterization of different combination of mutants, we show that RLK C function redundantly with RLK B and RLK D to regulate fertilities of male and female gametophytes. In *rlk c*, the

synergid and egg cells were not well specified, resulting in an increase of unfertilized ovules. Mutations in RLK B and RLK D could enhance phenotypes of *rlk c*. The *rlk c rlk b* plant exhibited severe defects in female gametophyte development, pollen tube guidance and seed production. The *rlk c rlk b* female gametophyte was arrested post-meitotically. It is most likely that RLK C and RLK B function redundantly to elicit a signal transduction pathway involved in female gametophyte development. By contrast, *rlk c rlk d-2* caused more severe defect in pollen fertility. In both cases, the major contribution for gamete fertility is from *RLK C* signaling due to no apparent phenotype in the *rlk b* and *rlk d* single mutants. In addition, the *rlk b rlk d-2* mutant did not show a phenotype, indicating their unique functions in reproduction. According to dominant-negative (DN) study, the *LAT52*p::DN-RLK C receptor lacking the kinase domain enhanced a defect in male fertility in the *rlk c* mutant. This confirms that the functional redundancy in RLK C is essential to regulate male fertility. Taken together, we provide evidence that RLK C, RLK B, and RLK D function to achieve full fertility of male and female gametophytes.

TABLE OF CONTENTS

LIST OF FIGURES

Chapter 2

Chapter 3

Chapter 4

LIST OF TABLES

CHAPTER 1

INTRODUCTION

Sexual reproduction is a major method of reproduction in flowering plants. It requires fusion of the reproductive gametes (egg and sperm). After fertilization, embryos are produced in the seeds. To achieve successful sexual reproduction, some important steps are required including gametogenesis, pollination and double fertilization. In compatible interaction, after pollen grains land on the receptive stigma, it will take up water and germinate consequently. Then, the pollen tube penetrates into the intercellular space between stigmatic tissues and transmitting tracts (TT) of the style. During pollination, the cell wall of pollen grain and tube physically contacts with the female tissues. Finally, the pollen tube reaches the ovary and delivers the sperm to the embryo sac (Lord and Russell, 2002). Like other cell signaling networks, pollen-pistil interaction is composed of several key components including the guiding cues, receptors and downstream regulators. However, the key player is still unknown. Some studies have shown biochemical and genetic evidence that signals from pollen or female tissues involved in pollen tube growth toward the ovule, such as TTS (transmitting tissue-specific) protein, GABA (gamma-aminobutyric acid), chemocyanin, SCA (stigma/style cysteine-rich adhesin), *Zea mays egg apparatus1*, cysteine-rich peptides (CRPs). However, how these signals are perceived and transmitted to attract the pollen tube is not well understood. Receptor-like kinases (RLKs) are proposed to be receptor partners for guiding cues in pollen-pistil communication. RLKs are involved in various plant developments by perception of signals through the cell surface and regulating

downstream signalling. They may function as receptors to mediate plant sexual reproduction during pollen-pistil interaction and/or gamete development.

Pollen Development

In flowering plant, the male gametophyte or pollen is developed from pollen mother cell (PMC) within the anther. The function of pollen is to produce two sperm cells and to carry them through the female tissues for double fertilization (Mascarenhas, 1990). Cellular event from the initiation of the microspore mother cell (PMC) until the production of microspores is called microsporogenesis. Microsporogenesis is composed of three main events: (a) meiosis; (b) the switch of life cycle phase from the sporophyte to gametophyte; (c) the early stage of microgametogenesis. In flowering plants, these events shortly occur within the same cell. Each diploid PMC undergoes meiosis to produce tetrads. After telophase of meiosis II, each haploid microspore is released from the callose wall of tetrad. Following meiosis, the individual microspore undergoes two mitotic divisions. The uninucleate microspore undergoes first mitosis, a symmetric division, to produce the bicellular pollen consisting of a large vegetative cell and the generative cell. The vegetative cell, non-germ line cell, functions as a somatic cell without further cell division. By contrast, the generative cell, germ line cell, then undergoes mitosis to give rise two sperm cells before pollen germination. In Arabidopsis, pollen is shed as a three-celled gametophyte (tri-cellular pollen), which contains two sperm nuclei and a vegetative nucleus (Borg et al., 2009).

Pollen Germination and Tube Growth

After pollen grains are released from the anther and land on a receptive stigma, some dynamic events are required for pollen to germinate and grow. Those main steps include the pollen hydration, the polar site selection, the pollen germination and the pollen tube growth. In compatible interaction, after pollen grain lands on the stigma, it will take up water (hydration) from the stigma surface to pollen. The mechanism involved in hydration causes the reactivation of metabolic machinery in pollen (Heslop-Harrison 1987). It has been shown that the hydration process is crucial for pollen germination. In Arabidopsis, *RARING-TO-GO* is required for normal dispersion of the pollen grain (Johnson and McCormick, 2001). The loss of the gene activity caused precociously germination of pollen inside the anther locule. During pollen hydration, a aquaporin-like protein regulates pollen germination (Dixit et al*.,* 2001). Some lipids and proteins involved in the synthesis of long-chain lipid are also required (Preuss et al., 1993 and Lolle and Cheung, 1993).

Following pollen hydration, a particular region of pollen grain will be polarized to specify the germination site. It has been shown that lipid and water are involved in polarity establishment in the pollen grain (Lush et al., 1998; Wolters-Arts et al., 1998). After it germinates through the aperture, the pollen tube travels directionally toward the female tissues and delivers sperm for double fertilization (Hepler et al., 2001). There are some cellular components associated with pollen tube growth including the Rho family of small GTPases, cytoskeleton array and vesicular trafficking. Among other GTPases in Rho family, only ROP GTPases associate with signaling network in Arabidopsis. ROP

GTPases, plant-specific Rac GTPases, act as molecular and signaling switch regulators to mediate various signaling transduction. ROP GTPases are guanine nucleotide-binding proteins whose activities depend on bound guanine nucleotides, the GTP-binding active or GDP-binding inactive form. ROP GTPase has shown as a key player to regulate various downstream pathways including ion fluxes, cytoskeleton organization, gene expression and vesicle trafficking (Fu et al., 2001; Lee and Yang, 2008) resulted in tip growth of pollen tube. In Arabidopsis, ROP GTPases are expressed in mature pollen and pollen tubes (Honys and Twell, 2004; Qin et al., 2009). In pollen tubes, ROPs is localized to the plasma membrane at the tip region. The oscillation of ROPs is in phase with tube growth (Hwang et al., 2005). ROPs control rate of tip growth via tip-localized calcium flux (Li et al., 1999) and dynamics of tip F-actin to maintain polar growth (Gu et al, 2005). In growing pollen tubes, ROPs control vesicle trafficking via RICs. RICs regulate exocytosis by targeting the vesicles and fusion to the plasma membrane (Lee et al., 2008). However, function of ROPs on endocytosis is largly unknown.

Cytoskeleton, an essential protein polymer in pollen tube, is a major target for signaling pathways in plant cells. Filamentous actin or F-actin, a 43 kD globular protein, plays a role in pollen tube growth. In growing pollen tubes, fine F-actin is abundant to transport vesicles at tip region (Fu et al., 2001). To study functions of F-actin in pollen tubes, an actin-disrupting drug, Latrunculin B, was used to suppress pollen tube growth *in vitro* (Kost et al., 1999). Interestingly, actin dynamics oscillate and lead tip growing, suggesting that F-actin dynamics control polarized growth (Fu et al., 2001). In ectopic expression of ROP1 pollen tube, actin dynamics was decreased at the tip region, resulted

in an accumulation of F-actin and an inhibition of pollen tube elongation. Actin binding proteins, such as profilins and actin-depolymerizing factors, are involved in the regulation of actin dynamics and reorganization. Profilins, 12-15 kD proteins, have major functions in sequestering G-actin and promoting actin assembly (Yokota and Shimmen, 2006). In self-incompatibility (SI) response of field poppy pollen, it was shown that actin is a target for SI signals, which is mediated by Ca^{2+}. In SI reaction, dramatic F-actin disruption is due to depolymerization of actin via profilins (Snowman et al., 2002). Therefore the incompatible pollen tube growth was inhibited in the female tissues. Actin-depolymerizing factors (ADFs) or cofilin, 15-20 kD proteins, bind both G-actin and F-actin to severe F-actin and increase treadmilling by 25 folds (Maciver and Hussey, 2002). ADFs activity is regulated by phosphorylation, pH and phosphatidylinositol 4,5-bisphosphate (PIP_2) (Helling et al., 2006).

Not only F-actin organization is involved in pollen tube growth but vesicular trafficking also associates to this tip-growing cell. In general, vesicle targeting is important in plant development, such as tip growth, morphogenesis and auxin polar transport. The endomembrane system is greatly dynamic in growing pollen tubes. It contains vacuoles, ERs, golgi networks, endosomes and small vesicles at the tip region (de Graaf et al., 2005). The polarity of pollen tube growth is determined by site of vesicle fusion and it also requires targeted vesicle transport (Franklin-Tong, 1999). During this process, golgi network and endosome produce vesicles transporting to the tip region. Then, these vesicles are packed with complex polysaccharides and glycoproteins and fuse to the plasma membrane to sustain rapid growth of cell walls (Roy et al., 1998).

Inhibition of targeting of exocytic and recycled vesicles to the tip region caused a reduction of pollen tube growth rate (de Graaf et al., 2005).

Vacuole has diverse functions in plants including cell growth, pH and ion homeostasis, storage of ions, metabolites and proteins, plant development and signal transduction. Pollen vacuoles are highly dynamics throughout pollen development. By use of cryo-fixation/freeze-substitution method, the ultrastructural strucuture and behavior of vacuoles were analyzed (Yamamoto et al., 2003). During tetrad stage and microspore formation, small vacuoles are accumulated in cytoplasm. Later on, in addition to dispersed vacuoles, a large vacuole is formed in microspores. Following the meiosis, a large vauole separates into numerous small vacuoles by tonoplast invagination. Shortly after the second mitosis of the generative nucleus, vacuoles disappear until the mature stage. In mature pollen, vacuoles are dynamic s(Hicks et al., 2004). In compatible interaction, after pollen grain lands on the stigma, pollen takes up water from the stigma. The mechanism involved in hydration causes phase switching from the desiccated state to the active state of pollen. During pollen germination, dynamics of vacuole biogenesis is required. Using a tonoplast specific marker, δ-TIP::GFP, small dispersed structures of vacuole could be seen in hydrated pollen grain. In early germinating pollen, tubular vacuoles were found in the grain. After germination, a large central vacuole appeared in the grain and the pollen tube. *VACUOLESS1 (VCL1)* plays role in rapid biogenesis of vacuole. However, the loss of *VCL1* activity, pollen caused partial male sterility but did not affect vacuole morphology in *vacuoless1*.

Lines of evidence suggest that the dynamics of some ions including Ca^{2+}, H^+ and K^+ play role in pollen tube growth. Ca^{2+} is known as an important ion for pollen germination and tube growth (Hepler, 1997). Ca^{2+} is taken up by pollen and functions to control pollen tube growth and direction of growth. In addition, Ca^{2+} was reported to be a second messenger for mediating inhibition of pollen tube growth in SI (self-incompatible response) (Franklin-Tong, 1999). In growing pollen tube, Ca^{2+} also differentially regulates vesicular trafficking including exocytosis and membrane recycling at the tip region (Malho and Camacho, 2002). Interestingly, the oscillation of Ca^{2+} gradient is in phase with tube growth rates (Holdaway-Clarke et al., 1997). It has been shown that both tip-focused intracellular Ca^{2+} gradient and tip-localized influx of extracellular Ca^{2+} are essential for tip growth regulation. Other molecules, such as Ca^{2+}-dependent protein kinases (CDPKs), calmodulin and some Ca^{2+}-binding proteins are key effectors to regulate pollen tube growth (Snedden and Fromm, 2001; Harmon et al., 2000). However, their biological functions are largely unknown. H^+ and pH gradient play role in tip growth regulation as well as Ca^{2+}. pH gradient at tip region associates with dynamics of other important components and mechanisms, such as vesicle trafficking and F-actin (Lovy-Wheeler et al., 2006 and Vidali et al., 2001). The endomembrane proteins called cation/proton exchangers (CHXs) have shown to be regulator of intracellular pH (Sze et al., 2004). In growing pollen tube, K^+ is required for turgor pressure maintenance (Holdaway-Clarke and Hepler, 2003). Interestingly, at least two CHXs (CHX21 and CHX23) are required to change the establishment of polarity and target pollen tube to the ovule (Lu et al., 2011).

Female Gametophyte Development

The development of female gametophyte includes megasporogenesis and megagametogenesis. While megasporogenesis is to generate the megaspore (haploid), megagametogenesis is to generate the female gametophyte (diploid). During megasporogenesis, a megaspore mother cell (MMC) undergoes meiosis to producee four haploid nuclei. In Arabidopsis, the developmental pattern of female gametophyte is called Polygonum type, which occurs in 70 percent of the flowering plants, such as rice, maize, tomato and tobacco. The pattern of megasporogenesis in Arabidopsis is called monosporic pattern (Huang and Russell, 1992). The female gametogenesis in *Arabidopsis* is divided into eight stages (Christensen et al., 1997). In developing ovule, a megaspore mother cell (MMC) undergoes meiosis to generate a tetrad of haploid megaspores, three of which at the micropylar end degenerate by programmed cell death. The other megaspore at the chalazal end of the embryo sac still function. The functional megaspore at the charazal end undergoes megagametogenesis and gives rise to the female gametophyte. First, the functional megaspore (stage FG1) undergoes mitosis to give rise to a two-nucleate cell (stage FG2). Then, those two nuclei migrate to two opposite poles, the chalazal and micropylar end of the embryo sac, and the vacuole is formed in the middle between those two nuclei (stage FG3). Shortly, each nuclei from each pole undergoes mitosis for the second and the third rounds (stage FG4) to give rise to four daughter nuclei at each pole (stage FG5). At the end, one nucleus from each pole migrates to the center of the embryo sac to form the polar nuclei. Then, the embryo sac becomes cellularized and cell walls are formed around those nuclei. Additinonally, the

polar nuclei fuse together during cellularization. The result of a series of mitosis of the functional megasopre without cytokinesis causes a seven-celled embryo sac with eight nuclei (stage FG6). Typically, the mature female gametophyte contains four different cell types: one egg cell, two synergids, one central cell and three antipodals. However, in Arabidopsis, the antipodal cells undergo cell death shortly before fertilization (Drews et al., 1998). Therefore, the mature female gametophyte consists of one egg cell, two synergids and one central cell. Recently, it has been shown that the gradient of auxin, a plant hormone required for cell growth and cell division, is involved in the patterning of Arabidopsis female gametophyte. During the syncitial development, the asymmetric auxin distribution is required (Pagnussat et al., 2009).

Pollination and Pollen Tube Guidnace

Pollination is an important process for sexual reproduction in plants. It is composed of several steps including recognition between pollen and pistil tissues. Due to the different steps of the pollen tube journey along the female tissues, from pollen grain germination through the gamete fusion, it has been predicted that the various guiding signals are required for each step of the pollen tube growth and guidance. However, most of these signals are still unknown and the pollen tube guidance process is still mysterious. In compatible interaction, after a pollen grain lands on the stigma surface, it hydrates and germinates consequently. Then, pollen tube penetrates into the intercellular space between stigmatic tissues and transmitting tract epidermis (TTE) of the style. Upon pollination, the cell wall of pollen grain and/or pollen tube contacts with the female tissues and this process is the directional process. Finally, pollen tube reaches the ovary

and delivers the sperm cells to the embryo sac in the ovule (Lord and Russell, 2002). Like any other cell signaling networks, pollen-pistil interaction is composed of some components including the potential cues, receptors and downstream regulators. Some studies show evidences of potential signals produced from female tissues to target pollen tube growth toward ovule and pollen-pistil recognition such as TTS (transmitting tissue-specific) protein, GABA (γ-aminobutyric acid), chemocyanin and SCA (stigma/style cysteine-rich adhesin) and ZEA MAYS EGG APPARATUS1 (ZmEA1).

Genetic and biochemical evidence has shown that both sporophytic and gametophytic tissues from pistil produce signal cues to guide the pollen tubes. Following pollination, pollen physically contacts with the stigma, hydrates and germinates. In the sporophytic tissues, such as the stigma and the style, pollen tubes grow into the intercellular space between stigmatic tissues and transmitting tract of the style (Lord and Russell, 2002). The extracellular matrix (ECM) of the style is a secretory tissue producing a glycoprotein called TTS (transmitting tissue-specific) glycoprotein. TTS was proposed to be a growth stimulant and pollen tube attractant in tobacco by generating a spatio-temporal gradient (Wu et al., 1995). In lily pistil, Chemocyanin, a 9.4 kDa molecule, was identified from ECM. This chemotropic molecule plays a role in guiding the pollen tube on stigma to the style. Chemocyanin is a member in the Phytocyanin family and functions with another small secreted protein called SCA [stigma/style cysteine-rich adhesins (SCA)] to accelerate the chemotropic activity (Kim et al., 2003). SCA, a 9.4 kDa protein, was isolated from lily style by *in vito* adhesion assay. Interestingly, it can attract the pollen tube from style to the ovule. Taken together, this

suggests that chemocyanin and SCA from lily are essential components for pollen-pistil interaction. However, how theses two molecules work together to mediate the chemotropic activity is still unclear. In Arabidopsis, the gradient of GABA (γ-aminobutyric acid) generated in transmitting tissues was proposed to target the pollen tube to the embryo sac (Wilhelmi and Preuss, 1996). *POP2* encodes a transaminase and functions to regulate a gradient formation of GABA at the micropylar end of the embryo sac. In *pop2* mutant, the pollen tube growth was affected due to the untypical GABA gradient (Palanivelu et al., 2003). Not only molecules produced from the female tissues are required for proper pollen tube guidance, the normal female tissues development is also critical. A defect in ovule development caused inhibition of pollen tube growth toward the embryo sac, suggesting that the guiding cue is generated in female tissues (Ray et al., 1997). A transmitting tract expressed gene called *NO TRANSMITTING TRACT (NTT)* encoding a C2H2/C2HC zinc finger transcription factor plays a role in transmitting tract development and pollen tube growth toward the ovule. *ntt* mutant displayed pollen tube growth inhibition at the base of the ovary (Crawford et al., 2007).

The final step of pollen tube guidance occurs in the female gametophyte or the embryo sac. Genetic evidence has shown that the different cell types of the female gametophyte are essential for the guidance. In synergids, *MYB98*, a member of the R2R3-MYB transcription factor family, is expressed. *myb98* mutant showed an impairment in synergid differentiation. The female gametophytic defect subsequently interfered with the pollen tube guidance (Kasahara et al., 2005). In *Torenia fournieri*, the diffusible guiding chemical was produced in both synergid cells by a laser ablation study (Higashiyama et

al., 2001). It is most likely that the micropylar guidance cue for pollen tubes comes from the synergids. Recently, two cysteine-rich polypeptides (CRPs), derived from the synergids, were identified. CRPs are members of a subgroup of defensin-like proteins and exclusively expressed in the synergids. These attractants are produced in the synergids and thereafter secreted to the surface of the egg apparatus in *Torenia* embryo sac. These diffusible molecules from the synergids function to target the pollen tubes (Okuda et al., 2009). Diversity of CRP is species-specific tube attraction (Kanaoka et al., 2011). In Arabidopsis, *feronia* (*fer*) mutant displayed defects in pollen tube reception and double fertilization. The pollen tubes can be accurately targeted to the embryo sac; however, they failed to arrest. Therefore, the pollen tube growth was continued inside the embryo sac without the sperm delivery. *FER* encoding a receptor-like kinase is expressed in synergids (Escobar-Restrepo et al., 2007). ZEA MAYS EGG APPARATUS1 (ZmEA1), a protein specifically expressed in the egg and synergids, also functions as a signal to attract the pollen tubes (Marton et al., 2005). Not only the synergid cell is required for pollen tube guidance toward the embryo sac but the central cell is also essential for this process. In Arabidopsis, the central cell development in *maa3* mutant was delayed and pollen tube guidance was affected. *MAA3* encodes a homolog of Sen1 helicase in *Saccharomyces cerevisiae*, required for RNA processing (Shimizu et al., 2008) The *central cell guidance* (*ccg*) mutant also had an impairment in pollen tube guidance. *CCG* encoding a nuclear protein is predominantly expressed in the central cell of the embryo sac (Chen et al., 2007). The studies suggest that the central cell is also important for the guidance from female tissues. To obtain successful pollen tube growth and guidance at

the micropyle of the embryo sac, the normal development of the female gametophyte and ovule is required. In Arabidopsis, the female gametophyte of *maa1* (*magatama1*) and *maa3* mutants was delayed. Therefore, the pollen tubes were not properly targeted to the embryo sac (Shimizu and Okada, 2000).

Lines of evidence suggest that some ions such as Ca^{2+} and K^{+} play a role in pollen tube guidance. Ca^{2+} is known as an important component for pollen tube growth. Ca^{2+} was also shown as an attractant to target pollen tubes to the female tissues (Rosen, 1968). However, its function as a guidance cue is still not well understood. Two endomembrane cation/proton exchangers (CHXs), CHX21 and CHX23, are essential for pollen tube guidance (Lu et al., 2011). In general, CHX23 regulates K^{+} transport. In double mutant of CHX21 and CHX23, pollen tubes failed to enter the ovules.

Double Fertilization

Upon pollination, pollen grains land on the compatible stigma of the pistil and the pollen tubes germinate and grow through the female sporophytic tissues and finally reach the ovules inside the ovary. The pollen tubes are guided from the female tissues and targeted to synergids in the female gametophyte. In Arabidopsis, the pollen tubes grow into one of the two synergids through the filiform apparatus. The invasion of the pollen tube inside the synergid(s) causes the degeneration of those shortly after the penetration. Eventually, the pollen tube growth ceases within the embryo sac. During double fertilization, the pollen tube delivers two sperm cells, which migrate and fuse with the egg cell and central cells to generate a diploid zygote and a triploid endosperm, respectively.

Receptor-Like Kinases (RLKs)

Receptor-like kinases (RLKs), a large monophyletic gene family, are involved in perception of signals through the cell surface. Arabidopsis genomes contain over 600 RLKs homologs (2.5% of the annotated protein-coding genes) (Shiu et al., 2004). Most of them share common structures including the extracellular domain, the transmembrane domain (TM) and the kinase domain (Walker, 1994). The amino-terminal extracellular domain functions to bind the ligands on the cell surface. The transmembrane domain allows these receptors to be located on the plasma membrane (PM). The carboxyl-terminus intercellular kinase domain, located in the cytosol, is the active domain to generate a downstream phosphorylation cascade. It has been shown that some known RLKs function as inactive monomer (Nam and Li 2002). After the ligand directly interacts with the extracellular domain of the receptor, the kinase domain is activated to induce a conformational change of the RLK (Shiu and Bleecker 2003). The modification in the extracellular domain results in dimerization and brings the cytoplasmic kinase domains into close proximity. Afterward, the transphosphorylation of the kinase domain occurs. In some cases, oligomerization is not required to activate RLKs. For instance, CrRLK1 shows autophosporlyation (Schulze-Muth et al., 1996). The kinase then phosphorylates the target proteins. RLKs can function in homodimerization and heterodimerization manner, suggesting that they are able to perceive a wide range of ligands (Johnson and Ingram, 2005).

In Arabidopsis, classification of RLKs is based on the extracellular domain. There are more than 21 different classes including the leucine-rich repeat (LRR), the lectin type (LecRLKs), the S-domain type, the wall-associated kinases (WAKs), the DUF26 domain, the proline-rich repeat and the CrRLK1L type (Shiu and Bleecker 2001a, Shiu and Bleecker 2001b; Becraft, 2002). The leucine-rich repeat (LRR)-RLKs are the most common motif spreading out more than 50% of the RLK family. The LRR-RLKs could be grouped into at least 13 subclasses based on the number of leucine repeats and their arrangements. The lectin RLK (LecRLK) is the second common class containing 42 members. They have the extracellular domain similar to legume lectins. The S-locus RLKs (SRKs) contain a B-lectin oragglutinin and a PAN motif. The wall-associated kinases (WAKs) contain the epidermal growth factor (EGF) repeats. The plant specific DUF26 family contains four conserved cysteins. The proline-rich repeat RLKs are plant specific type. However, their functions remain poorly understood. The CrRLK1L (*Catharanthus roseus* RLK1-like), a plant specific family, contains putative carbohydrate-binding domains. It has been shown that the CrRLK1Ls play a role in vegetative and gametophyte development. For example, ANXUR1/2 and FERONIA function in development of male and female gametophyte, respectively. RLKs are able to be classified by their kinase domains (Krupa et al., 2004). The plant RLKs all appear to be serine/threonine protein kinase. However, the biological functions of most gene member are still unknown. It has been published that RLKs function in various aspects of plant development such as organ shape, inflorescence architecture (Shpak et al., 2003), early anther development (Hord et al., 2006), root hair patterning, guard cell

morphogenesis. Besides, RLKs function in defense response to against pathogens and hormone perception (Wang and He, 2004; Belkhadir and Chory, 2006). RLKs are also involved in plant sexual reproduction, such as self-incompatibility (Walker, 1994).

RLKs and Plant Hormone Perception

Plant steroid hormone called brassinosteroids (BRs) is known as a key player to mediate cell growth and development. It has been shown that BR signaling requires a leucine-rich-repeat receptor kinase BRASSINOSTEROID INSENSITIVE 1 (BRI1). BR binds to the extracellular domain of BRI1 (Wang and He, 2004; Belkhadir and Chory, 2006), which then heterodimerizes BRI1-associated receptor kinase (BRI1-ASSOCIATED KINASE1/BAK1/AtSERK3 (Nam et al., 2002). BAK1 encodes an LRR-RLK with 5 LRR domains and functions as a co-receptor in both BR signaling and immune response. LRR domains of BAK1 are required for the recruitment to a ligand-bound LRR-RLK and then allow the kinase domain to physically interact for the subsequence transphosphorylation. BAK1 and BRI1 share similar gene expression and subcellular localization patterns. *BIN2 (BRASSINOSTEROID INSENSITIVE 2)* encodes a glycogen synthase kinase-3 (GSK3)-like kinase, which functions as a negative regulator for BR response. BIN2 phosphorylates positive regulators of BR response called BZR1 and BZR2/BES1 and leads to degradation of these proteins. Disruption in BR signaling leads to dwarfism, delayed flowering and photomorphogenesis in the dark (Friedrichsen and Chory, 2001).

RLKs and Defense Against Pathogens

To defend against harmful pathogens, plants require recognition of pathogen-derived molecules to activate their defense mechanisms. Flagellin, which is the major protein produced from bacterial flagella, functions as a resistance (*R*) gene product in plant–pathogen interaction (Nam, 2001). Other *R* gene products have been discovered including *avrXa21* virulence and tomato Pto (Dardick and Ronald, 2006); Dong et al., 2009). Even though some resistance (*R*) gene products are already identified and characterized, the receptors involved in pathogen perception largely remain unknown. LRR-RLKs are predicted to physically interact to those *R* gene products. Some studies have identified that plant FLAGELLIN SENSITIVE 2 (FLS2) RLK acts as a receptor for bacterial flagellin protein (Danna et., 2011). FLS2 phosphorylates a mitogen-activated protein kinase (MAPK) and then activates some defense genes and transcriptional factors. Similar to BR perception, BAK1 is involved in FLS2 signaling. BAK1 does not directly participate the binding between FLS2 and flagellin but it is required to activate the kinase of FLS2 via transphosphorylation. *avrXa21,* an *R* gene product produced from bacteria *Xanthomonas oryzae*, binds to an LRR and a kinase domain of LRR-containing protein called rice Xa21 (Lee et al., 2009). The recognition of pathogen-derived molecules leads to the phosphorylation of kinase domain of RLK to transduce the signal to downstream mechanisms, such as hypersensitive response (HR), programmed cell death (PCD) and finally synthesis of defense proteins (Montesano et al., 2003).

RLKs and Plant Development

Some RLKs have identified to be involved in plant development including shoot apical meristem (SAM) maintenance, gametophyte development and cell morphogenesis (Becraft, 2002). The mechanism of SAM maintenance is already well understood. During plant life cycle, SAM plays a crucial role in cell differentiation to produce lateral organs and in cell proliferation to self-renew the stem cell pool. In order to balance a proper population of these stem cells, an LLR-RLK CLAVATA1 (CLV1) is required. Loss of *CLV1* activity, size of apical meristem greatly expands, suggesting that CLV1 pathway regulates stem cell proliferation and differentiation in SAM (Clark et al., 1997). CLV1 heteromerizes CLV2/CORYNE and functions as receptor complex to bind a glycopeptide ligand CLV3 (Rojo et al., 2002). CLV2 encodes a LRR-RLK required for the stability of CLV1. Mutation in CLV1, CLV2 and CLV3 causes an ectopic accumulation of stem cells and enlargement of SAM. However, the recognition mechanism between CLV1 and CLV3 remains poorly understood. Recently, a model for CLV1-CLV3 interaction has been proposed. It has been shown that CLV3 induces transport of CLV1 to the lytic vacuoles. Loss of *CLV3* function, CLV1 is highly expressed on the PM (Nimchuck et al., 2011).

RLKs and Sexual Plant Reproduction

It has been shown that some RLKs play role in development of sporophytic tissues in reproductive organs. EXCESS MICROSPOROCYTES1/ EXTRA SPOROGENOUS CELL (EMS1/EXS) is an LRR-RLK expressed in the early stage of anther. Lack of *EMS/EXS* activity causes the numerous archesporial cells per anther

locule. In addition, the tapetum does not form in *ems1/exs* mutant. This suggests that *EMS/EXS* functions to restrict a proper number of archesporial cells. TAPETAL DETERMINANT1 (TPD1) is a ligand for EMS/EXS. TPD, a small peptide, is essential for tapetum development. TPD might be the ligand for EXS.

RLKs play roles in not only development of sporophytic tissues but also pollen-pistil interaction. The study on pollen-pistil interaction is well understood in self-incompatibility (SI) mechanism, which rejects self pollen to prevent inbreeding and promote outcrossing. The rejection of self-pollen could be occurred either during pollen lands on the stigma or during pollen tube grows inside the pistil. In *Brassica,* it has been shown that SI system is controlled by a complex *S-locus* with different haplotypes. These haplotypes from *S-locus* indicate the pollen phenotypes (Nasrallah, 1997). For example, if the haploid pollen carries the similar S-haplotype of the diploid pistil, the pollen is rejected by the pistil resulted in the inhibition of pollen tube growth. By contrast, if the haploid pollen carries different S-haplotypes of the diploid pistil, the pollen tube is allowed to grow toward the ovule. The evidences showed that SRK (S-locus receptor-like kinases) and SLG (S-locus glycoprotein), which are encoded at the *S-locus,* involve in pollen-pistil recognition (Nasrallah, 1997; Stein et al., 1991). Both proteins are highly expressed in *Brassica* stigma, which is consistent to their functions in pollen-pistil interaction. *SRK* encodes a serine/threonine kinase while *SLG* encodes a secreted glycoprotein (Stein and Nasrallah, 1993). In addition, calcium is reported to be a second messenger for mediating inhibition of pollen tube growth in SI (Franklin-Tong, 1999). Other genes related to *SRK* are identified in self-compatible species, such as *Arabidopsis*

lyrata (Schierup et al., 2001). More than 40 SRKs have been discovered in Arabidopsis. Evidence showed that SRKs in stigma physically interact with SCR (S-locus cysteine-rich) ligands produced from pollen wall (Shimizu et al., 2008), suggesting their roles in compatible pollinations. In tomato, LAT52, a pollen-specific small protein, is essential for pollen germination. LAT52 binds to a pollen LRR-RLK called LePRK2 to transduce the signal to downstream cascade and promote pollen germination (Zhang et al*.,* 2008). During pollen germination, LeSTIG1, another small protein produced from the stigma, binds to LePRK to regulate pollen tube growth (Tang et al*.,* 2004). LePRKs are localized to the plasma membrane of tomato pollen tube and partially dephosphorylate when they are incubated in the presence of style exaudate (Muschietti et al., 1998). Evidences suggest that ROP GTPase is required for the signaling via RLKs. A pollen-specific RopGEF binds to LePRK (Kaothien et al., 2005). In tobacco, another RLK, NTS16, was discovered (Li and Gray, 1997). Evidence showed that *NTS16,* expressed in the style, is involved in compatible interaction. Another RLK FERONIA was identified as a key player to mediate pollen tube reception in Arabidopsis (Escobar-Restrepo et al., 2007). *FERONIA* is predominantly expressed in the synergid cells. Loss of *FERONIA* activity caused a defect in pollen tube reception, suggesting its function through pollen-pistil communication. FERONIA phosphorylates RopGEF and subsequently activates RopGEF activity to switch an inactive ROP into active ROP. Taken together, this suggests that RLKs are potential receptor in both incompatible and compatible signaling.

REFERENCES

Arabidopsis Genome Initiative. (2000). Analysis of the genome sequence of the flowering plant *Arabidopsis thaliana*. Nature, 408: 796-815.

Becraft, P. (2002). Receptor kinase signaling in plant development. Annual Review of Cell and Developmental Biology, 18: 163-92.

Belkhadir, Y., and Chory, J. (2006). Brassinosteroid signaling: A paradigm for steroid hormone signaling from the cell surface. Science, 314: 1410-1411.

Borg M., Brownfield L., Twell D. (2009). Male gametophyte development: A molecular perspective. Journal of Experimental Botany, 60: 1465-1478.

Boisson-Dernier, A., Kessler, S.K. and Grossniklaus, U. (2011). The walls have ears: the role of plant CrRLK1Ls in sensing and transducing extracellular signals. Journal of Experimental Botany, 62: 1581–1591.

Chen, Y.H., Li, H.J., Shi, D.Q., Yuan, L., Liu, J., Sreenivasan, R., Baskar, R., Grossniklaus, U., Yang, W.C. (2007). The central cell plays a critical role in pollen tube guidance in *Arabidopsis.* Plant Cell, 19: 3563–3577.

Clark, S.E., Williams, R.W., and Meyerowitz, E.M. (1997). The *CLAVATA1* gene encodes a putative receptor kinase that controls shoot and floral meristem size in Arabidopsis. Cell, 89: 575-585.

Crawford, B.C.W., Ditta, G., Yanofsky, M.F. (2007). The NTT gene is required for transmitting-tract development in carpels of Arabidopsis thaliana. Current Biology, 17: 1101–1108.

Danna, C.H., Millet, Y.A., Koller, T., Han, S-.W., Bent, A.F., Ronald, P.C., Ausubel, F.M. (2011). The Arabidopsis flagellin receptor FLS2 mediates the perception of Xanthomonas Ax21 secreted peptides. Proceedings of the National Academy of Sciences of the United States of America, 108: 9286-9291.

Dardick, C. and Ronald, P. (2006). Plant and animal pathogen recognition receptors signal through non-RD kinases. PLoS Pathogen, 2: e2.

De Graaf, B., Cheung A.Y., Andreyeva T., Levasseur K., Kieliszewski K., Wu H-M. (2005). Rab 11 GTPase-regulated membrane trafficking is crucial for tip-focused pollen tube growth in tobacco. Plant Cell, 17: 2564–2579.

Dixit R., Rizzo C., Nasrallah M., Nasrallah J. (2001). The Brassica MIP-MOD gene encodes a functional water channel that is expressed in the stigma epidermis. Plant Molecular Biology 45: 51-62.

Dong, J., Xiao, F., Fan, F., Gu, L., Cang, H., Martin, G.B., and Chai, J. (2009). Crystal structure of the complex between Pseudomonas effector AvrPtoB and the tomato Pto kinase reveals both a shared and a unique interface compared with AvrPto-Pto. Plant Cell, 21: 1846–1859.

Drews, G. N., Lee, D. and Christensen, C. A. (1998). Genetic analysis of female gametophyte development and function. Plant Cell, 10: 5-17.

Escobar-Restrepo, J.M., Huck, N., Kessler, S., Gagliardini, V., Gheyselinck, J., Yang, W.C., and Grossniklaus, U. (2007). The FERONIA receptorlike kinase mediates male-female interactions during pollen tube reception. Science, 317: 656-660.

Franklin-Tong, V.E. (1999). Signaling and the modulation of pollen tube growth. The Plant Cell, 11: 727-738.

Friedrichsen, D. and Chory, J. (2001). Steroid signaling in plants: from the cell surface to the nucleus. Bioessays, 23: 1028-1036

Fu Y., Wu G., Yang Z. (2001). Rop GTPase-dependent dynamics of tip-localized F-actin controls tip growth in pollen tubes. The Journal of Cell Biology, 152: 1019-1032.

Gu Y., Fu Y., Dowd P., Li S., Vernoud V., Gilroy S., Yang Z. (2005). A Rho family GTPase controls actin dynamics and tip growth via two counteracting downstream pathways in pollen tubes. The Journal of Cell Biology, 169: 127-138.

Guyon V, Tang WH, Monti MM, Raiola A, Lorenzo GD, McCormick S, Taylor LP (2004) Antisense phenotypes reveal a role for SHY, a pollen-specific leucine-rich repeat protein, in pollen tube growth. Plant Journal, 39: 643-654.

Harmon, A.C., Bribskov, M., and Harper, J.F. (2000). CDPKs: A kinase for every Ca^{2+} signal? Trends in Plant Science, 4: 154-159.

Helling D., Possart A., Cottier S., Klahre U., Kost B. (2006). Pollen tube tip growth depends on plasma membrane polarization mediated by tobacco PLC3 activity and endocytic membrane recycling. Plant Cell, 18: 3519–3534.

Hepler, P.K. (1997). Tip growth in pollen tubes: Calcium leads the way. Trends in Plant Science, 2: 79-80.

Hepler, P.K., Vidali, L., Cheung, A.Y. (2001). Polarized cell growth in higher plants. Annual Review of Cell Developmental Biology, 17: 159-187.

Heslop-Harrison, J. (1987). Pollen germination and pollen tube growth. International Review of Cytology 107: 1-78.

Hicks, G.R., Rojo, E., Hong, S., Carter, D.G., Raikhel, N.V. (2004). Geminating pollen has tubular vacuoles, displays highly dynamic vacuole biogenesis, and requires VACUOLESS1 for proper function. Plant Physiology, 134: 1227-1239.

Higashiyama, T., Hamamura, Y. (2008). Gametophytic pollen tube guidance. Sexual Plant Reproduction 21: 17-26.

Higashiyama, T., Kuroiwa, H., Kawano, S., Kuroiwa, T. (1998). Guidance in vitro of the pollen tube to the naked embryo sac of torenia fournieri. Plant Cell 10: 2019-2032.

Higashiyama, T., Yabe, S., Sasaki, N., Nishimura, Y., Miyagishima, S., Kuroiwa, H., Kuroiwa, T. (2001). Pollen tube attraction by the synergid cell. Science, 293: 1480-1483.

Holdaway-Clarke T.L., Feijo J.A., Hackett G.R., Kunkel J.G., Hepler P.K. (1997). Pollen tube growth and the intracellular cytosolic calcium gradient oscillate in phase while extracellular calcium influx is delayed. Plant Cell, 9: 1999-2010.

Holdaway-Clarke, T.L., Hepler, P.K. (2003). Control of pollen tube growth: role of ion gradients and fluxes. New Phytologist, 159: 539-563.

Honys, D., Twell, D. (2003). Comparative analysis of the Arabidopsis pollen transcriptome. Plant Physiol **132:** 640-652.

Honys, D., Twell, D. (2004). Transcriptome analysis of haploid male gametophyte development in Arabidopsis. Genome Biology, 5: R85.

Hord, C.L.H., Chen, C., DeYoung, B.J., Clark, S.E., Ma, H. (2006). The BAM1/BAM2 receptor-like kinases are important regulators of Arabidopsis early anther development. Plant Cell, 18: 1667–1680.

Huck, N., Moore, J.M., Federer, M., and Grossniklaus, U. (2003). The Arabidopsis mutant *feronia* disrupts the female gametophytic control of pollen tube reception. Development, 130: 2149-2159.

Hwang, J.U., Gu, Y., Lee, Y.J., Yang, Z. (2005). Oscillatory ROP GTPase activation leads the oscillatory polarized growth of pollen tubes. Molecular Biology of the Cell, 16: 5385-5399.

Ishikawa, F., Suga, S., Uemura, T., Sato, M.H., Maeshima, M. (2005). Novel type aquaporin SIPs are mainly localized to the ER membrane and show cell-specific expression in Arabidopsis thaliana. FEBS Lett **579:** 5814-5820.

Iwano, M., Entani, T., Shiba, H., Kakita, M., Nagai, T., Mizuno, H., Miyawaki, A., Shoji, T., Kubo, K., Isogai, A. (2009). Fine-tuning of the cytoplasmic Ca2+ concentration is essential for pollen tube growth. Plant Physiol **150:** 1322-1334.

Johnson, K.L., and Ingram, G.C. (2005). Sending the right signals: Regulating receptor kinase activity. Current Opinions in Plant Biology, 8: 648-656.

Johnson, M.A., Lord, E. (2006). Extracellular Guidance Cues and Intracellular Signaling Pathways that Direct Pollen Tube Growth, Plant Cell Monograph, 3: 223-242.

Johnson, M.A., von Besser, K., Zhou, Q., Smith, E., Aux, G., Patton, D., Levin, J.Z., Preuss, D. (2004). Arabidopsis hapless mutations define essential gametophytic functions. Genetics, 168: 971-982.

Johnson, S.A., McCormick, S. (2001). Pollen germinates precociously in the anthers of raring-to-go, an Arabidopsis gametophytic mutant. Plant Physiology, 126: 685-695.

Jones-Rhoades, M.W., Borevitz, J.O., Preuss, D. (2007). Genome-wide expression profiling of the Arabidopsis female gametophyte identifies families of small, secreted proteins. Plos Genetics, **3:** 1848-1861.

Kanaoka, M.M., Kawano, N., Matsubara, Y., Susaki, D., Okuda, S., Sasaki, N., Higashiyama, T. (2011). Identification and characterization of TcCRP1, a pollen tube attractant from *Torenia concolor*. Annals of Botany,

Kaothien, P., Ok, S.H., Shuai, B., Wengier, D., Cotter, R., Kelley, D., Kiriakopolos, S., Muschietti, J., McCormick, S. (2005). Kinase partner protein interacts with the LePRK1 and LePRK2 receptor kinases and plays a role in polarized pollen tube growth. Plant Journal, 42: 492-503.

Kasahara, R.D., Portereiko, M.F., Sandaklie-Nikolova, L., Rabiger, D.S., Drews, G.N. (2005). MYB98 is required for pollen tube guidance and synergid cell differentiation in Arabidopsis. The Plant Cell, 17: 2981-2992.

Kim, S., Mollet, J.C., Dong, J., Zhang, K.L., Park, S.Y., Lord, E.M. (2003). Chemocyanin, a small basic protein from the lily stigma, induces pollen tube chemotropism. Proceedings of the National Academy of Sciences of the United States of America, 100: 16125-16130.

Kost, B., Mathur J., Chua, N.H. (1999). Cytoskeleton in plant development. Current Opinion in Plant Biology, 2: 462-470.

Krupa, A., Abhinandan, K.R., Srinivasan, N., (2004). KinG: a database of protein kinases in genomes. Nucleic Acids Research, 32: D153-D155.

Lalanne, E., Twell, D. (2002). Genetic control of male germ unit organization in Arabidopsis. Plant Physiology, 129: 865-875.

Lee, S.W., Han, S.W., Sririyanum, M., Park, C.J., Seo, Y.S., Ronald, P.C. (2009). A type I-secreted, sulfated peptide triggers XA21-mediated innate immunity. *Science* **326,** 850–853.

Lee, Y.J., Szumlanski, A., Nielsen, E., Yang, Z. (2008). Rho-GTPase-dependent filamentous actin dynamics coordinate vesicle targeting and exocytosis during tip growth. The Journal of Cell Biology, 181: 1155-1168.

Lee, Y.J. and Yang, Z. (2008). Tip growth: signaling in the apical dome. Current Opinion in Plant Biology, 11: 662-671.

Li, H., Lin, Y., Heath, R.M., Zhu, M.X. and Yang, Z. (1999). Control of pollen tube tip growth by a Rop GTPase-dependent pathway that leads to tip-localized calcium influx. Plant Cell, 11: 1731-1742.

Li, H.Y., Gray, J.E. (1997). Pollination-enhanced expression of a receptor-like protein kinase related gene in tobacco styles. Plant Molecular Biology, 33: 653–665.

Lind, J.L., Bonig, I., Clarke, A.E., Anderson, M.A. (1996). A style-specific 120-kDa glycoprotein enters pollen tubes of Nicotiana alata in vivo. Sexual Plant Reproduction 9: 75-86.

Lolle, S.J. and Cheung, A.Y. (1993). Promiscuous germination and growth of wild-type pollen from Arabidopsis and related species on the shoot of the Arabidopsis mutant, fiddlehead. Developmental Biology, 155: 250–258.

Lord, E.M. and Russell, S.D. (2002). The mechanisms of pollination and fertilization in plants. Annual Review of Cell and Developmental Biology, 18: 81–105.

Lovy-Wheeler, A., Kunkel, J.G., Allwood, E.G., Hussey, P.J., Hepler, P.K. (2006). Oscillatory increases in alkalinity anticipate growth and may regulate actin dynamics in pollen tube of lily. Plant Cell, 18: 2182-2193.

Lu, Y., Chanroj, S., Zulkifli, L., Johnson, M.A., Uozumi, N., Cheung, A. and Sze, A. (2011). Pollen Tubes Lacking a Pair of K^+ Transporters Fail to Target Ovules in *Arabidopsis*. Plant Cell, 23: 81-93.

Lush W.M., Grieser F., Wolters-Arts M. (1998). Directional guidance of *Nicotiana alata* pollen tubes *in vitro* and on the stigma. Plant Physiology, 118: 733-741.

Luu, D.T., Qin, X., Morse, D., Cappadocia, M. (2000). S-RNase uptake by compatible pollen tubes in gametophytic self-incompatibility. Nature 407: 649-651.

Maciver, S.K. and Hussey P.J. (2002). The ADF/cofilin family: Actin-remodeling proteins. Genome Biology, 3: reviews 3007.1–3007.12.

Malho, R. and Camacho, L. (2004). Signaling the cytoskeleton in pollen tube germination and growth. In: Hussey PJ, ed. The plant cytoskeleton in cell differentiation and development. Annual Plant Review Series UK, Blackwell Publishers: 240–264.

Malho, R., Read, N.D., Trewavas, A.J., Pais, M.S. (1995). Calcium Channel Activity during Pollen Tube Growth and Reorientation. Plant Cell **7:** 1173-1184.

Malho, R. and Trewavas, A.J. (1996). Localized Apical Increases of Cytosolic Free Calcium Control Pollen Tube Orientation. Plant Cell, 8: 1935-1949.

Mascarenhas, J.P. (1990). Gene activity during pollen development. Annual Review of Plant Physiology and Plant Molecular Biology l41: 317-338.

Marton, M.L., Cordts, S., Broadhvest, J. and Dresselhaus, T. (2005). Micropylar pollen tube guidance by egg apparatus 1 of maize. Science, 307: 573-576.

McCormick, S. (2004). Control of male gametophyte development. Plant Cell, 16: S142-153.

Montesano, M., Brader, G., and Paiva, N.L. (2003). Pathogen derived elicitors: searching for receptors in plants. Molecular Plant Pathology, 4: 73-79.

Muschietti, J., Eyal, Y., McCormick, S. (1998). Pollen tube localization implies a role in pollen-pistil interactions for the tomato receptor-like protein kinases LePRK1 and LePRK2. Plant Cell, 10: 319-330.

Nam, J. (2001). New aspects of gene-for-gene interactions for disease resistance in plant. Plant Pathology Journal, 17: 83-87.

Nam, K.H., and Li, J. (2002). BRI1/BAK1, a receptor kinase pair mediating brassinosteroid signaling. Cell, 110: 203-212.

Nasrallah, J.B. (1997). Signal perception and response in the interactions of self-incompatibility in *Brassica.* Essays in Biochemistry, 32: 143-160.

Nimchuck, Z.L., Tarr P.T., Ohno, C., Qu, X. and Meyerowitz, E.M. (2011). Plant stem cell signaling involves ligand-dependent trafficking of the CLAVATA1 receptor kinase. Current Biology, 21: 345-352.

Okuda, S., Tsutsui, H., Shiina, K., Sprunck, S., Takeuchi, H., Yui, R., Kasahara, R.D., Hamamura, Y., Mizukami, A., Susaki, D. (2009). Defensin-like polypeptide LUREs are pollen tube attractants secreted from synergid cells. Nature, 458: 357-361.

Pagnussat, G.C., Alandete-Saez, M., Bowman, J.L., Sundaresan, V. (2009). Auxin-dependent patterning and gamete specification in the Arabidopsis female gametophyte. Science, **324:** 1684-1689.

Palanivelu, R., Brass, L., Edlund, A.F., Preuss, D. (2003). Pollen tube growth and guidance is regulated by POP2, an Arabidopsis gene that controls GABA levels. Cell, 114: 47-59.

Palanivelu, R., Preuss, D. (2006). Distinct short-range ovule signals attract or repel *Arabidopsis thaliana* pollen tubes in vitro. Bmc Plant Biology 6: -

Pierson, E.S., Miller, D.D., Callaham, D.A., van Aken, J., Hackett, G., Hepler, P.K. (1996). Tip-localized calcium entry fluctuates during pollen tube growth. Developmental Biology, 174: 160-173.

Preuss, D., Lemieux, B., Yen, G., Davis, R.W. (1993). A conditional sterile mutation eliminates surface components from Arabidopsis pollen and disrupts cell signaling during fertilization. Genes and Development 7: 974-985.

Qin, Y., Leydon, A.R., Manziello, A., Pandey, R., Mount, D., Denic, S., Vasic, B., Johnson, M.A., Palanivelu, R. (2009). Penetration of the stigma and style elicits a novel transcriptome in pollen tubes, pointing to genes critical for growth in a pistil. PLoS Genet 5: e1000621

Ray, S., Park, S.S., Ray, A. (1997). Pollen tube guidance by the female gametophyte. Development, 124: 2489-2498.

Rojo, E., Sharma, V.K., Kovaleva, V., Raikhel, N.V. and Fletcher, J.C. (2002). CLV3 is localized to the extracellular space where it activates the Arabidopsis CLAVATA stem cell signaling pathway. Plant Cell, 14:1-10.

Rosen, W.G. (1968). Ultrastructure and physiology of pollen. Annual Review of Plant Physiology, 19: 435-462.

Roy, S., McPherson, R.A., Apolloni, A., Yan, J., Clyde-Smith, J., Hancock, J.F. (1998). Molecular Cell Biology, 18: 3947-3955.

Schierup, M.H., Mable, B.K., Awadalla, P. and Charlesworth, D. (2001). Identification and characterization of a polymorphic receptor kinase gene linked to the self-incompatibility locus of *Arabidopsis lyrata*. Genetics, 158: 387–399.

Schulze-Muth, P., Irmler, S., Schroder, G., and Schroder, J. (1996). Novel type of receptor-like protein kinase from a higher plant *Catharanthus roseus* cDNA, gene, intramolecular autophosphorylation, and identification of a threonine important for auto- and substrate phosphorylation. Journal of Biological Chemistry, 271: 26684-26689.

Shimizu, K.K., Ito, T., Ishiguro, S. and Okada, K. (2008). *MAA3* (*MAGATAMA3*) helicase gene is required for female gametophyte development and pollen tube guidance in *Arabidopsis thaliana*. Plant and Cell Physiology, 49: 1478-1483.

Shimizu, K.K. and Okada, K. (2000). Attractive and repulsive interactions between female and male gametophytes in Arabidopsis pollen tube guidance. Development, 127: 4511-4518.

Shimizu, K.K., Shimizu-Inatsugi, R., Tsuchimatsu, T., and Purugganan, M.D. (2008). Independent origins of self-compatibility in *Arabidopsis thaliana.* Molecular Ecology, 17: 704-714.

Shiu, S.-H., and Bleecker, A.B. (2001a). Plant receptor-like kinase gene family: Diversity, function and signaling. Science STKE, re22.

Shiu, S.-H., and Bleecker, A.B. (2001b). Receptor-like kinases from Arabidopsis form a monophyletic gene family related to animal receptor kinases. Proceeding of the National Academy of Science U.S.A., 98: 10763-10768.

Shiu, S.-H., and Bleecker, A.B. (2003). Expansion of the receptor-like kinase/pelle gene family and receptor-like kinase proteins in Arabidopsis. Plant Physiology, 132: 530-543.

Shui, S.-H., Karlowski, W.M., Pan, R., Tzeng, Y.-H., Mayer, K.F.X., and Li, W.-H. (2004). Comparative analysis of the receptor-like kinase family in Arabidopsis and rice. Pant Cell, 16:1220-1234.

Shpak, E.D., Lakeman, M.B. and Torii, K.U. (2003). Dominant-negative receptor uncovers redundancy in the Arabidopsis ERECTA leucine-rich repeat receptor-like kinase signaling pathway that regulates organ shape. Plant Cell, 15: 1095-1110.

Snedden, W.A., Fromm, H. (2001). Calmodulin as a versatile calcium signal transducer in plants. New Phytology, 151: 35–66.

Snowman, B.N., Kovar, D.R., Shevchenko, G., Franklin-Tong, V.E., Staiger, C.J. (2002). Signal-mediated depolymerization of actin in pollen during the self-incompatibility response. Plant Cell, 14: 2613-2626.

Stein, J.C., and Nasrallah, J.B. (1993). A plant receptor-like gene, the S-locus receptor kinase of *Brassica oleracea* L., encodes a functional serine threonine kinase. Plant Physiology, 101: 1103-1106.

Stein, J.C., Howlett, B., Boyes, D.C., Nasrallah, M.E., and Nasrallah, J.B. (1991). Molecular cloning of a putative receptor protein kinase gene encoded at the self-incompatibility locus of *Brasica oleracea*. Proceeding of the National Academy of Sciences USA, 88: 8816–8820.

Sze, H., Padmanaban, S., Cellier, F., Honys, D., Cheng, N.H., Bock, K.W., Conéjéro, G., Li, X., Twell, D., Ward, J.M. (2004). Expression patterns of a novel AtCHX gene family highlight potential roles in osmotic adjustment and K^+ homeostasis in pollen development. Plant Physiology, 136: 2532–2547

Tang, W., Kelley, D., Ezcurra, I., Cotter, R., McCormick, S. (2004). LeSTIG1, an extracellular binding partner for the pollen receptor kinases LePRK1 and LePRK2, promotes pollen tube growth in vitro. Plant Journal, 39: 343-353.

Tang, W.H., Ezcurra, I., Muschietti, J., McCormick, S. (2002). A cysteine-rich extracellular protein, LAT52, interacts with the extracellular domain of the pollen receptor kinase LePRK2. Plant Cell, 14: 2277-2287.

Vidali, L., McKenna, S.T., Hepler, P.K. (2001). Actin polymerization is necessary for pollen tube growth. Molecular Biology of the Cell, 12: 2534–2545

von Besser, K., Frank, A.C., Johnson, M.A., Preuss, D. (2006). Arabidopsis HAP2 (GCS1) is a sperm-specific gene required for pollen tube guidance and fertilization. Development, 133: 4761-4769.

Walker, J.C. (1994). Structure and function of the receptor-like protein kinases of higher plants. Plant Molecular Biology, 26: 1599-1609.

Wang, Y., Zhang, W.Z., Song, L.F., Zou, J.J., Su, Z., Wu, W.H. (2008). Transcriptome analyses show changes in gene expression to accompany pollen germination and tube growth in Arabidopsis. Plant Physiology, 148: 1201-1211.

Wang, Z.Y., and He, J.X. (2004). Brassinosteroid signal transduction-choices of signals and receptors. Trends in Plant Science, 9: 91-96.

Wilhelmi, L.K. and Preuss, D. (1996). Self-sterility in *Arabidopsis* due to defective pollen tube guidance. Science, 274: 1535-1537.

Wolters-Arts, M., Lush, W.M., Mariani, C. (1998). Lipids are required for directional pollen-tube growth. Nature, 392: 818-821.

Wu, H.M., Wang, H., Cheung, A.Y. (1995). A pollen tube growth stimulatory glycoprotein is deglycosylated by pollen tubes and displays a glycosylation gradient in the flower. Cell, 82: 395-403.

Yamamoto, Y., Nishimura, M., Hara-Nishimura, I., Noguchi, T. (2003). Behavior of vacuoles during microspore and pollen development in *Arabidopsis thaliana*. Plant Cell Physiology, 44: 1192–1201.

Yang, Z. and Fu, Y. (2007). ROP/RAC GTPase signaling. Current Opinion in Plant Biology, 10: 490-494.

Yokota, E. and Shimmen, T. (2006). The actin cytoskeleton in pollen tubes: Actin and actin binding proteins. In The Pollen Tube, Malho R., ed (Berlin/Heidelberg, Germany: Springer), pp. 139–155.

Zhang, D., Wengier, D., Shuai, B., Gui, C.P., Muschietti, J., McCormick, S., Tang W.H. (2008). The pollen receptor kinase LePRK2 mediates growth-promoting signals and positively regulates pollen germination and tube growth. Plant Physiology, 148: 1368-1379.

CHAPTER 2

Leucine Rich Repeat Receptor-Like Kinase C (LRR-RLK C) Functions in Arabidopsis Sexual Reproduction

ABSTRACT

Sexual reproduction is a critical process in flowering plants. To achieve successful reproduction, some important events are required including gametogenesis, pollination and fertilization. In this chapter, a reverse genetic approach was used to clarify the biological function of a novel LRR-RLK, named as RLK C, during sexual reproduction in Arabidopsis. Phenotypic characterization of the loss-of-function of *RLK C* reveals that *rlk c* plants showed subtle defects in seed production and pollen tube guidance. By use of cell-specific markers, the synergid and egg cells were not specified in some *rlk c* embryo sacs. According to the segregation analysis, the genetic transmission efficiencies were partially affected through male and female gametophytes. However, pollen fertility appeared normal. The expression pattern of *RLK C* was determined by GUS assay. RLK Cp-GUS was expressed in both vegetative and reproductive tissues. In the embryo sac, *RLK C* was highly expressed at the synergids. The *rlk c* plant carrying the genomic region of wild-type *RLK C* displayed normal seed production and pollen tube guidance. Taken together, we proposed that RLK C is required for the fertility of gametophyte.

INTRODUCTION

Leucine-rich repeat (LRR) RLKs are the most common motif spreading out more than 50% (216 members) of the RLK family in Arabidopsis. They are transmembrane proteins involved in various signal transduction pathways. LRR-RLKs could be grouped into at least 13 subfamilies from 2-22 LRR repeats (LRR I to LRR XIII) based on the number of the leucine repeats and their arrangements (Dievart and Clark 2004). Generally, the LRR domain is characterized by the consensus sequence LxxLxLxxNxLxx of approximately 24 amino acids with the conserved leucines (Braun and Walker 1996). The variety of residues probably causes structural difference and binding specificity of the LRRs (Kajava and Kobe 2002). Some of these LRR-RLK genes have been characterized in Arabidopsis. However, functions of most LRR-RLK genes are still unknown. It has been demonstrated that LRR-RLKs function in different aspects of plant growth and development, such as organ shape, inflorescence architecture, early anther development (Hord et al, 2006), cell morphogenesis, hormone perception and disease resistance. For example, CLAVATA1 regulates cell differentiation in shoot apical meristem (SAM) (Clark et al., 1997). ERECTA is involved in organ shape and inflorescence architecture (Shpak et al, 2003). BRI1 signaling is required for brassinosteroid perception (Li and Chory 1997). HAESA controls floral organ abscission (Jinn et al., 2000). Nevertheless, few evidence to date has been shown that LRR-RLKs involved in gametophyte development and its function, such as pollen tube guidance. During pollination, the cell wall of pollen grain and/or pollen tube physically contacts with the female tissues. Finally, the pollen tube reaches the ovary and delivers the sperm

to the female gametophyte (Lord and Russell, 2002). It is likely that the interaction between pollen and pistil is required for pollination and pollen tube guidance. Lines of evidence have shown that RLKs are involved in cell-cell communication. They function as receptors to perceive the signals from the outside of the cell, amplify and transduce the signals to the downstream components. The putative ligands for these membrane receptors could be small molecules, peptides or plant hormones (Benschop et al., 2007). Due to the large number of member in this gene family, RLKs might function redundantly among closely related member.

In this chapter, *RLK C* encoding a leucin-rich repeat (LRR)-RLK with Ser/Thr kinase activity was characterized. RLK C belongs to LRR III-type of the LRR-RLK subfamily with 47 members. It has been shown that members of LRR III type are involved in hormone and abiotic stress responses, including auxin and drought tolerant (Hove, 2010). MRLK (Meristematic Receptor-Like Kinase)/ IMK 3 is spatial expressed in shoot and root acal meristems. Evidence has shown that MRLK phosphorylates and binds to a MADS-box protein AGL24 *in vitro* (Fujita et al., 2003). According to their subcellular localizations, it is suggested that the MRLK signaling pathway induces AGL24 translocation from the cytoplasm to the nucleus. It is likely that the RLK signaling is involved in phosphorylation of AGL24 transcription factor. TMKL1 or Transmembrane Kinase-Like might be involved in silique maturation based on Northern blot analysis (Valon et al., 1993). RKL 1 is predominantly expressed in stomata cells, hydathodes, trichomes and floral organ abscission zone (Tarutani et al., 2004). RLK 902, highly related to RKL 1, is strongly expressed in root tips, lateral root primordia, stipules

and abscission zone. However, double mutations in *RKL 1* and *RLK 902* did not show apparent phenotype, suggesting functional redundancy (Tarutani et al., 2004). Evidence shows that RLK C is involved in mannitol tolerance (Hove, 2010). In this study, a reverse genetics and molecular approaches were used to identify *RLK C*. A T-DNA insertion line was obtained and named as *rlk c*. We demonstrate that the RLK C signaling pathway requires other players to mediate sexual reproduction in *Arabidopsis*.

MATERIALS AND METHODS

Phylogenetic Analysis of the Extracellular Domains of Receptor-Like Kinases in *Arabidopsis* Pollen

A public oligo-based expression profiling (Affymetrix GeneChips) analysis of pollen revealed that approximately 180 *RLKs* of the total number of *RLKs* in the genome were represented. They are distributed among 7 subfamilies, including the leucine-rich repeat (LRR), the lectin type (LecRLKs), the S-domain (SD) type, PERKL, the wall-associated kinases (WAKs), the DUF26 domain and the CrRLK1L type subfamilies. To generate the distance tree of pollen RLKs in *Arabidopsis*, the information of those were collected form TAIR (The Arabidopsis Information Resource), ncbi (The National Center for Biotechnology Information), PlantsP (http://plantsp.genomics.purdue.edu/) and Shiu and Bleecker (2001). The amino acid sequences encoded the extracellular domain of each RLK were aligned by ClustalW (Thompson et al., 1994) to generate the distance mapping tree (Figure 2.1A). At4g23740 is a gene member of a family of LRR-RLK. In this subfamily, it contains two other LRR-RLKs, At1g06840 and At1g63430 (Figure 2.1B). At4g23740, At1g06840 and At1g63430 were selected for further studies and were named

as RLK C, RLK B and RLK D, respectively. RLK C, RLK B and RLK D belong to LRR III, LRR VI and LRR VIII of the LRR-RLK subfamily. They share approximately 20% identical to each other.

Plant Materials and Plant Growth Condition

Arabidopsis thaliana accession Columbia-0 (Col-0) plants used in this study were grown in the growth room and chamber at the University of California, Riverside. To surface clean Arabidopsis seeds, 70% ethanol and the sterilization solution (20% bleach, 0.05% tween 20 and double-distilled water) were added to the seeds for 5 minutes. Seeds were washed thoroughly 3-5 times with sterile water to remove the bleach residue and seeds were immediately planted on petri dishes containing plant growth medium: one-half strength Murashige and Skoog (MS) salts (Sigma), 0.5% sucrose, 0.8% phyto agar (Research Products International Corp.), 1xB5 (1,000x in distilled water: 10% myo-inositol, 0.1% nicotinic acid and 0.1% pyroxidine HCI) and 1xThiamin (2,000x in distilled water: 0.2% thiamin HCI) pH5.8 with 1M KOH. Seeds were kept at 4°C for 3-4 days to break dormancy. After the cold treatment, the petri dish was placed in the growth room. Seven to 10-day-old seedlings were transferred to soil (Sunshine Mix#1, Sun Gro Horticulture) at 22°C under a 16 light/ 8 dark-hour photoperiod with 200 μEm-2s-1 illumination. To study function of *RLK C* (At4g23740), a T-DNA insertion allele (SALK_005132) was obtained from Arabidopsis Biological Resource Center (ABRC; Alonso et al., 2003).

PCR and RT-PCR ANALYSIS

Genomic DNAs from T-DNA insertion line were extracted from the mature leaves for PCR-based genotyping using gene-specific primers generated by the T-DNA primer design tool (http://signal.salk.edu/tdnaprimers.2.html); 5'-ATGCAACCAACT CGTTCACTC-3' and 5'-AAGCTCCACAACGTTTTCATG-3' and T-DNA-specific primers (5'-ATTTTGCCGATTTCGGAAC-3'). Reverse transcriptase (RT)-PCR was performed to determine the expression level of *RLK C* in *rlk c* and wild-type plants. Total RNAs were isolated from various plant tissues, such as root, mature rosette leaf, pistil and open flower using RNeasy mini Kit (Qiagen). In a reverse transcriptase reaction, the double-strand cDNAs were synthesized (Superscript II, Invitrogen) and used as templates in RT-PCR using gene specific primers for *RLK* C (5'-ATGGAAGCTTTGAGG ATTTATCTATGG-3' and 5'-AACAGTCAACACAAACGCCAAAG-3'); for *ACTIN3,* 5'-GGAACAGTGTGACTCACACCATC-3' and 5'-AAGCTGTTCTTTCCCTCTACG C- 3' as amplification control).

Analysis of Seed Set in Mature Siliques

To analyze seed production in *rlk c*, the mature siliques were incubated in 100% ethanol over night and the numbers of seeds and unfertilized ovules per a silique were examined.

Analysis of *In vivo* Pollen Tube Growth and Guidance with Aniline Blue Staining

Aniline blue staining was performed to observe pollen tube growth inside the pistils. The anthers from mature floral buds (stage 12) were emasculated and plants were kept in the growth room for 24 hours. Plants used as pollen donor were taken from the

growth room and kept at room temperature for an hour before pollination. Self and reciprocal-cross pollination were carried out. Fresh pollen grains from the mature flowers (stage 13) were used to manually apply on the stigma surface of the emasculated pistil. The pollinated pistils were harvested after pollination for 18-24 hours. Pistils were fixed in fixative solution (3:1 v/v ethanol and acetic acid) for 2 hours at room temperature. The pistils were dehydrated using the following concentrations of ethanol series: 95%, 70%, 50% and 30% (10-15 minutes for each change at room temperature) and softened by 8M NaOH overnight. The softening pistils were washed with distilled water to remove the NaOH residue and stained with decolorized aniline blue for 2 hours as described by Mori et al. (2006). Pollen tube growth behavior inside the female tissues was observed under a fluorescence microscope (Nikon Microphot FXA, Nikon) and images were captured with a Spot Insight Camera (Diagnostic Instruments Inc.).

Pollen Analysis

(A) Pollen Viability Vest by FDA Staining

The viability of the *rlk c* pollen grains was assessed by FDA staining (Heslop-Harrison and Heslop-Harrison, 1970). Pollen was collected from freshly dehisced anthers and immersed in the pollen growth liquid media. Pollen was incubated at 28°C for 30 minutes. A drop of 0.5 μg/mL FDA (fluoreacein diacetate) was added to the pollen growth media and observed immediately with a Nikon ECLIPSE microscope (Nikon Instruments) equipped with epifluorescence and fluorescein isothiocyanate (FITC) filter.

(B) Vacuole Analysis by Neutral Red Staining

To investigate vacuoles, mature pollen grains were collected and applied with 0.02% (w/v) neutral red for 30 minutes at room temperature as described by Lee et al., (2008). Samples were observed under a bright-field microscope.

(C) *In vitro* Pollen Germination Test

The anthers were brushed on pollen growth medium (18% sucrose, 0.01% Boric acid, 1mM $CaCl_2$, 1mM $Ca(NO_3)_2$, 1mM $MgSo_4$ pH 7.0 and 0.5% Select agar). The petri dishes were incubated at 28°C for 4 hours before analysis. Pollen tube growth was observed with a Nikon ECLIPSE microscope (Nikon Instruments) and images were captured with a Hamamatsu Digital Camera (Hamamatsu Photomics).

(D) Pollen Nuclei Analysis by DAPI staining

Mature pollen grains were collected and placed on slide. A few drop of DAPI (4', 6-diamidino phenylindole) solution (0.1 M Sodium phosphate pH 7.0, 1 mM EDTA, 0.1% Triton X-100 and 0.4 μg/ml) was added to pollen, and was observed by a fluorescence microscope with UV filter.

Cleared Whole-Mount Preparation

Inflorescences were harvested and fixed in the fixative solution (3:1 v/v ethanol and acetic acid) for 2 hours at room temperature. Tissues were then rehydrated using the following concentrations of ethanol series: 95%, 70%, 50% and 30% (10-15 minutes for each change at room temperature) and cleared in Hoyer's solution (100 g chloral hydrate, 25 mL glycerol and 50 mL distilled water) for 3 hours and observed under a Nikon

ECLIPSE microscope (Nikon Instruments). Images were captured with a Hamamatsu Digital Camera (Hamamatsu Photomics).

GUS Expression Analysis

Genomic DNAs from the mature leaves were used as templates to generate promoter-GUS construct by use of gene specific primers (5'-CGTCCTATCAAATCCG TCCCG-3' and 5'-ACAGAAATGTGTTTGTTGAACCGG-3'). The transgene was introduced into the *rlk c* mutant. To perform GUS expression analysis, GUS assay was performed in 5 day-old seedlings and 7 week-old plants. Plant tissues were harvested and fixed in 40% acetone for an hour at room temperature. The pistils were incubated in GUS staining buffer (10 mM EDTA, 100 mM sodium phosphate, pH 7.0, 0.5 mM potassium ferrocyanide, 0.5 mM potassium ferricyanide) and 0.1% Triton X-100 with 1 mM 5-bromo-4-chloro-β-glucuronide) at 37°C at least 3 hours as described by Vielle-Calzada et al. (2000). The pistils were fixed in the fixative solution (3:1 v/v ethanol and acetic acid) for 2 hours at room temperature and rehydrated using the following concentrations of ethanol series: 95%, 70%, 50% and 30% at room temperature and cleared in Hoyer's solution for 3 hours. Samples were observed under a Nikon microscope (Nikon Microphot FXA, Nikon) and images were captured with a Spot Insight Camera (Diagnostic Instruments Inc.).

RESULTS

RLK C is Expressed in Both Vegetative and Reproductive Organs

To determine gene expression level by reverse transcriptase (RT)-PCR, total RNAs were isolated from roots of 10-day-old seedlings, rosette leaves and open flowers of wild-type *Arabidopsis* plants and subjected to RT-PCR. The anlysis revealed that the transcript expression of *RLK C* was detected in most plant tissues, such as roots, rosette leaves, pistils and open flowers (Figure 2.2A). To investigate the expression profile of *RLK C*, the transgenic reporter plants expressing the β-glucuronidase (GUS) gene under the control of *RLK C* promoter were generated. Analysis of GUS expression revealed that *RLK C* activities were both in underground and above-ground tissues. In *RLK C*::GUS plants, *GUS* activity was found in both vegetative and reproductive organs. At the root tip of 5-day-old seedlings, *RLK C*::GUS plants showed GUS signal in the meristematic region, stele, vascular tissues and pericycle (Figure 2.3A-D). The epidermis and root hairs were free of GUS staining (Figure 2.3D). GUS expression was detected in the secondary root primordia (Figure 2.3B, C, E and F). In above-ground tissues, GUS activity was observed at the first true leaves and cotyledons (Figure 2.3A). GUS staining was strongest at the region between hypocotyls and primary roots. The mature rosette and cauline leaves showed strong GUS activity particularly in the vasculature (Figure 2.3G, H and I), trichomes (Figure 2.3I and J) and hydathodes of the leaf base (Figure 2.3G). No GUS activity was detectable in guard cells of the rosette and cauline leaves.

In reproductive stage, GUS signal was observed in the inflorescences (Figure 2.4A). No GUS activity was detected at the first and second whorl of floral organs, the

sepeals and petals, at any developmental stages of the flower (Figure 2.5B). In male organs, GUS staining was observed in the anther filaments with strong expression in the vascular tissues (Figure 2-4B). GUS staining was undetectable in the delveoping pollen and mature pollen grains after 3-hour GUS assay. However, after the incubation time was prolonged to 3 days, GUS activity was detected in the mature pollen grains (Figure 2.4D and E) and pollen tubes (Figure 2.4E and F).

After 1-day GUS assay, the expression of *RLK C*::GUS was detected early in the styles and ovaries of stage 10 flowers. GUS signal was barely visible in the stigmatic papillaes and transmitting tracts of the ovaries at any developmental stages of flower (Figure 2-5B). Upon pollination (flower stage 13), the pistils showed GUS activity in the styles and the ovaries (Figure 2.4B). GUS expression was also detected in mature embryo sac (Figure 2.4C). After 3-hour GUS assay, the GUS expression could be observed at the egg apparatus. After fertilization, GUS signal was visible at the stigmatic cells and the abscission zone of the developing siliques (Figure 2.5A). GUS activity was barely visible in young embryo (Figure 2.5B). In mature siliques, the expression was undetectable in the seeds and silique wall (Figure 2.5C).

***rlk c* Showed Defects in Pollination and Seed Production**

The genomic structure of *RLK C* was shown in Figure 2.2B. To study the functions of LRR-RLK C gene (At4g23740) in *Arabidopsis*, a T-DNA insertion allele (SALK_005132) was obtained from ABRC (Alonso et al., 2003). The T-DNA insertion site for *RLK C* was also shown in Figure 2.2B. The *rlk c* allele has a T-DNA insertion located on the first exon of *RLK C*. To investigate the functions of *RLK C* during the

reproductive stage, the homozygous line was used to determine gene expression level by RT-PCR from the open flowers. The analysis revealed that the transcript level of *RLK C* was undetectable using gene-specific primers sets (Figure 2.2C).

To determine whether loss of *RLK C* activity can alter reproduction in *rlk c*, analysis of seed production was performed. The data indicated a significant decrease of seed production for self-pollinated *rlk c* (Figure. 2.6B). The unfertilized ovules dispersed randomly from the top to the bottom of the silique. The average seed number per a silique in *rlk c* was 44.46 ± 3.62 (n = 50; $P < 0.01$; Figure 2.6G), which is statistically different compared with wild-type (52.9 ± 4.53; n = 52; Figure 2.6A). No aborted seeds were observed in the siliques, suggesting that the embryogenesis is normal. To examine further that pollination process also affect in *rlk c*, i*n vivo* aniline blue staining was performed. The results showed normal pollen tube growth toward the base of the pistil in self-pollinated *rlk c* (Figure 2.6D). In addition, mutant pollen tubes could grow to the bottom of the pistil at a normal growth rate as compared to wild-type, approximately 16-18 hours after pollination. By 18 hours after pollination, most of the pollen tubes could reach the bottom of the pistil and enter the embryo sac. The result revealed a significant decrease of correct pollen tube guidance in the *rlk c* mutant (87.84 ± 8.63; n = 1,044; $P < 0.01$; Figure 2.6E and H), compared with wild-type plant in which 97.18% ± 1.72 of ovules recruited the pollen tubes (n = 1,062; Figure 2.6C and E). The *rlk c* pollen tubes could grow normally in the transmitting tracts; however, some did not make a turn toward the funiculus of the ovules (Figure 2.6F). This suggests that the decrease of correct tube guidance leads to a decrease seed production in *rlk c*. To investigate double fertilization

in *rlk c*, the pistils were self-pollinated and harvested after manual pollination for 3 days. In wild-type, most ovules were successfully fertilized, indicated by the formation of developing embryo and endosperm (93.98% ± 3.23%; n = 548; Figure 2.7A and B). Quantification of the results showed a significant decrease of fertilized ovules in *rlk c* plants (82.08% ± 13.31%; n = 703; $P < 0.01$; Figure 2.7D). Some ovules were unfertilized as shown in Figure 2.7C. The percentage of fertilized ovules was comparable to that of correct pollen tube attraction. Based on embryogenesis study, after fertilization, the *rlk c* embryos normally developed (Figure 2.7H-F). Taken together, this suggests that the decrease of fertilization was due to problem in pollen tube attraction.

Defects in Female and Male Gametes Contributed to Seed Set Phenotype in *rlk c*

(A) Transmission Through Female and Male gametes is Affected in *rlk c*

To determine the efficiency of gene transmission in the *rlk c* mutant, reciprocal crosses between *rlk c* $^{(+/-)}$ and wild-type and segregation analysis were carried out. The F1 progeny were scored for Kanamycin-resistant to Kanamycin-sensitive seedlings. The result revealed the ratio of 0.61:1 (n = 739) when wild-type pollen grains pollinated on the *rlk c* $^{(+/rlk\ c)}$ pistils (Table 2.1). By contrast, when *rlk c* $^{(+/rlk\ c)}$ pollen grains pollinated on wild-type pistils, the ratio of 0.88:1 (n = 1,176) was revealed. Both ratios were distorted from the expected ratio of 1:1, suggesting that the T-DNA insertion inactivates *RLK C*, which is partially required for both female and male gametes. Thus, the T-DNA is partially transmitted to the progeny.

(B) *rlk c* Displayed Abnormal Pollen Tube Guidance

To explain the effect of loss-of-function mutation on pollination and fertilization, reciprocal cross was performed between *rlk c*$^{(rlk\ c/rlk\ c)}$ and wild-type plants. The pollinated pistils were stained with aniline blue to determine *in vivo* pollen tube behavior. In self-pollinated wild-type pistils, pollen tube guidance was normal. The percentage of the correct guidance in self-pollinated wild-type was 98.11% ± 1.12% (n = 1,062). Reciprocal analysis revealed significant decrease of correct pollen tube attraction when *rlk c* acted as pollen (92.66% ± 3.24%; n = 1,044; $P < 0.01$) and pistil donor (90.83% ± 4.26%; n = 436; $P < 0.01$; Figure 2.8B). This suggests that both female and male gametophytes partially contribute to defect in pollen tube guidance in *rlk c*.

(C) Pollen Fertility is Not Altered in *rlk c*

rlk c anthers appeared to develop normally as compared to wild-type anthers. Pollen viability of *rlk c* was assessed by fluorescein diacetate (FDA) (Figure 2.9B). The result showed that 83.01% ± 1.18% (n = 924; Figure 2.9E) of *rlk c* pollen grains was viable, compared with pollen grains from wild-type plants (90.44% ± 6.20%; n = 1,705; $P < 0.05$; Figure 2.9A). Similat to wild-type pollen, all *rlk c* pollen carries 3 normal nuclei: 2 sperm nuclei amd 1 vegetative nucleus, indicating normal pollen development (Figure 2.9D). In order to examine the percentage of pollen germination in *rlk c*, *in vitro* germination test was performed in comparison to wild-type pollen. The result revealed normal pollen germination in *rlk c* (73.35% ± 5.00%; n = 1,441; $P < 0.05$) and wild-type (74.62% ± 5.35%; n = 2,116; Figure 2.9F). This data supports that pollen development and fertility of *rlk c* are normal.

rlk c Displayed Normal Development of the Ovule

To confirm that the pollen attraction defect is not caused by aberrant ovule development, the whole-mount of various developmental stages of *rlk c* ovules were prepared. The result revealed normal ovule morphology in *rlk c* (Figure 2.10B, D, F and H). Similar to wild-type, the initiation and patterning of young ovule appeared normal. The ovule primordia were initiated from the placental wall (stage 1; Figure 2.10B). Subsequently, the primordium differentiates into a finger-like structure at flower stage 10. The integument was developed from the chalaza and grew toward the nucellus (stage 2; Figure 2.10D). The inner integument of the ovule is first formed in flower stage 11. Shortly, the outer integument is initiated close to the inner integument. In the next stage, the whole ovule expands, the funiculus elongates and the integuments surround the nucellus at stage 13. At stage 3, the megaspore mother cell (MMC) undergoes meiosis to give rise to four megaspores. The surviving megaspore in each developing ovule underwent megagametogenesis to produce the female gametophyte (Figure 2.10F). Until stage 4, the mature ovule containing the embryo sac was normally developed (Figure 2.10H). This suggests normal development of female sporophytic tissues in *rlk c*.

RLK C Affects Synergid and Egg Specifications

It is possible that the female gametophyte of *rlk c* was abnormal, resulting in a reduction of correct pollen tube guidance. To investigate whether cell specification is affected in the *rlk c* female gametophyte, the expressions of two cell-typed specific GUS markers were analyzed. We introduced ET1119 (an egg cell marker; Figure 2.11A) and ET884 (a synergid marker; Figure 2.11C) into the *rlk c* plants. The expressions of each

marker line were investigated in F2 progeny. Analysis of ET119 and ET884 expression in F2 plants showed decrease number of ovules expressing GUS. In wild-type, the percentages of female gametophytes without ET1119 and ET884 expression were 3.05% ± 2.00% (n = 98) and 4.20% ± 4.36% (n = 131), respectively. By contrast, the percentages of female gametophytes without ET1119 and ET884 expression in *rlk c* were 24.2% ± 4.49% (n = 219; $P < 0.01$; Figure 2.13E) and 19.40% ± 4.30% (n = 134; $P < 0.01$; Figure 2.13F). The alterations of egg and synergid are likely due to defect in cell specification. This abnormal embryo sac with the loss of synergid and egg cell identity can cuase an abberrent pollen tube guidance in *rlk c* plant.

RLK C Rescues the *rlk c* Mutant Phenotype

To determine whether the gametophytic defects in *rlk c* were caused by the loss of *RLK C* activity, the complementation experiment was performed. A complementation construct was created to introduce a binary vector carrying the genomic region of wild-type *RLK C* including the endogenous promoter (1,200bp upstream of the translational start site) and the complete genomic coding region into the *rlk c* mutant background. The transgenic plants in T1 generation were tested for a presence of both complemented construct and the *rlk c* allele. T3 transformants were used to determine the *RLK C* level and to examine reproductive phenotypes, including seed production, pollen viability and pollen tube attraction (Figure 2.12). The result showed that the complemented *rlk c* plants restored *RLK C* transcript level and mutant phenotypes (Figure 2.12H), suggesting that RLK C was expressed. The complemented *rlk c* plants carrying the complementation construct displayed normal seed production and pollen viability (Figure 2.12A and C). In

both wild-type and complemented *rlk c* plants, the mature pollen grains were intacted and viable, indicating normal pollen fertility (Figure 2.12C and D). In the complemented *rlk c* plant, pollen tubes grew normally in the female tissues from transmitting tracts toward the funiculus and entered the embryo sac (Figure 2.12E and F). The percentage of correct pollen attraction in self-pollinated wild-type and the complemented plants were 97.18 ± 1.72% (n = 1,504) and 97.61 ± 1.92% (n = 3,404), respectively. The data was not significantly different from that of wild-type plants (Figure 2.12G). In addition, most ovules from the *rlk c* mutant carrying *RLK C* were able to recruit the pollen tubes. This data suggested that pollen viability and pollination phenotypes caused by loss of *RLK C* function was successfully complemented by the introduction of *RLK C* under control of the native promoter.

To confirm that fertilization process in complemented plants is rescued by the complementation construct, analysis of fertilization was performed. The result indicated that double fertilization in transgenic plants expressing *RLK C* was normal, as compared with wild-type (Figure 2.12I). Most ovules were fertilized, indicated by the formation of developing embryo and endosperm. The percentage of fertilized ovules in the complemented line was 93.80% ± 5.43% (n = 1,178). This data was not statistically different compared with wild-type, in which 93.98% ± 3.23% (n = 548) of ovules were fertilized. Analysis of silique in the complemented plants also confirmed that pollination and fertilization were normal. The abortion of seeds caused by unfertilization and embryogenesis defect were not observed (Figure 2.12A). The average seed number per a silique in wild-type, complemented line and *rlk c* were 49.33 ± 4.96 (n = 60), 48.64 ±

2.90 (n = 64) and 44.0 ± 3.62 (n = 50), respectively (Figure 2.12B). Taken together, defects in sexual reproduction, such as decreases of seed production, pollen fertility, pollen tube growth and guidance, in the *rlk c* mutant were rescued by complementation with *RLK C*. This suggests that defects in sexual reproduction were due to the loss of *RLK C* activity.

DISCUSSION

LRR-RLK C Plays an Essential Role in Pollen Tube Attraction

In this study, the characterization of the *rlk c* mutant was described. We demonstrate that the RLK C signaling pathway is required for female gametophytic development resulting in correct pollen tube attraction in *Arabidopsis thaliana*. RLK C belongs to LRR III-type of the LRR-RLK subfamily. Among 47 members in LRR III, none have a known function in reproduction. The loss-of-function mutant of *RLK C* exhibited a slightly decrease of fertilized ovules. Some ovules remained untargeted by the pollen tubes, indicating a subtle defect in pollen tube guidance, as shown in *in vivo* aniline blue staining (Figure 2.6D). As a result, some pollen tubes did not enter the embryo sac and seed production was decreased. However, pollen tube growth and guidance were normal on the transmitting tracts of style and ovary. According to gene transmission analysis, both female and male transmission efficiencies were distorted in the *rlk c* mutant (Table 2.1), indicating defects in both female and male gametophytes.

To determine whether pollen tube guidance defect is contributed by female or male gametophytes, reciprocal crosses and *in vivo* aniline blue staining was performed. The analysis showed that the guidance phenotype could not be observed when the *rlk c*

pollen grains were pollinated on wild-type pistil. The *rlk c* pollen tubes were able to target to wild-type ovules and consequently fertilize the female gametophytes suggesting normal pollen tube attraction and fertilization. In addition, pollen development and pollen tube growth appeared normal through wild-type pistils. Although male transmission efficiency was slightly reduced, defect in the male gametophyte was not observed in the *rlk c* mutant. It is likely that the RLK C signaling pathway requires other players to mediate the male gametophyte. Interestingly, when wild-type pollen grains were pollinated the *rlk c* pistils, the average number of untargeted ovules was slightly increased, indicating subtle guidance defect from the female gametophyte consisting with the partial distortion of the female transmission. Using the transgenic reporter *Arabidopsis* plants expressing the β-glucuronidase (GUS) gene under the control of *RLK C* promoter revealed that *RLK C* promoter activity was predominantly at the micropylar end of the unfertilized embryo sac (Figure 2.4C). However, after fertilization, GUS signal was barely visible in the young embryos and undetectable in the mature seeds. These suggest that the spatial expression of *RLK C* transcript is consistent with our proposed function of RLK C on pollen tube guidance. Lines of evidence show that the female gametophyte plays a crucial role in pollen tube growth to the female gametophyte (Higashiyama et al., 2001; Hulskamp et al., 1995b; Ray et al., 1997). It is most likely that the micropylar guidance cues are produced from the synergids (Higashiyama et al., 2001). To confirm that RLK C is involved in pollen tube attraction, a complementation construct carrying the genomic region of wild-type *RLK C* gene was introduced into the *rlk c* background. The analysis revealed that defects in seed production and pollen tube

guidance were rescued by this wild-type *RLK C* construct, suggesting that RLK C is required for pollen tube attraction. This study demonstrates that megagametogenesis of *rlk c* appears aberrant. In addition, the synergid and the egg are not specified in some embryo sacs (Figure 2.11D and F), suggesting that the cell identity of the synergid and egg in the *rlk c* female gametophyte were altered.

Here, we propose that the RLK C signaling pathway is required for female gametophytic development resulting in accurate pollen tube guidance and seed formation in *Arabidopsis thaliana*. However, RLK C is expressed throughout the vegetative tissues, such as secondary root primordia and leaves (Figure2.3). It is possible that function of RLK C is not restricted to the reproductive stage. To understand the RLK C signaling pathway, more studies will be useful. It is important to confirm the localization of RLK C to clarify subcellular roles of RLK C in the female gametophyte and the synergids. To investigate the activity of the kinase domain of RLK C, kinase assay should be performed to verify the phosphorylation.

REFERENCES

Benschop, J.J., Mohammed, S., O'Flaherty, M., Heck, A.J.R., Slijper, M. and Menke, F.L.H. (2007). Quantitative phosphoproteomics of early elicitor signaling in Arabidopsis. Molecular Cell Proteomics, 6: 1198–1214.

Braun D.M., Walker, J.C. (1996). Plant transmembrane receptors: new pieces in the signaling puzzle. Trends in Biochemical Sciences, 21: 70-73.

Clark, S.E., Williams, R.W., and Meyerowitz, E.M. (1997). The *CLAVATA1* gene encodes a putative receptor kinase that controls shoot and floral meristem size in Arabidopsis. Cell, 89: 575-585.

Dievart, A., and Clark, S.E. (2004). LRR-containing receptors regulating plant development and defense. Development, 131: 251-261.

Fujita, H., Takemura, M., Tani, E., Nemoto, K., Yokota, A. and Kohchi, T. (2003). An *Arabidopsis* MADS-box protein, AGL24, is specifically bound to and phosphorylated by meristematic receptor-like kinase (MRLK). Plant Cell Physiology, 44: 735–742.

Heslop-Harrison, J. and Heslop-Harrison, Y. (1970). Evaluation of pollen viability by enzymatically induced fluorescence; intracellular hydrolysis of fluorescein diacetate. Stain Technology, 45: 115-120.

Higashiyama, T., Yabe, S., Sasaki, N., Nishimura, Y., Miyagishima, S., Kuroiwa, H., Kuroiwa, T. (2001). Pollen tube attraction by the synergid cell. Science, 293: 1480-1483.

Hord, C.L.H., Chen, C., DeYoung, B.J., Clark, S.E., and Ma, H. (2006). The BAM1/BAM2 receptor-like kinases are important regulators of Arabidopsis early anther development. Plant Cell, 18: 1667–1680.

Hove, (2011). Probing the roles of LRR RLK genes in *Arabidopsis thaliana* roots using a custom T-DNA insertion set.

Jinn, T.-L., Stone, J.M. and Walker, J.C. (2000). HAESA, an Arabidopsis leucine-rich repeat receptor kinase, controls floral organ abscission. Genes Development, 14: 108-117.

Kajava, A.V. and Kobe, B. (2002). Assessment of the ability to model proteins with leucine-rich repeats in light of the latest structural information. Protein Sciences, 11: 1082–1090.

Lee, Y., Kim E.-S., Choi, Y., Hwang, I., Staiger, C.J., Chung, Y.Y. and Lee, Y. (2008). The Arabidopsis phosphatidylinositol 3-Kinase is important for pollen development. Plant Physiology, 147: 1886-1897.

Li, J.M., and Chory, J. (1997). A putative leucine-rich repeat receptor kinase involved in brassinosteroid signal transduction. Cell, 90: 929–938.

Lord E.M. and Russell S.D., (2002). The mechanisms of pollination and fertilization in plants. Annual Review of Cell and Developmental Biology, 18: 81–105.

Mori, T., Kuroiwa, H., Higashiyama, T., and Kuroiwa, T. (2006). Generative Cell Specific 1 is essential for angiosperm fertilization. Nature Cell Biology, 8: 64-71.
Ray S., Park S.S., Ray A. (1997). Pollen tube guidance by the female gametophyte. Development, 124: 2489-2498.

Shiu, S.-H., and Bleecker, A.B. (2001a). Plant receptor-like kinase gene family: Diversity, function and signaling. Science STKE, re22.

Shiu, S.-H., and Bleecker, A.B. (2001b). Receptor-like kinases from Arabidopsis form a monophyletic gene family related to animal receptor kinases. Proceeding of the National Academy of Science U.S.A., 98: 10763-10768.

Shpak, E.D., Lakeman, M.B. and Torii, K.U. (2003). Dominant-negative receptor uncovers redundancy in the Arabidopsis ERECTA leucine-rich repeat receptor-like kinase signaling pathway that regulates organ shape. Plant Cell, 15: 1095-1110.

Tarutani, Y., Morimoto, T., Sasaki, A., Yasuda, M., Nakashita, H., Yoshida, S., Yamaguchi, I., Suzuki, Y. (2004). Molecular characterization of two highly homologous receptor-like kinase genes, RLK902 and RKL1, in *Arabidopsis thaliana*. Bioscience, Biotechnology and Biochemistry, 68: 1935–1941.

Thompson, J.D., Higgins, D.G., Gibson, T.J. (1994). CLUSTAL W: improving the sensitivity of progressive multiple sequence alignment through sequence weighting, position specific gap penalties and weight matrix choice. Nucleic Acids Research, 22: 4673-4680.

Valon, C., Smalle, J., Goodman, H.M., Giraudat, J. (1993). Characterization of an *Arabidopsis thaliana* gene (TMKL1) encoding a putative transmembrane protein with an unusual kinase-like domain. Plant Molecular Biology, 23: 415-421.

Vielle-Calzada, J.-P., Baskar, R., and Grossniklaus, U. (2000). Delayed activation of the paternal genome during seed development. Nature, 404: 91-94.

Figure 2.1 Distance mapping tree of the extracellular domain of receptor-like kinases expressed in *Arabidopsis thaliana* pollen. (A) Amino acid sequences of 180 RLKs expressed in pollen were aligned and analyzed using default parameters of ClustalW (Thompson et al., 1994). (B) A partial map for 3 LRR-RLKs used in further study.

Figure 2.1

A

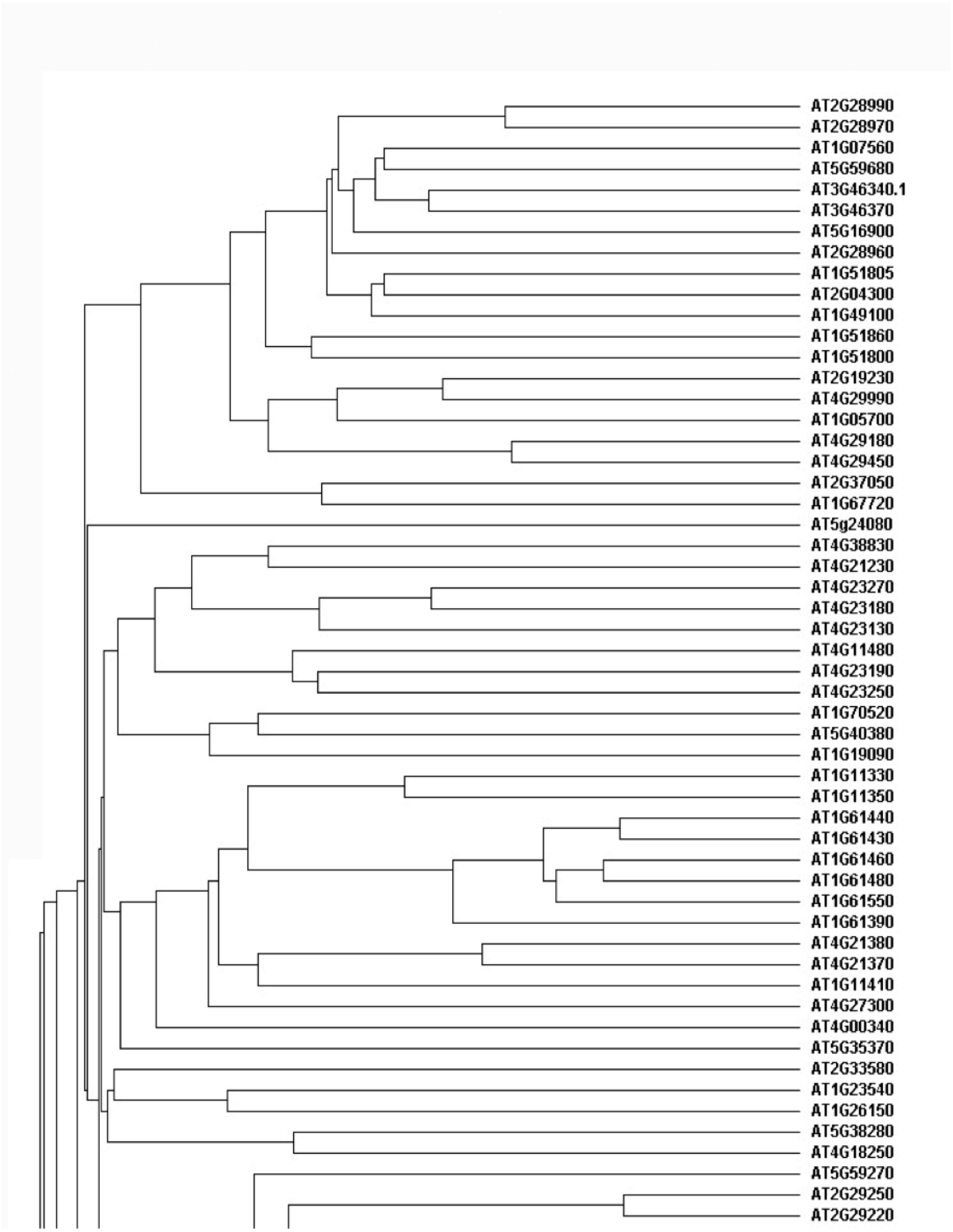
AT2G28990
AT2G28970
AT1G07560
AT5G59680
AT3G46340.1
AT3G46370
AT5G16900
AT2G28960
AT1G51805
AT2G04300
AT1G49100
AT1G51860
AT1G51800
AT2G19230
AT4G29990
AT1G05700
AT4G29180
AT4G29450
AT2G37050
AT1G67720
AT5g24080
AT4G38830
AT4G21230
AT4G23270
AT4G23180
AT4G23130
AT4G11480
AT4G23190
AT4G23250
AT1G70520
AT5G40380
AT1G19090
AT1G11330
AT1G11350
AT1G61440
AT1G61430
AT1G61460
AT1G61480
AT1G61550
AT1G61390
AT4G21380
AT4G21370
AT1G11410
AT4G27300
AT4G00340
AT5G35370
AT2G33580
AT1G23540
AT1G26150
AT5G38280
AT4G18250
AT5G59270
AT2G29250
AT2G29220

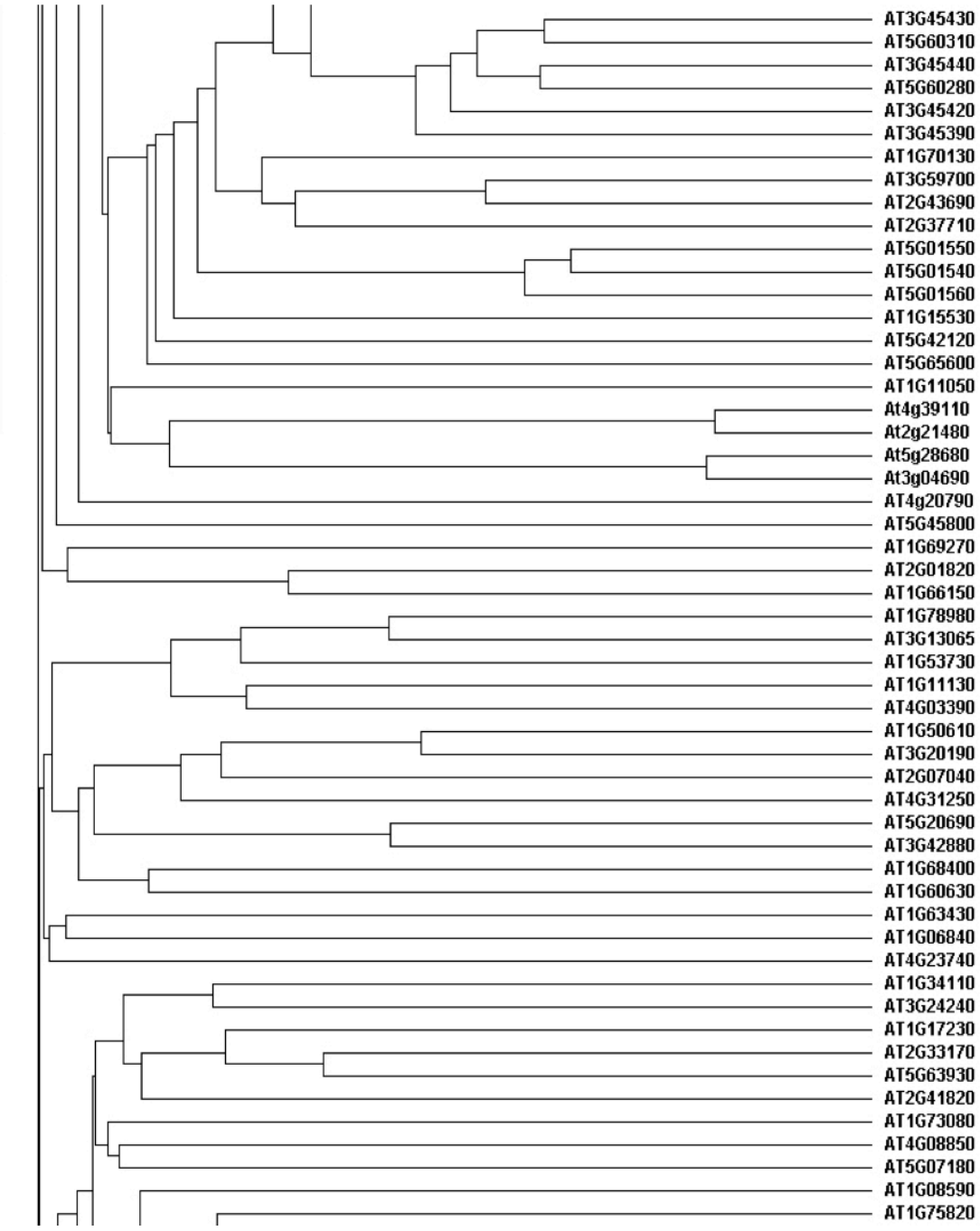
AT3G45430
AT5G60310
AT3G45440
AT5G60280
AT3G45420
AT3G45390
AT1G70130
AT3G59700
AT2G43690
AT2G37710
AT5G01550
AT5G01540
AT5G01560
AT1G15530
AT5G42120
AT5G65600
AT1G11050
At4g39110
At2g21480
At5g28680
At3g04690
AT4g20790
AT5G45800
AT1G69270
AT2G01820
AT1G66150
AT1G78980
AT3G13065
AT1G53730
AT1G11130
AT4G03390
AT1G50610
AT3G20190
AT2G07040
AT4G31250
AT5G20690
AT3G42880
AT1G68400
AT1G60630
AT1G63430
AT1G06840
AT4G23740
AT1G34110
AT3G24240
AT1G17230
AT2G33170
AT5G63930
AT2G41820
AT1G73080
AT4G08850
AT5G07180
AT1G08590
AT1G75820

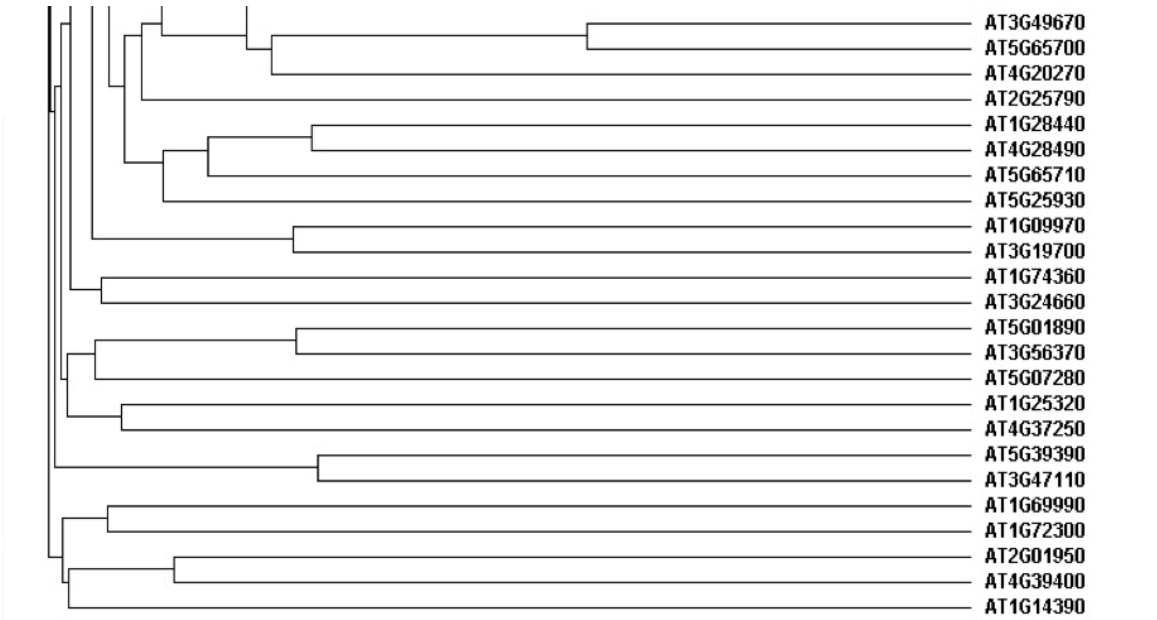
AT3G49670
AT5G65700
AT4G20270
AT2G25790
AT1G28440
AT4G28490
AT5G65710
AT5G25930
AT1G09970
AT3G19700
AT1G74360
AT3G24660
AT5G01890
AT3G56370
AT5G07280
AT1G25320
AT4G37250
AT5G39390
AT3G47110
AT1G69990
AT1G72300
AT2G01950
AT4G39400
AT1G14390

B

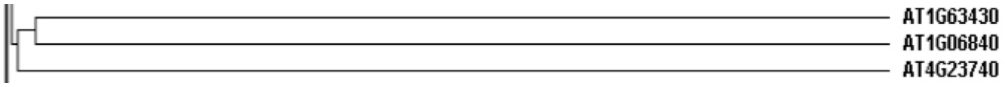
AT1G63430
AT1G06840
AT4G23740

Figure 2.2 *RLK C* transcript levels in various tissues and gene structure of a T-DNA insertion allele of LRR-RLK C. (A) Tissue-specific expression of Arabidopsis *RLK C* revealed by semi-quantitative RT-PCR. *ACTIN3*, Actin gene-specific primer set was used for PCR as the control. (B) Genomic structure of *rlk c* (SALK_005132) showing T-DNA insertion site in the first exon of *RLK C*. Exons are represented by black boxes and introns by lines. (C) RT-PCR analysis of Arabidopsis *RLK C* transcript levels in wild-type and *rlk c* using RLK C gene-specific primer set. *ACTIN3*, Actin gene-specific primer set was used for PCR as the control.

Figure 2.2

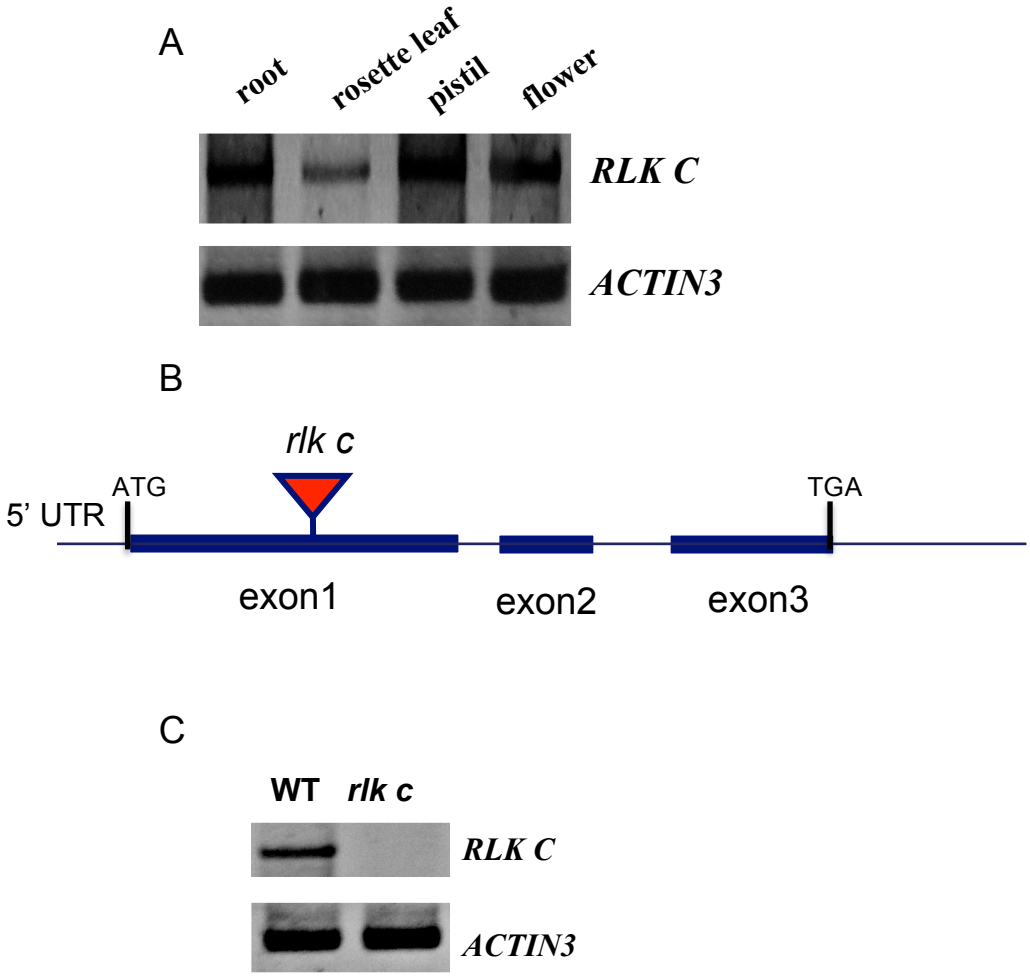
A
root
rosette leaf
pistil
flower
RLK C
ACTIN3
B
rlk c
ATG
TGA
5' UTR
exon1
exon2
exon3
C
WT
rlk c
RLK C
ACTIN3

Figure 2.3 Promoter-GUS Analysis of *RLK C* in vegetative tissues. GUS expression was driven by *RLK C* promoter. (A) GUS expression was detected in 5-day-old seedling grown on MS medium. (B) GUS expression was detected at the root tips. (C) GUS expression was found in the primary root. (D) An enlarged view of C (red box) showing that GUS was expressed in the meristematic region, the stele, the vascular tissues and the pericycle. (E) GUS expression was detected in the secondary root primordia. (F) GUS was expressed in the later stage of secondary root formation. (G) Strong GUS expression was observed at the margin of the rosette leaf and hydrathodes (red box). (H) GUS expression was detected at the base of the cauline leaf. (I) GUS was expressed in the veins and the trichomes. (J) An enlarged view of I (red box) showing GUS expression in a trichome.

Figure 2.3

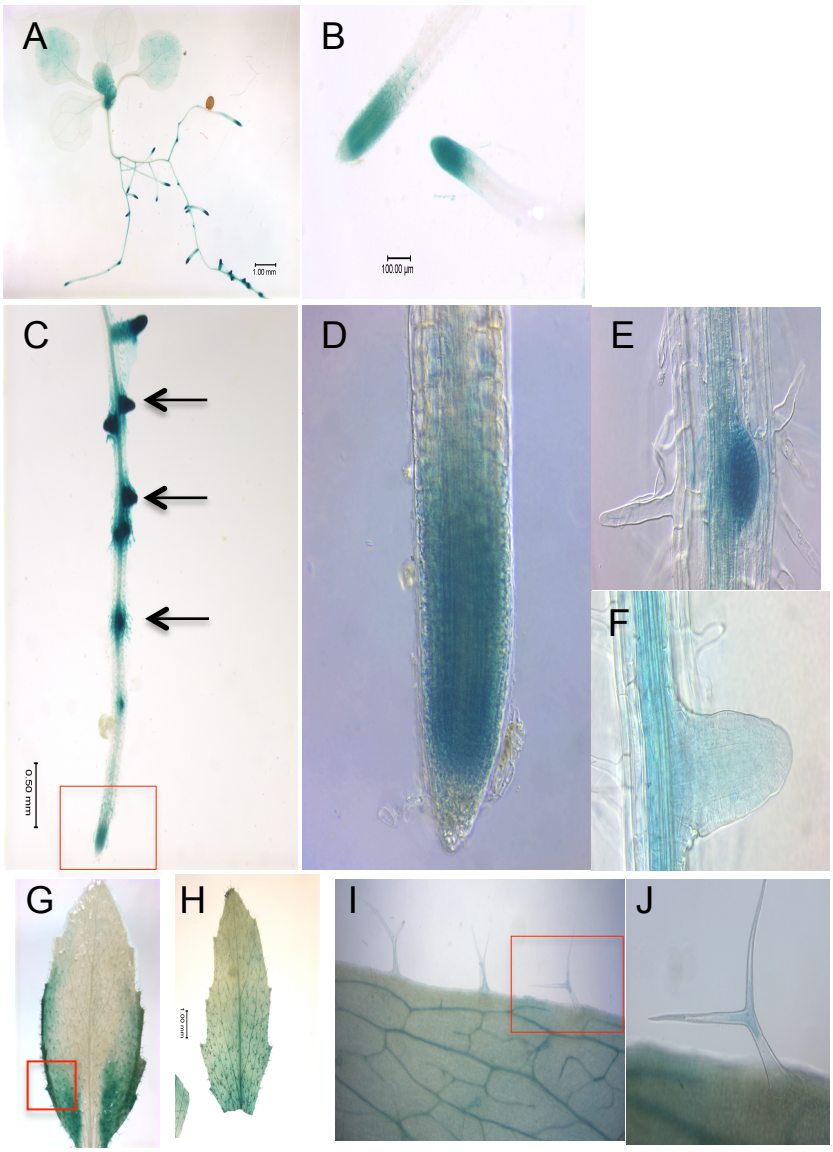

Figure 2.4 Promoter-GUS Analysis of *RLK C* in reproductive tissues. (A) GUS expression was detected in the inflorescence. (B) GUS was expressed in open flower. GUS expression was detectable in the pistil (style and ovary) and anther filaments. (C) Strong GUS expression was observed in the synergids of the mature embryo sac. (D) GUS expression was in the pollen grains after 3-day assay. (E) GUS expression was in pollen grain and tube. (F) GUS activity was detected in pollen tube at the micropyle of the ovules. Abbreviation, s, stigma; st, style; an, anther; fi, anther filament

Figure 2.4

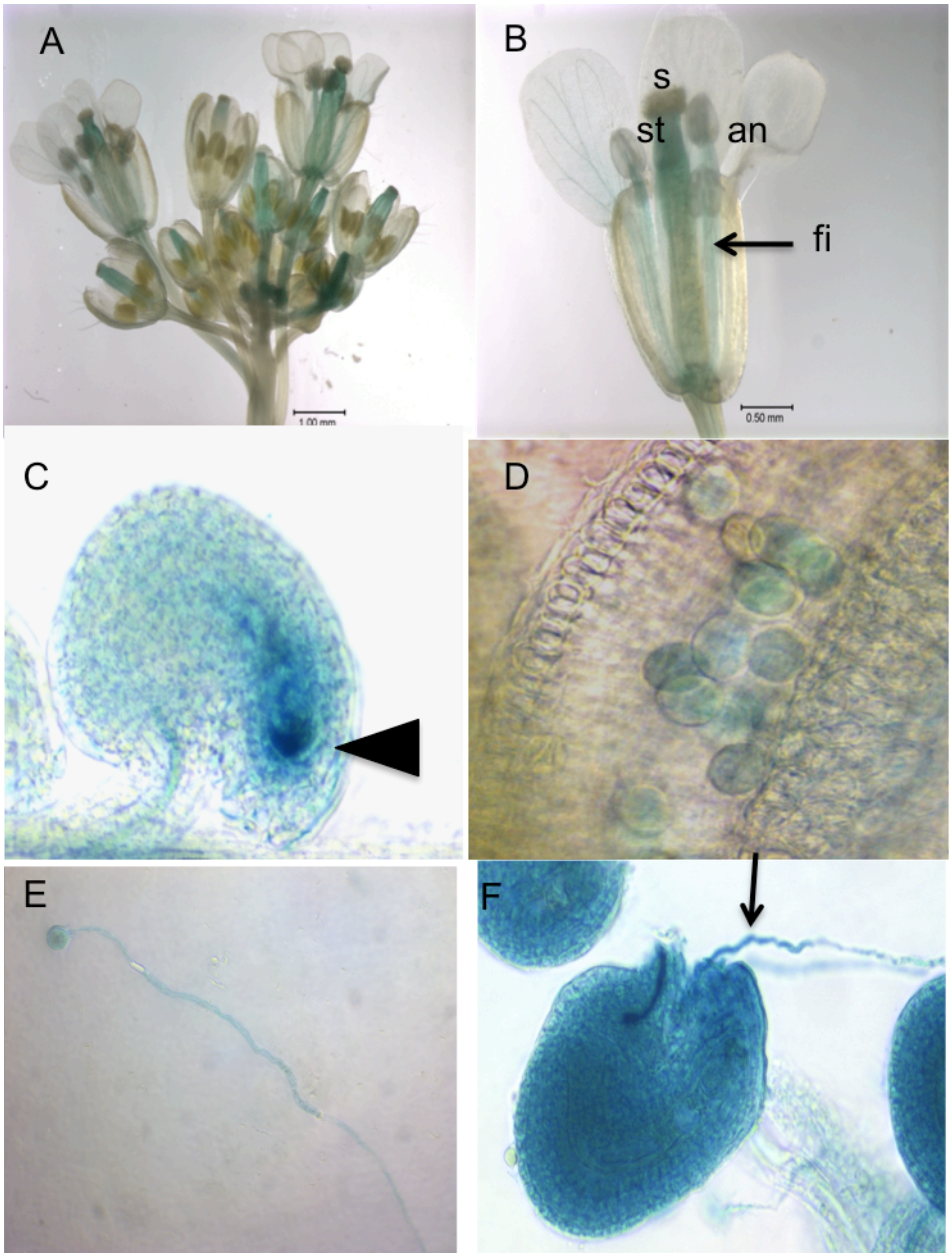

Figure 2.5 Promoter-GUS Analysis of *RLK C* in siliques. (A) GUS expression was detected in different developmental stages of siliques after fertilization. (B) Very weak GUS signal was visible in young developing seed (2 days after fertilization). (C) GUS activity was undetectable in developing seeds (7 days after fertilization).

Figure 2.5

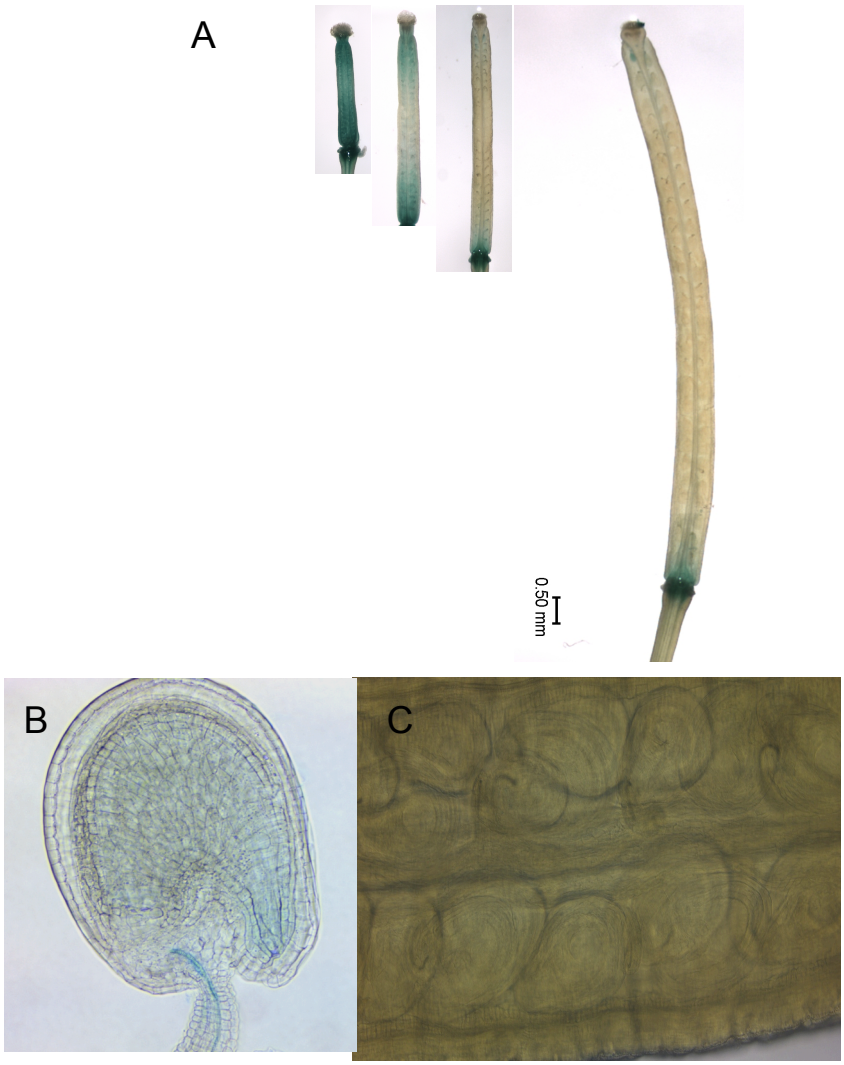

Figure 2.6 Defects in seed production and *in vivo* pollination of *rlk c.* Siliques of wild-type (A) and *rlk c* (B) were dissected to examine the average number of seed per a silique. Arrows indicate gaps found in the *rlk c* silique. (C and D) Pollen tube growth was examined by aniline blue staining in wild-type (C) and *rlk c* (D) pistils. s, stigma; st, style; o, ovule. (E) Quantitative analysis of seed production in wild-type and *rlk c*. The number of seed per a silique was count. (F) Quantitative analysis of *in vivo* pollen tube guidance in wild-type and *rlk c* after aniline blue staining. The number of ovules receiving pollen tube (correct guidance) was counted and shown in a percentage (± S.D.).

Figure 2.6

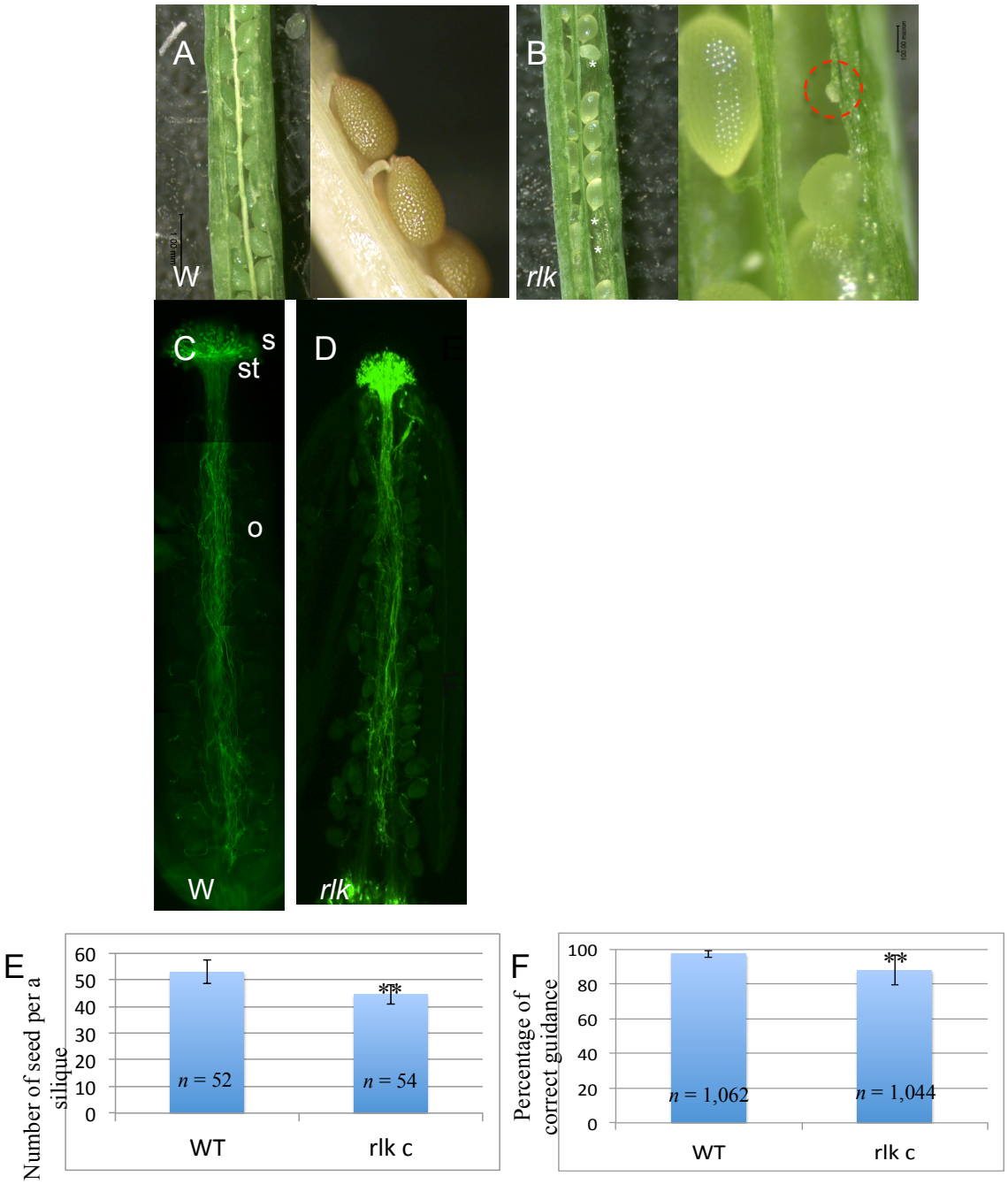
A
W
B
rlk
C
s
st
o
W
D
rlk
E
Number of seed per a silique
60
50
40
30
20
10
0
n = 52
n = 54
**
WT
rlk c
F
Percentage of correct guidance
100
80
60
40
20
0
n = 1,062
n = 1,044
**
WT
rlk c

Figure 2.7 Analysis of fertilization and early embryogenesis in *rlk c.* (A) Analysis of fertilization was performed at 3 days after pollination. Pistils were dissected and cleared to examine the fertilized ovules (arrow). (B) The formation of young embryo (star) and endosperm (arrow) after double fertilization. (C) Unfertilized ovule found in the *rlk c* pistil. No sign of fertilization was observed. Black arrow represents the central cell. White arrow represents egg cell. (D) Quantitative analysis of fertilization in wild-type and *rlk c*. The number of fertilized ovules was counted and shown in the percentage (± S.D.). (E-G) Early embryogenesis analysis of *rlk c*. Stars indicate embryos. (E) Octant embryo. (F) Heart-shaped embryo. (G) Torpedo embryo. (H) Aborted ovule was found in *rlk c* mature silique.

Figure 2.7

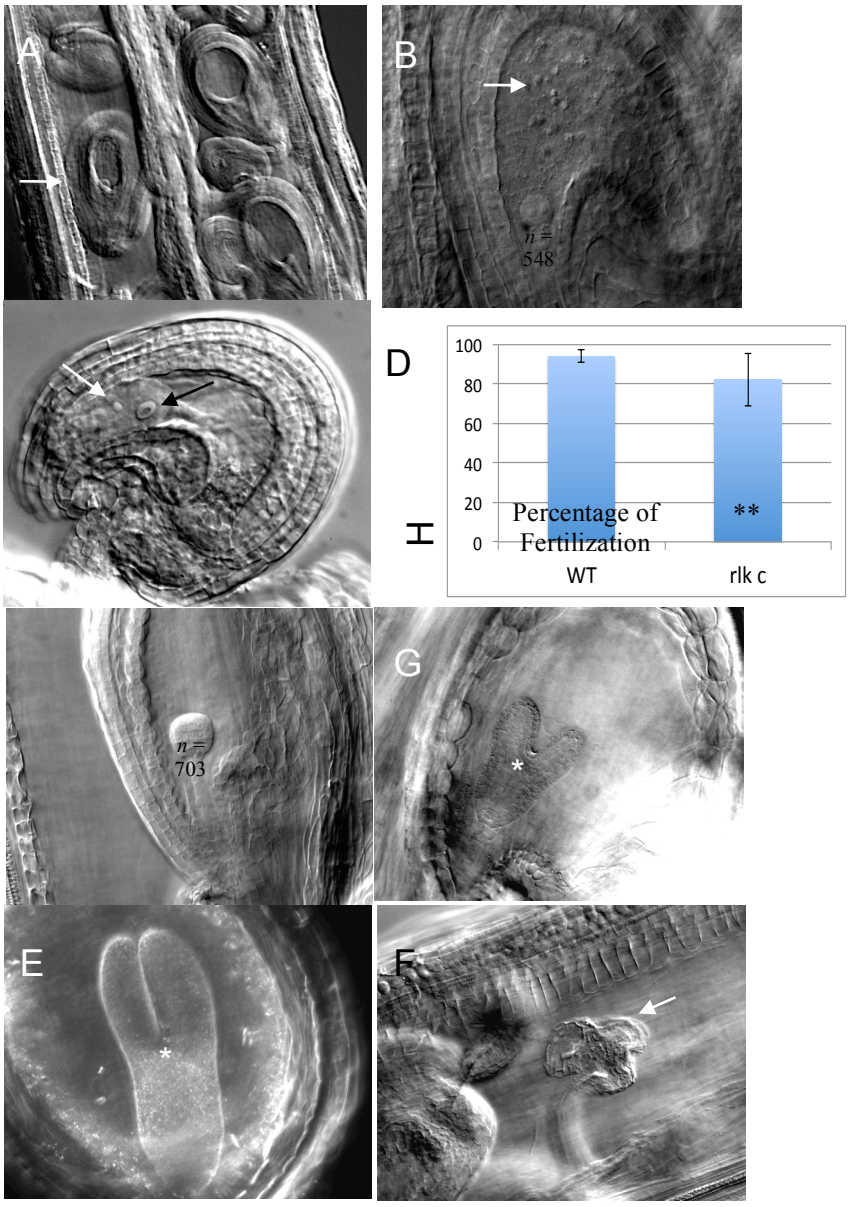
A
B
n = 548
D
100
80
60
40
20
0
Percentage of Fertilization
**
WT
rlk c
H
n = 703
G
*
E
*
F

Figure 2.8 *In vivo* reciprocal cross in pollination and fertilization of *rlk c*. (A, B and C) *In vivo* pollen tube growth was visualized by aniline blue staining in each cross. (D) Quantitative analysis of seed production in reciprocal cross. The number of seed per a silique was count in the mature silique. (E) Quantitative analysis of *in vivo* pollen tube guidance in reciprocal cross between wild-type and *rlk c* after aniline blue staining. The number of ovules receiving pollen tube (correct guidance) was counted and shown in a percentage (± S.D.).

Figure 2.8

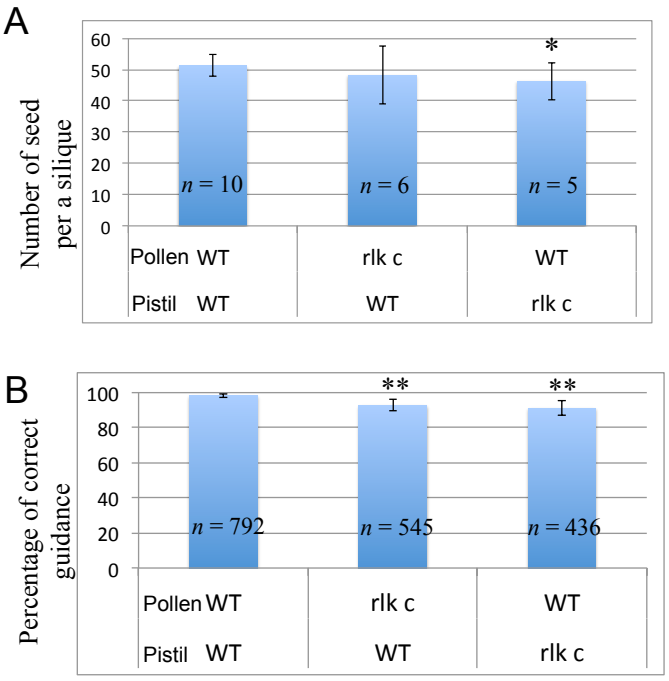
A
Number of seed per a silique
60
50
40
30
20
10
0
n = 10
n = 6
n = 5
*
Pollen WT
rlk c
WT
Pistil WT
WT
rlk c
B
Percentage of correct guidance
100
80
60
40
20
0
n = 792
n = 545
n = 436
**
**
Pollen WT
rlk c
WT
Pistil WT
WT
rlk c

Figure 2.9 Pollen viability and germination of *rlk c*. Fluorescence microscopy of FDA-stained pollen derived from wild-type (A) and *rlk c* (B) plants. FDA stains live pollen grains bright-green. (C and D) DAPI staining of wild-type pollen (C) and *rlk c* pollen (D). (E) Quantitative analysis of pollen viability in wild-type and *rlk c* after FDA staining. The number of viable pollen was counted and shown in a percentage (± S.D.). (F) Quantitative analysis of *in vitro* pollen germination in wild-type and *rlk c*. Pollen was grown on pollen growth media at 28 C for 4 hours. The number of germinated pollen was counted and shown in a percentage (± S.D.).

Figure 2.9

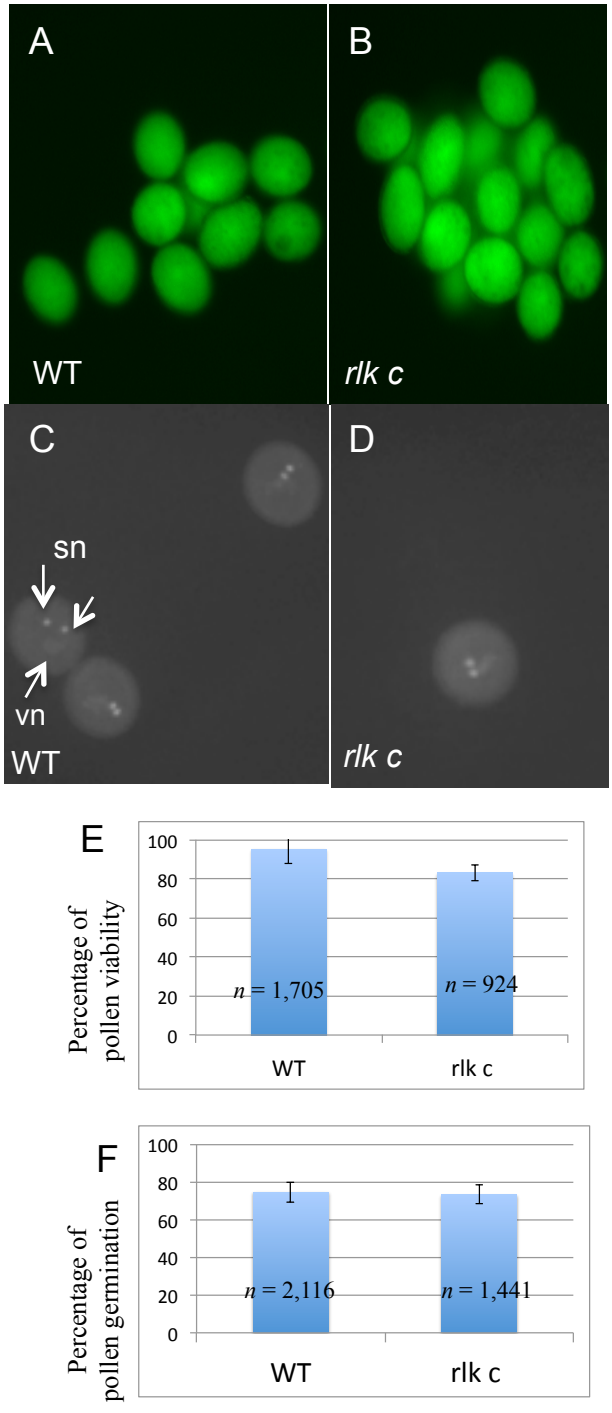
A
WT
B
rlk c
C
sn
vn
WT
D
rlk c
E
Percentage of pollen viability
100
80
60
40
20
0
n = 1,705
n = 924
WT
rlk c
F
Percentage of pollen germination
100
80
60
40
20
0
n = 2,116
n = 1,441
WT
rlk c

Figure 2.10 Ovule development of *rlk c*. Whole-mount pistils of wild-type (A,C,E and G) and *rlk c* (B, D, F and H) were prepared. Ovule primordia at stage 1 in wild-type (A) and *rlk c* (B). The integuments (i) were developed from the chalaza and grew toward the nucellus at stage 2 in wild-type (C) and *rlk c* (D). At stage 3, surviving megaspores were shown in wild-type (E) and *rlk c* (F). At stage 4, mature ovules containing the embryo sac were developed in wild-type (G) and rlk c (H). Abbreviations: fu, funiculus; i, integument.

Figure 2.10

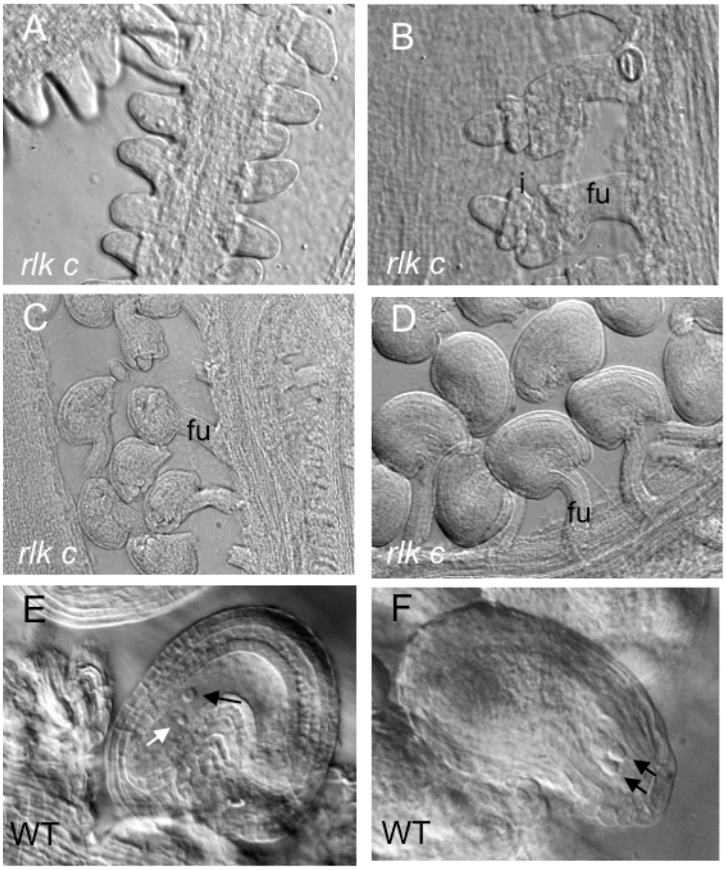

Figure 2.11 Cell specifications of *rlk c* female gametophyte. (A) Expression of the specific egg marker (ET1119) in a micropylar cell of wild-type embryo sac. (B) ET1119 was expressed in *rlk c* embryo sac. (C) Expression of the specific synergid marker (ET884) in two micropylar cells of wild-type embryo sac. (D) ET884 expression was undetectable in *rlk c* embryo sac, indicated by red stars. (E) Quantitative analysis of ovules showing ET884 expression in wild-type and *rlk c* embryo sac. Error bars indicate SD.

Figure 2.11

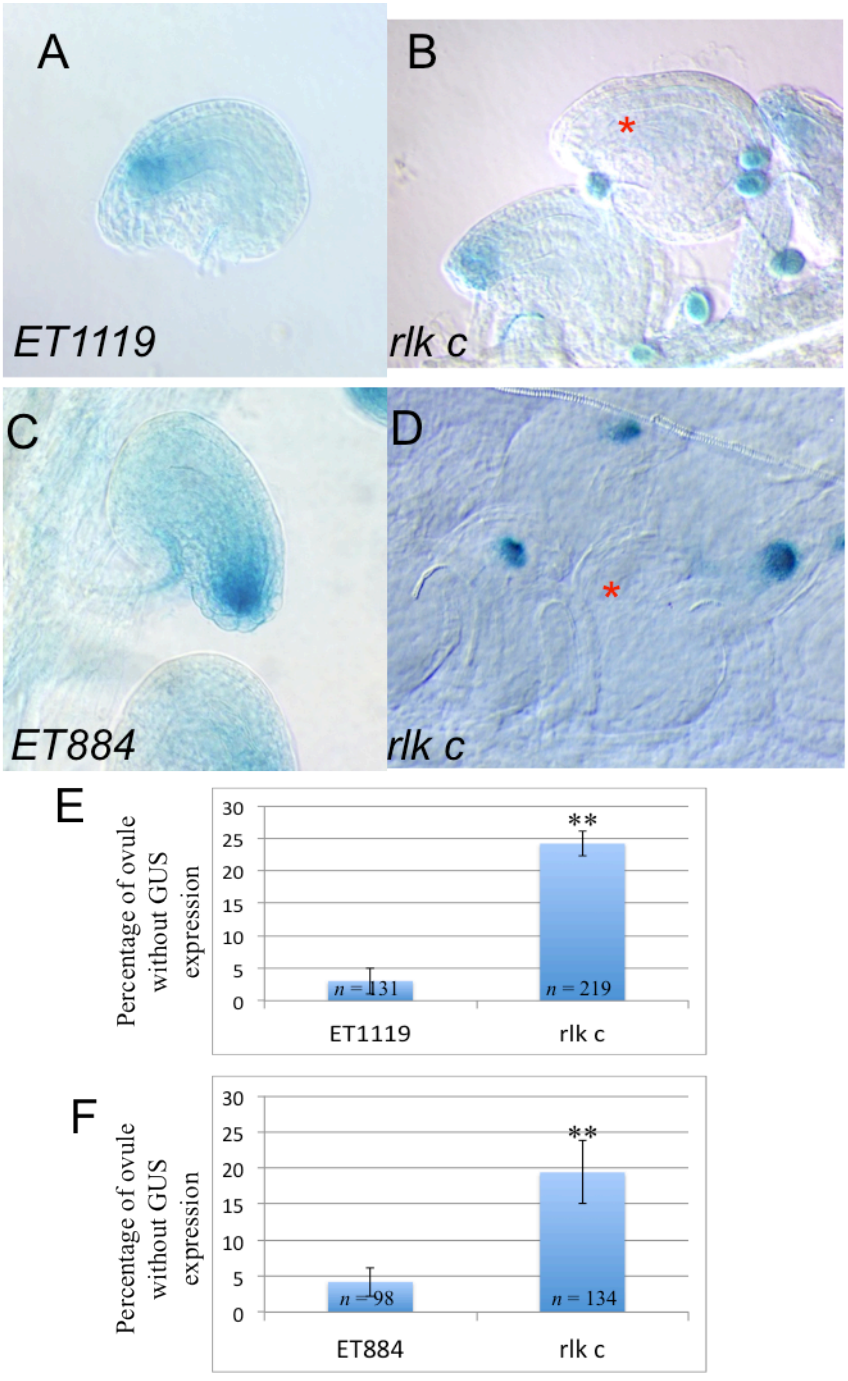
A
ET1119
B
rlk c
C
ET884
D
rlk c
E
Percentage of ovule without GUS expression
30
25
20
15
10
5
0
**
n = 131
n = 219
ET1119
rlk c
F
Percentage of ovule without GUS expression
30
25
20
15
10
5
0
**
n = 98
n = 134
ET884
rlk c

Figure 2.12. RLK C fully complements reproductive defects in *rlk c*. (A) Mature siliques of *rlk c* carrying a construct encoding wild-type RLK C. (B) Quantitative analysis of seed production in wild-type, *rlk c* and complemented line. The number of seed per a silique was count. (C) Normal pollen viability of complemented line after FDA staining. (D) Quantitative analysis of pollen viability in wild-type, *rlk c* and complemented line after FDA staining. The number of viable pollen was counted and shown in a percentage (± S.D.). (E and F) Pollen tube growth and guidance were examined in pistils of complemented line by aniline blue staining. No evidence of unfertilized ovules was observed. (G) Quantitative analysis of *in vivo* pollen tube guidance in wild-type, *rlk c* and complemented line. The number of ovules receiving pollen tube, indicating correct guidance was counted. (H) RT-PCR analysis of Arabidopsis *RLK C* transcript levels in wild-type, *rlk c* and complemented line using RLK C gene-specific primer set. *ACTIN3*, Actin gene-specific primers were used for PCR as the control. (I) Quantitative analysis of double fertilization in wild-type, *rlk c* and complemented line. The number of fertilized ovules was examined. (J) Quantitative analysis of *in vivo* pollen tube guidance in reciprocal cross between wild-type plant and complemented line. The number of ovules receiving pollen tube, indicating correct guidance was shown in a percentage (± S.D.).

Figure 2.12

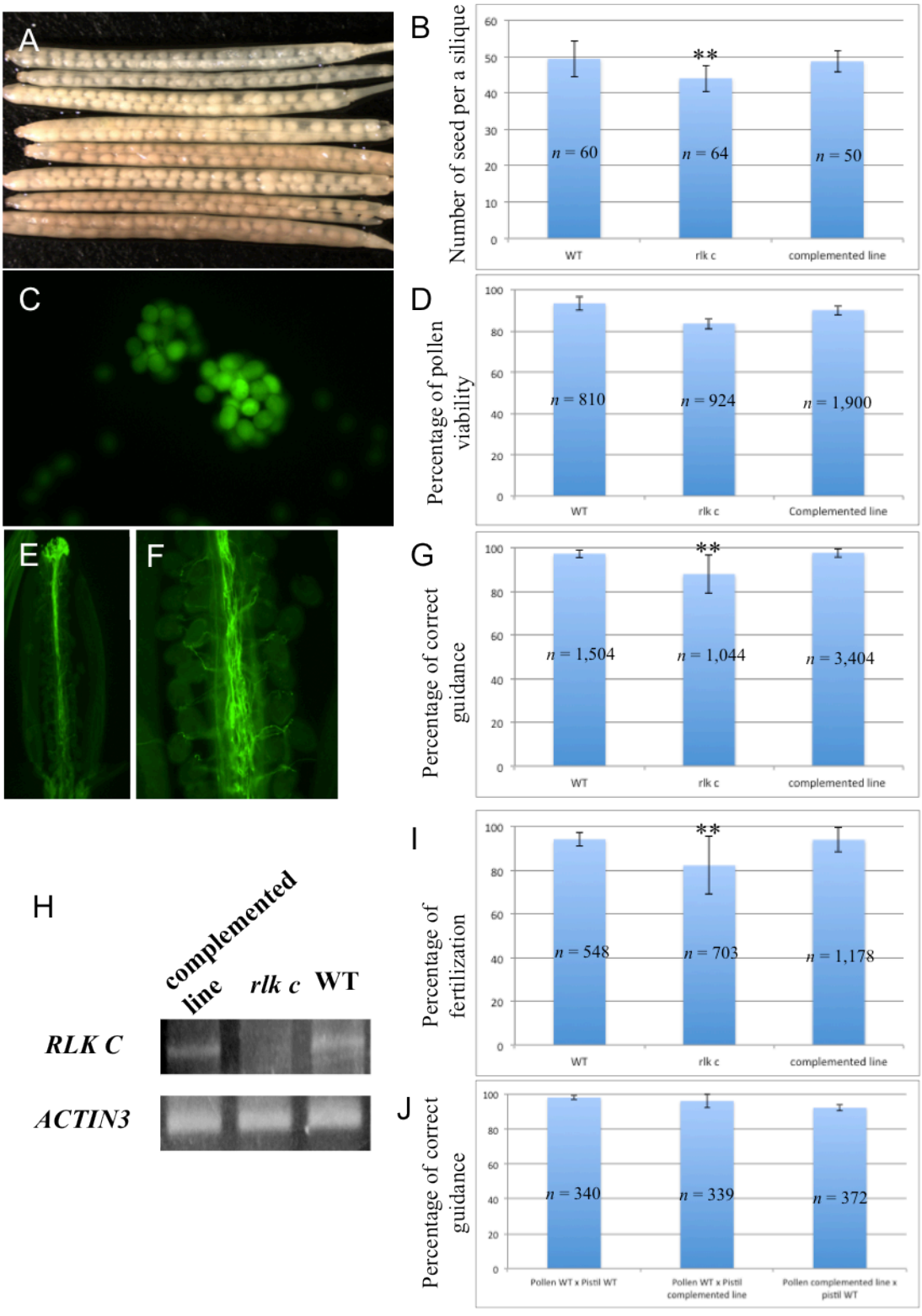
A
B
Number of seed per a silique
60
50
40
30
20
10
0
**
n = 60
n = 64
n = 50
WT
rlk c
complemented line
C
D
Percentage of pollen viability
100
80
60
40
20
0
n = 810
n = 924
n = 1,900
WT
rlk c
Complemented line
E
F
G
Percentage of correct guidance
**
n = 1,504
n = 1,044
n = 3,404
WT
rlk c
complemented line
H
complemented line
rlk c
WT
RLK C
ACTIN3
I
Percentage of fertilization
**
n = 548
n = 703
n = 1,178
WT
rlk c
complemented line
J
Percentage of correct guidance
n = 340
n = 339
n = 372
Pollen WT x Pistil WT
Pollen WT x Pistil complemented line
Pollen complemented line x pistil WT

Table 2-1 Segregation analysis for the *rlk c* mutant

Experiment	Parent (F0)		Segregation in F1 plants	Expected ratio	Observed ratio
	Pollen donor	Pistil donor			
Reciprocal fertilization	WT $^{(+/+)}$	*rlk c* $^{(+/-)}$	WT $^{(+/+)}$: *rlk c* $^{(+/-)}$	1 : 1	1 : 0.61 ** (*n* = 739)
	rlk c $^{(+/-)}$	WT $^{(+/+)}$	WT $^{(+/+)}$: *rlk c* $^{(+/-)}$	1 : 1	1 : 0.88 * (*n* = 1,176)

* Significantly different from the expected ratio (χ^2 , $p < 0.05$)

** Significantly different from the expected ratio (χ^2 , $p < 0.01$)

CHAPTER 3

Leucine Rich Repeat Receptor-like Kinases (LRR-RLKs) Signaling Functions Redundantly in Gamete Fertility

ABSTRACT

In this chapter, a reverse genetic approach was used to identify two more LRR-RLKs (RLK B and RLK D). The *rlk b* and *rlk d* mutants did not show obvious reproductive phenotype. However, *rlk c* displayed slight defects in seed production and pollen tube guidance. To understand their functions in sexual reproduction, different combinations of double mutations were generated; *rlk c rlk b*, *rlk c rlk d-2* and *rlk b rlk d-2*. We show that RLK C function redundantly with RLK B and RLK D to regulate male and female fertilities. First, mutations in RLK B and RLK D enhanced phenotypes in the *rlk c* mutant. The *rlk c rlk b* plant exhibited more severe defects in seed production and pollen tube guidance. The failure in pollen tube guidance in *rlk c rlk b* is likely due to the irregular development of the female gametophyte resulting in programmed cell death (PCD) in mature embryo sac. This suggests that RLK C and RLK B function redundantly to regulate female fertility. Second, the *rlk c rlk d-2* double mutant caused a significant decrease of pollen fertility. In both cases, it is likely that the major contribution for sexual fertility is from *RLK C* signaling due to no apparent phenotype in the *rlk b* and *rlk d* single mutants. In addition, *rlk b rlk d-2* did not show a phenotype, indicating their unique functions in reproduction. Taken together, we proposed that the RLK C signaling pathway requires the overlapping of RLK B and RLK D signaling pathway to mediate the fertilities of male and female gametophytes.

INTRODUCTION

Pollen-pistil interaction is required for sexual reproduction. Some lines of evidence have demonstrated that the guidance signals from the female tissues, such as the female gametophyte, lead the pollen tube to grow and correctly target toward the egg apparatus (Higashiyama et al., 2001). However, receptors on *Arabidopsis* pollen for this pollen-pistil communication are not identified yet. According to microarray analysis, about 200 RLKs have been detected in *Arabidopsis* pollen and pollen tubes (Honys and Twell, 2003). Thus, some of these might function as receptor involved in pollen-pistil recognition. In tomato pollen, two RLKs (LePRK1 and LePRK2) were identified and they function only in the presence of style exaudate (Muschietti et al., 1998). In *Arabidopsis*, *ANXUR1/2*, the closely related *FERONIA*, are expressed in the pollen tube. In *anx1/anx2* mutants, the pollen tubes ruptured before arriving the ovules, suggesting their roles in regulation the timing of pollen tube rupture (Miyazaki et. al., 2009). Taken together, these support that male-female interaction is mediated by RLKs.

In this chapter, two *RLK*s (*RLK B* and *RLK D*) both encoding leucin-rich repeat (LRR)-RLKs were characterized in Arabidopsis. RLK B and RLK D belong to the LRR-RLK subfamily. RLK B and RLK D are members of LRR VI and LRR VIII, respectively. Among 11 members in LRR VI, only ScORK17 was published (Germain et.al, 2008). In tomato, evidence has shown that a member of LRR VI, ScORK17 or *Solanum chacoense* Ovule Receptor Kinase, is involved in female gametophyte development and embryogenesis. *ScORK17* was barely expressed in any reproductive tissues before fertilization. By contrast, after fertilization, the expression level was significantly

increased in the ovary tissues. An introduction of a transgene carrying a full-length *ScORK17* driven by a *CaMV 35S* promoter into *A. thaliana* led to defective female gametophyte and reduced seed production. Approximately 43% of ovules developed aberrant functional megaspores, indicating abnormal megagametogenesis. Nevertheless, it is possible that the inappropriate expression is due to *CaMV 35S* activity. In addition, overexpression of *ScORK17* in *S. chacoense* did not show any reproductive phenotypes. In LRR VIII, there are 23 members. Most of these LRR-RLK members have shown no biological function. In sugarcane, it has been shown that SHR5 is involved in the association between plants and endophytic nitrogen-fixing bacteria (Vinagre et.al, 2006). Based on semi-quantitatice RT-PCR data, *SHR5* expression was greatly reduced in plants associated with the diazotrophic endophytes. In this chapter, a reverse genetic approach was used to identify RLK B and RLK D. Three T-DNA insertion lines for *RLK B* and *RLK D* were obtained and named these alleles as *rlk b*, *rlk d-1* and *rlk d-2*. To understand their functions in sexual reproduction, different combinations of double mutations were generated; *rlk c rlk b*, *rlk c rlk d-2* and *rlk b rlk d-2*. We demonstrate that the RLK C signaling pathway requires RLK B and RLK D to mediate sexual reproduction in *Arabidopsis*.

MATERIALS AND METHODS

Plant Materials and Plant Growth Condition

Arabidopsis thaliana accession Columbia-0 (Col-0) plants used in this study were grown in the growth room and chamber at the University of California, Riverside. To surface clean Arabidopsis seeds, 70% ethanol and the sterilization solution (20% bleach, 0.05% tween 20 and double-distilled water) were added to the seeds for 5 minutes. Seeds were washed thoroughly 3-5 times with sterile water to remove the bleach residue and seeds were immediately planted on petri dishes containing plant growth medium: one-half strength Murashige and Skoog (MS) salts (Sigma), 0.5% sucrose, 0.8% phyto agar (Research Products International Corp.), 1xB5 (1,000x in distilled water: 10% myo-inositol, 0.1% nicotinic acid and 0.1% pyroxidine HCI) and 1xThiamin (2,000x in distilled water: 0.2% thiamin HCI) pH5.8 with 1M KOH. Seeds were kept at 4°C for 3-4 days to break dormancy. After the cold treatment, the petri dish was placed in the growth room. Seven to ten day-old seedlings were transferred to soil (Sunshine Mix#1, Sun Gro Horticulture) at 22°C under a 16 light/ 8 dark-hour photoperiod with 200 μEm-2s-1 illumination.

To study functions of *RLK B* (At1g63430) and *RLK D* (At1g06840), one or two T-DNA insertion alleles per RLK gene were obtained from Arabidopsis Biological Resource Center (ABRC; Alonso et al., 2003) and Syngenta Arabidopsis Insertion Library (SAIL; Sessions et al., 2002). The T-DNA insertion sites for each gene were shown in Figure 3.1C and D. The *rlk b* allele (SALK_111226) has a T-DNA insertion located on the first intron of *RLK B*. For RLK D, two T-DNA insertion alleles were

obtained, *rlk d-1* (SALK_039722) and *rlk d-2* (CS842841). The *rlk d-1* and *rlk d-2* allele have their T-DNA insertions located on the first exon and the eight intron of *RLK D*, respectively. The *rlk d-2* mutant was obtained from SAIL collection (SAIL_1160_G06.V) harboring pCSA110 T-DNA, which carries GUS driven by a pollen-specific *LAT52* promoter and a BASTA resistance cassette for the herbicide Basta.

PCR and RT-PCR Analysis

Genomic DNAs from each T-DNA insertion lines were extracted from the mature leaves for PCR-based genotyping using gene-specific primers generated by the T-DNA primer design tool (http://signal. salk.edu/tdnaprimers.2.html); for *rlk b*, 5'-TCTCTCTC TTTCTCGCCACAC-3' and 5'-TGCAGGTACGTTATTTGACCC-3'; for *rlk d-1*, 5'-TTCAGGTAATGGATGAGACCG-3' and 5'-ACGGAGGCCTTAATTATCAGG-3'; for *rlk d-2*, 5'-AATTCAGCTCTCTTTCCTGCC-3' and 5'-TCCTGTCACCATAAGGACT GG-3' and T-DNA-specific primers (for *rlk c*, *rlk b* and *rlk d-1*, 5'-ATTTTGCCGATT TCGGAAC-3'; for *rlk d-2*, 5'-GCCTTTTCAGAAATGGATAAATAGCCTTGCTTCC-3').

Reverse transcriptase (RT)-PCR was performed to determine the expression levels of each RLK gene in wild-type and loss-of-function mutants. Total RNAs were isolated from various plant tissues roots of 10-day-old seedlings, mature rosette leaves, pistils and open flowers) by RNeasy mini Kit (Qiagen). In a reverse transcriptase reaction, the double-strand cDNAs were synthesized (Superscript II, Invitrogen) and used as templates in RT-PCR using gene specific primers for *RLK*s (for *RLK B*, 5'-TGTTCG TTAGCTCTTGTTCTTGGTCTC-3' and 5'-AGCCAAATCTGCA ACCTCTCTCTG-3';

for *RLK D*, 5'-TTGACGGAAGAAGGTGGTGAAGTT-3' and 5'-TATAGGTCCACAC AATCGAAGCAGATT-3'; for *ACTIN3,* 5'-GGAACAGTGTGAC TCACACCATC-3' and 5'-AAGCTGTTCTTTCCCTCTACGC- 3' as amplification control).

Analysis of Seed Set in Mature Siliques

To analyze seed production in the *rlk* mutants, the mature siliques were incubated in 100% ethanol over night and the numbers of seeds and unfertilized ovules per a silique were counted.

Analysis of Pollen Tube Guidance

(A) *In vivo* Pollen Tube Growth and Guidance with Aniline Blue Staining

Aniline blue staining was performed to observe pollen tube growth inside the pistils. The anthers from mature floral buds (stage 12) were emasculated and plants were kept in the growth room for 24 hours. Plants used as pollen donor were taken from the growth room and kept at room temperature for an hour before pollination. Self and reciprocal-cross pollination were carried out. Fresh pollen grains from the mature flowers (stage 13) were used to manually apply on the stigma surface of the emasculated pistil. The pollinated pistils were harvested after pollination for 18-24 hours. Pistils were fixed in fixative solution (3:1 v/v ethanol and acetic acid) for 2 hours at room temperature. The pistils were dehydrated using the following concentrations of ethanol series: 95%, 70%, 50% and 30% (10-15 minutes for each change at room temperature) and softened by 8M NaOH overnight. The softening pistils were washed with distilled water to remove the NaOH residue and stained with decolorized aniline blue for 2 hours as described by Mori et al. (2006). Pollen tube growth behavior inside the female tissues was observed under a

fluorescence microscope (Nikon Microphot FXA, Nikon) and images were captured with a Spot Insight Camera (Diagnostic Instruments Inc.).

(B) *In vivo* Pollen Tube Growth by GUS Assay

In vivo GUS assay was performed as described by Palanivelu et al. (2006). Pollen from mature flowers (stage 13) was used to apply on the stigma of the emasculated pistil. The pistils were harvested after pollination for 18 hours and fixed in the 80% (v/v) acetone at least an hour. The pistils were incubated in GUS staining buffer (10 mM EDTA, 100 mM sodium phosphate, pH 7.0, 0.5 mM potassium ferrocyanide, 0.5 mM potassium ferricyanide) and 0.1% Triton X-100 with 1 mM 5-bromo-4-chloro-β-glucuronide) at 37°C overnight, observed with a Nikon microscope (Nikon Microphot FXA), and images were captured with a Spot Insight Camera (Diagnostic Instruments Inc.).

(C) Semi–*in vivo* Assay for Pollen Tube Guidance

To analyze Arabidopsis pollen tube guidance, semi-*in vivo* assay was performed as described by Palanivelu et al, (2006). The anthers from mature floral buds (stage 12) were emasculated and plants were kept in the growth room for 24 hours. Fresh pollen from mature flowers (stage 13) was used to apply on the stigma of the emasculated pistil under a stereo microscope. The pollinated pistils were harvested after pollination for an hour. The pistils were cut at the junction between the style and the ovary and placed horizontally on a plate containing pollen growth media. Within 2-3 hours, the remaining ovaries were dissected and the ovules were removed from the ovaries. The ovules were placed on the plate. Pollen tube guidance was observed with a Nikon ECLIPSE

microscope (Nikon Instruments) and images were captured with a Hamamatsu Digital Camera (Hamamatsu Photomics).

Pollen Analysis

(A) Pollen Viability Test by FDA Staining

The viability of the *rlk* pollen grains was assessed by FDA staining (Heslop-Harrison and Heslop-Harrison, 1970). Pollen was collected from freshly dehisced anthers and immersed in the pollen growth liquid media. Pollen was incubated at 28°C for 30 minutes. A drop of 0.5 μg/mL FDA (fluoreacein diacetate) was added to the pollen growth media and observed immediately with a Nikon ECLIPSE microscope (Nikon Instruments) equipped with epifluorescence and fluorescein isothiocyanate (FITC) filter.

(B) Vacuole Analysis by Neutral Red Staining

To investigate vacuoles, mature pollen grains were collected and applied with 0.02% (w/v) neutral red for 30 minutes at room temperature as described by Lee et al., (2008). Samples were observed under a bright-field microscope.

(C) *In vitro* Pollen Germination Test

In vitro assay was used to determine pollen tube germination. The anthers were brushed on pollen growth medium (18% sucrose, 0.01% Boric acid, 1mM $CaCl_2$, 1mM $Ca(NO_3)_2$, 1mM $MgSo_4$ pH 7.0 and 0.5% Select agar). The plates were incubated at 28°C for 4 hours before analysis. Pollen tube growth was observed with a Nikon ECLIPSE microscope (Nikon Instruments) and images were captured with a Hamamatsu Digital Camera (Hamamatsu Photomics).

(D) Pollen Nuclei Analysis by DAPI staining

Mature pollen grains were collected and placed on slide. A few drop of DAPI (4', 6-diamidino phenylindole) solution (0.1 M Sodium phosphate pH 7.0, 1 mM EDTA, 0.1% Triton X-100 and 0.4 μg/ml) was added to pollen, and was observed by a fluorescence microscope with UV filter.

Cleared Whole-Mount Preparation

Inflorescences were harvested and fixed in the fixative solution (3:1 v/v ethanol and acetic acid) for 2 hours at room temperature. Tissues were then rehydrated using the following concentrations of ethanol series: 95%, 70%, 50% and 30% (10-15 minutes for each change at room temperature) and cleared in Hoyer's solution (100 g chloral hydrate, 25 mL glycerol and 50 mL distilled water) for 3 hours and observed under a Nikon ECLIPSE microscope (Nikon Instruments). Images were captured with a Hamamatsu Digital Camera (Hamamatsu Photomics).

RESULTS

Tissue-Specific Expression of *RLK B* and *RLK D* by RT-PCR

To determine gene expression levels by reverse transcriptase (RT)-PCR, total RNA was isolated from roots, mature rosette leaves, pistils and open flowers of wild-type plants. RT-PCR anlysis revealed that the transcript of *RLK B* and *RLK D* were expressed in most tissues (Figure 3.1A and B). The expression level of *RLK B* was high in root, pistil and open flower but lower in mature leaves (Figure 3.2A). The expression of *RLK D* transcript was high in pistil and open flower but lower in root and mature leaf (Figure 3.2B). As compared to *RLK B* and *RLKC*, *RLK D* showed low expression in root. As

shown in Figure 2.2A, the expression of *RLK C* was also high in the flower and pistil. According to their overlapping expresstion patterns in the flower, they suggest that RLK C, RLK B and RLK D might function redundantly.

***rlk b, rlk d-1* and *rlk d-2* Displayed No Obvious Reproductive Phenotypes**

The genomic structures of two LRR-RLK genes, *RLK B* (At1g63430) and *RLK D* (At1g06840) and T-DNA insertion sites were shown in Figure 3.1C and D. The *rlk b* allele has a T-DNA insertion located on the first intron of *RLK B*. The *rlk d-1* and *rlk d-2* allele have their T-DNA insertions located on the first exon and the eight intron of *RLK D*, respectively. To investigate the putative functions of RLK B and RLK D during reproductive stage, the homozygous lines of *rlk b* and *rlk d* were used to determine their gene expression levels in open flowers. RT-PCR analysis revealed that transcripts of *RLK B* and *RLK D* were undetectable in their T-DNA insertion alleles using gene-specific primers sets (Figure 3.1E and F). The *RLK C* expression level was not affected neither *rlk b* nor *rlk d* mutant (Figure 3.1F). In addition, the expression levels of *RLK B* and *RLK D* were not interfered in the *rlk c* mutant. These suggest no crosstalk in gene regulation among these RLKs.

To determine whether the loss of *RLK* activity can alter reproduction process in the mutants, analysis of seed production was performed after self-pollination of wild-type and the *rlk* mutants. The data indicated normal seed production observed for *rlk b* (48.41 ± 4.36; $n = 34$; $P < 0.05$; Figure 3.2B), *rlk d-1* (49.92 ± 5.13; n = 43; $P < 0.05$; Figure 3.2C) and *rlk d-2* (48.68 ± 3.25; $n = 31$; $P < 0.05$; Figure 3.2D). These results were not statistically different compared with wild-type (53.00 ± 4.47; $n = 41$; Figure 3.2A and E).

Thereafter, those plants were fertile and their offspring seeds were able to germinate. To examine pollination and pollen tube growth, i*n vivo* aniline blue staining was performed in each mutant. The results revealed normal pollen tube growth toward the base of the pistil in all three alleles (Figure 3.2H and J). Pollen tubes from each mutant could grow to the bottom of the pistil at a normal growth rate as compared to wild-type. By 18 hours after pollination, most of pollen tubes could reach the bottom of the pistil and enter the embryo sac. The percentage of correct guidance from the pollen tubes of *rlk b*, *rlk d-1* and *rlk d-2* were 95.65% ± 2.69% (n = 1,240; $P < 0.05$), 93.26 ± 6.10 (n = 1,111; $P < 0.05$) and 91.35 ± 5.96 (n = 740; $P < 0.05$), respectively. These results are not statistically different compared with wild-type (96.17 ± 1.75; n = 1,251; Figure 3.2A and F), suggesting normal pollen tube growth and guidance in the *rlk b, rlk d-1* and *rlk d-2* mutants.

To investigate further that double fertilization is altered in *rlk b, rlk d-1* and *rlk d-2*, pistils were self-pollinated and harvested after manual pollination for 3 days and the number of fertilized ovules was counted. In wild-type, most ovules were successfully fertilized indicated by the formation of developing embryo and endosperm. The percentage of fertilized ovules in wild-type was 93.98% ± 3.23% (n = 548). Quantification of the results showed normal fertilization in *rlk b* (93.89% ± 4.78%; n = 262; $P < 0.05$), *rlk d-1* (95.58% ± 5.00%; n = 278; $P < 0.05$) and *rlk d-2* (90.00% ± 8.13%; n = 398; $P < 0.05$; Figure 3.3J).

Transmissions Through Both Gametes are Normal in *rlk b, rlk d-1* and *rlk d-2*

To confirm normal transmission by both gametes in the mutants, transmission efficiency was determined from reciprocal crosses between *rlk* $^{(+/rlk)}$ and wild-type plants. The F1 progeny from each cross were scored at 1:1 for *rlk* $^{(+/rlk)}$ to wild-type $^{(+/+)}$ by PCR-based genotyping for *rlk b* and *rlk d-1* and by Basta-resistance screening for *rlk d-2*. Reciprocal crosses reveled the ratio of 0.98:1 (n = 117; χ^2 = 0.08; $P < 0.05$) and 0.96:1 (n = 109; χ^2 = 0.10; $P < 0.05$) when *rlk b* $^{(+/rlk\ b)}$ functioned as pistil and pollen donor, respectively (Table 3.1). These observed ratios were close to the expected ratio of 1:1, indicating normal tranmission through both female and male gametes of *rlk b*. In *rlk d-1*, the ratio of 0.90:1 (n = 180; χ^2 = 0.18; $P < 0.05$) and 0.92:1 (n = 94; χ^2 = 0.18; $P < 0.05$) when *rlk d-1* $^{(+/rlk\ d\text{-}1)}$ functioned as pistil and pollen donor, respectively was revealed. These ratios from *rlk d-1* plants were close to the ratio of 1:1 (Table 3.2), suggesting that the transmission through both gametophytes was normal. In *rlk d-2*, the ratio of 0.96:1 (n = 273; χ^2 = 0.09; $P < 0.05$) and 0.94:1 (n = 92; χ^2 = 0.04; $P < 0.05$) when *rlk d-2* $^{(+/rlk\ d\text{-}2)}$ acted as pistil and pollen donor, respectively was revealed (Table 3.3), indicating normal gene transmission through both gametophytes. Taken together, T-DNA insertion in the *rlk b* and *rlk d* mutants did not affect both gametophytes, suggesting normal transmission through both gametes. This finding is consistent with no apparent phenotypes observed in *rlk b* and *rlk d*.

rlk c rlk d-2 and *rlk c rlk b* Exhibited Seed Set and Pollen Attraction Phenotypes more Severe than that of the *rlk c* mutant

To determine whether RLK C, RLK B and RLK D are functionally redundant in plant reproduction, three different double homozygous mutants (*rlk c rlk b, rlk c rlk d-2* and *rlk b rlk d-2)* were generated. The homozygous lines were used to determine their gene expression levels in the open flowers. RT-PCR analysis revealed that the transcript levels in each plant were undetectable using gene-specific primers sets (Figure 3.3K). The difference in the vegetative organs between each *rlk* double mutants and wild-type were not observed (data not shown). However, *rlk c rlk b* and *rlk c rlk d-2* plants produced less seeds than wild-type plants (Figure 3.3B and C). Average seed number per a silique of *rlk c rlk b*, *rlk c rlk d-2* and wild-type were 23.75 ± 6.20 (n = 20; $P < 0.01$; Figure 3.3B), 37.81 ± 8.74 (n = 27; $P < 0.05$; Figure 3.3C) and 54.25 ± 2.83 (n = 20), respectively (Figure 3.3E). In addition to the reduced seed formation, the mature siliques from *rlk c rlk b* plant were shorter than wild-type. Moreover, the mature siliques from *rlk c rlk b* and *rlk c rlk d-2* plants had many gaps, suggesting a problem in pollination or double fertilization. However, the self-pollinated *rlk b rlk d-2* plant developed normal siliques, which did not show any gaps (Figure 3.3D). This indicates normal pollination and fertilization. Average seed number per a silique of *rlk b rlk d-2* was 49.36 ± 7.48 (n = 19; Figure 3.3E). Only *rlk c rlk b* and *rlk c rlk d-2* but not *rlk b rlk d-2* exhibited more severe seed set than *rlk c* mutant.

To examine pollen tube behavior inside the pistils, the limited number of pollen grains was pollinated on the pistils and aniline blue staining was performed. The result showed normal pollen tube growth toward the base of the pistil and normal pollen tube attraction in all double mutants (Figure 3.3F-I). However, a significant decrease of successful guidance was observed for *rlk c rlk d-2* (81.54% ± 10.12%; $n = 809$; $P < 0.05$; Figure 3.3G) and *rlk c rlk b* (54.07% ± 12.57%; $n = 435$; $P < 0.01$; Figure 3.3H and I), compared to *rlk c* mutant. This suggests that a defect in pollen tube attraction in *rlk c rlk d-2* and *rlk c rlk b* cause a decrease of seed production. Both *rlk c rlk d-2* and *rlk c rlk b* plants exhibited pollen attraction phenotype more severe than that of *rlk c* mutant (Figure 3.3J). As expected, the *rlk b rlk d-2* mutant showed normal pollen tube guidance (92.86% ± 5.14%; $n = 140$), compared to wild-type (96.17 ± 2.83%; $n = 500$). This data is consistent with the normal seed production.

The *rlk c rlk d-2* and *rlk c rlk b* Mutants Show Reduced Gene Transmission

To investigate whether the mutation in the double mutants affect male or female gametophyte, segregation analysis was performed. For example, to determine the efficiency of gene transmission in the *rlk c rlk b* double mutant, reciprocal crosses between *rlk c rlk b* (*rlk c* $^{(+/-)}$ *rlk b* $^{(+/-)}$) and wild-type were carried out. The F1 progeny were scored by PCR-based genotyping. Their progeny from each cross were scored at 1:1:1:1 for *rlk c* $^{(+/+)}$ *rlk b* $^{(+/+)}$, *rlk c* $^{(+/+)}$ *rlk b* $^{(+/-)}$, *rlk c* $^{(+/-)}$ *rlk b* $^{(+/+)}$ and *rlk c* $^{(+/-)}$ *rlk b* $^{(+/-)}$ plants. As also shown in Table 3.4, the result revealed the ratio of 1:0.3:0.4:0.3 ($n = 80$) and 1:0.54:0.15:0.08 ($n = 76$) when *rlk c rlk b* acted as pistil and pollen donor, respectively. These ratios were distorted from the expected ratio of 1:1:1:1, suggesting

that the transmission efficiencies for female and male gametophytes were distorted in *rlk c rlk b*. The result revealed the ratio of 1:0.70:0.70:0.68 (n = 176) and 1:0.66:0.64:0.68 (n = 312) when *rlk c rlk d-2* acted as pistil and pollen donor, respectively (Table 3.5). The ratio from *rlk c rlk d-2* was affected in both female and male gametophytes, suggesting that the transmission efficiencies for female and male gametophytes was affected in *rlk c rlk d-2* double mutant.

***rlk c rlk b* Showed Abnormal Pollen Tube Attraction**

To explain the effect of double mutations on reproduction, reciprocal crosses were performed between *rlk* double mutants and wild-type. The pistils were stained with aniline blue to determine *in vivo* pollen tube behavior. As control, percentage of the correct guidance in self-pollinated wild-type was 91.53% ± 10.24% (n = 425). Reciprocal analysis revealed the pollen tube attraction phenotype in *rlk c rlk b* was caused by defective in the female gametophyte. When the *rlk c rlk b* pollen grains pollinated on wild-type pistils, the attraction was normal (93.67% ± 6.49%; n = 237; $P < 0.05$; Figure 3.4A and C). Interestingly, the percentage accurate attraction was significantly reduced when wild-type pollen grains pollinated onto the *rlk c rlk b* pistils (57.89% ± 5.33%; n = 223; $P < 0.01$; Figure 3.4B, D and I). Many *rlk c rlk b* ovules could not correctly target the pollen tube (Figure 3.4D). In addition, female guidance defect in *rlk c rlk b* was more severe than the *rlk c* mutant.

To verify the defect in ovular guidance from *rlk c rlk b* pistils, *in vivo* GUS assay was performed. *LAT52*p::GUS pollen grains were pollinated on the *rlk c rlk b* and wild-type pistils. The result confirms that guidance defect in *rlk c rlk b* was caused by the

pistils. As control, most of *LAT52*p::GUS pollen tubes perfectly targeted to the wild-type ovules (Figure 3.4E and G). By contrast, some *LAT52*p::GUS pollen tubes could grow toward the *rlk c rlk b* ovules. Many of them did not enter the embryo sac (Figure 3.4F and H), suggesting guidance defect from the female tissues of *rlk c rlk b*.

***rlk c rlk b* Showed Guidance Defect by Semi–*In Vivo* Analysis**

Based on our previous finding, pollen tube guidance defect in *rlk c rlk b* was caused by the female tissues. However, it is possible that defect in pollen tube attraction may originate from a malfunction of the sporophytic tissues, such as the transmitting tract in the style and the ovary, resulting in an inhibition of pollen tube growth to emerge toward the funiculus. We sought to determine whether pollen tube attraction phenotype in *rlk c rlk b* is due to the defective in the transmitting tract tissues, semi–*in vivo* study was performed. As control, wild-type pollen tubes germinated on wild-type stigma and grown toward the cutting edge of the style (Figure 3.5A). Afterward, pollen tubes emerged to the solid media and accurately targeted to the micropyle of wild-type ovules (Figure 3.5C), indicating normal pollen tube guidance (64.81% ± 18.25%; $n = 108$). By contrast, the percentage of the correct attraction was significantly decreased when wild-type pollen grains pollinated on the *rlk c rlk b* pistils (40.63% ± 12.28%, $n = 60$; $P < 0.01$; Figure 3.5B, D and E). Here, we report that defective in pollen tube guidance of *rlk c rlk b* was affected by the ovular tissues but not the style.

***rlk c rlk b* female gametophyte is arrested post-meiotically.**

To confirm that pollen attraction defect is not caused by aberrant ovule development, the whole-mount of various developmental stages of *rlk c rlk b* ovules were prepared. The result revealed that ovule morphology of *rlk c rlk b* was normal. Similar to wild-type, the initiation and patterning of young ovule appeared normal. Until stage 4, the mature ovule containing the female gametophyte was normally developed (Figure 3.6A and B). This suggests normal development in the sporophytic tissues. However, it is possible that the female gametophyte of the *rlk c rlk b* mutant was abnormal, resulting in a reduction of the correct guidance. To determine whether the female gametophyte of *rlk c rlk b* is functional, aniline blue was used to stain callose wall of the female gametophyte. In wild-type Arabidopsis, no evidence of callose accumulation was observed in embryo sac during anthesis (Figure 3.6E and F). By contrast, *rlk c rlk b* embryo sac produced many non-functional female gametophytes, indicated by high intensity of the fluorescent signal after aniline blue staining (Figure 3.6G and H). The percentage of non-functional embryo sac in *rlk c rlk b* was higher than that of wild-type (Figure 3.6H). It is most likely that female gametogenesis of *rlk c rlk b* is altered. To determine whether development of *rlk c rlk b* female gametophyte is affected, the inflorescences of wild-type and *rlk c rlk b* plants were cleared and observed under DIC. More than 50% of *rlk c rlk b* female gametophytes showed normal development, which was similar to wild-type (Figure 3.6I and J). Many were arrested and exhibited a large nucleus inside the embryo sac (Figure 3.6K). To investigate which developmental stage of *rlk c rlk b* female gametophyte is arrested, aniline blue was used to determine an event of degeneration of 3 non-functional

megaspores after meiosis. Evidence indicated that all *rlk c rlk b* female gametophytes could showed programmed cell death (PCD) of 3 megaspores at the micropylar end, suggesting that the meiotic phase of *rlk c rlk b* female gametophyte was normal (Figure 3.6L-N). It is most likely that the female gametophyte of *rlk c rlk b* was arrested at FG1 stage. In previous chapter, we also showed that synergid and egg cell specifications of the *rlk c* mutant were interfered (Figure 2.11). Taken together, these suggest that *RLK C* and *RLK B* function redundantly to mediate female gametophyte development.

***rlk c rlk d-2* Showed Partial Male Sterile and Abnormalities in Pollen Fertility**

To analyze pollen phenotype in double mutants, pollen viability was assessed by fluorescein diacetate (FDA). Many pollen grains from double mutants failed to stain FDA. However, only *rlk c rlsk d-2*, not *rlk c rlk b* and *rlk b rlk d-2* displayed decreased pollen viability more severe than that of wild-type (Figure 3.7G). Approximately 68.48% ± 6.19% (n = 1,142) of *rlk c rlk d-2* pollen grains were viable (Figure 3.7E and F), compared with pollen grains from wild-type plants (90.44% ± 6.20%; n = 1,705; $P < 0.01$) and *rlk c* plants (83.01% ± 1.18%; n = 924; $P < 0.05$), respectively. Pollen viability in *rlk c rlk b* (84.03% ± 2.99%; n = 645; $p < 0.05$) and *rlk b rlk d-2* (85.08% ± 9.63%; n = 858; $P < 0.05$) were normal as compared with wild-type. To investigate further in pollen morphology, mature pollen grains from double mutants were treated with 0.02% (v/v) neutral red. In mature wild-type pollen grains, numerous dispersed small vacuoles were observed in red after neutral staining (Figure 3.8A). Most *rlk c rlk b* and *rlk b rlk d-2* pollen grains had normal vacuolar morphology (data not shown). The frequency of aberrant pollen grains with abnormal vacuoles was significantly increased in *rlk c rlk d-2*

(11.88% ± 0.25%; n = 791; P < 0.01; Figure 3.8B-D), compared with pollen grains from wild-type plants (6.26% ± 1.41%; n = 559; Figure 3.8A). To determine whether the abnormality in *rlk c rlk d-2* pollen grain affects pollen function, the *in vitro* germination test was performed in comparison to wild-type pollen. The result revealed that the average percentage of pollen germination was significantly reduced in *rlk c rlk d-2* (50.25% ± 1.98%; n = 603; P < 0.01), compared to wild-type (74.62% ± 5.12%; n = 2,116) and *rlk c* (73.35% ± 5.00%; n = 1,441). This result indicates partial male sterility in *rlk c rlk d-2*.

To investigate which stage of pollen development is impaired in *rlk c rlk d-2*, both the whole-mount preparation of different anthers stages were carried out. There was no evidence of abnormal anther at any different stage and pollen development in *rlk c rlk d-2* was not affected (data not shown). Similar to wild-type, at stage 5, The pollen mother cells (PMCs) were produced within the anther locule (Figure 3.9B). PMCs were enclosed with thick callose wall. At stage 7, tetrads were generated and surrounded by callose wall, suggesting complete tetrad formation (Figure 3.9D). At anther stage 8, wild-type microspores were released from the callose wall (Figure 3.8E). At this stage, *rlk c rlk d-2* pollen grains were still in tetrad, which is similar to *rlk d-2* (Figure 3.9F). Finally, the mature pollen grains were formed even though some aborted pollen grains were observed (Figure 3.9H). These results suggest that male gametogenesis is not affected in *rlk c rlk d-2*.

DISCUSSION

RLK C, RLK B and RLK D Function Redundantly to Mediate Sexual Reproduction in Arabidopsis

In this chapter, two more LRR-RLK genes (*RLK B and RLK D*) were identified. We demonstrate that *RLK B*, *RLK C* and *RLK D* have different redundant functions in plant reproduction. RLK C (LRR III), RLK B (LRR VI) and RLK D (LRR VIII) belong to the LRR-RLK subfamily. They contain the extracellular LRR domains with different number of LRR repeats. The extracellular domains of each predicted RLKs share approximately 20% amino acid identity to RLK C. In chapter 2, we demonstrated that RLK C is involved in pollen tube guidance primarily through the female gametophyte. In this chapter, we show that the loss-of-function mutants of *RLK B* and *RLK D* did not display any apparent reproductive phenotypes and their transmission efficiencies appeared normal, suggesting that *RLK B* and *RLK D* are redundant. It is likely that loss-of-function of *RLK B* and *RLK D* is compensated by *RLK C* activity. According to our genetic studies, *RLK C, RLK B* and *RLK D* function redundantly in different manners. Loss of-function mutations in *RLK C* and *RLK B* loci exhibited severe aberrant pollen tube guidance and seed production. The *rlk c rlk b* mutant also exhibited the early programmed cell death (PCD) in mature female gametophyte, resulted in defect in the micropylar guidance. This suggests that RLK B overlaps in the RLK C signaling pathway to regulate the female fertility. Furthermore, loss-of-function mutations in *RLK C* and *RLK D* loci caused a greatly decrease of pollen fertility, suggesting a redundant function in *RLK C* and *RLK D.* As mentioned, mutations in both RLK B and RLK D could

enhance phenotype in *rlk c* in different ways. However, mutations in *RLK B* and *RLK D* did not show visible phenotype, indicating their unique roles in sexual reproduction. Based on our phenotypic analysis of 3 LRR-RLK double mutants, we provide evidence that RLK C, RLK B and RLK D play roles in development of male and female structures to achieve fully fertility in pollen and female gametophyte.

RLK C and RLK B Function Redundantly to Regulate Female Gametophyte Development

It is likely that RLK C and RLK B function redundantly to control female gametophyte development resulting in accurate pollen tube guidance. The function of *RLK C and RLK B* is required for the initiation of female gametogenesis. The *rlk b* mutant did not show detectable reproductive phenotype while *rlk c* showed slight defectives in pollen fertility, synergid and egg specifications, pollen tube guidance and seed production. The *rlk c rlk b* double mutant displayed more severe defects in female gametophyte development, pollen tube guidance and seed production, indicating that *RLK C* and *RLK B* function redundantly in sexual reproduction. In addition, it is likely that the major contribution for development of the female gametophyte is from *RLK C* due to no apparent phenotype in the *rlk b* mutant. We sought to determine whether pollen tube guidance defect is contributed by which gametophyte, *in vivo* aniline blue staining and semi-*in vivo* study were performed in the double mutant. Growth of the *rlk c rlk b* pollen tube was normal in wild-type transmitting tracts. However, the pollen tubes were not correctly targeted to the ovules, resulting in many unfertilized ovules. This suggests that the guidance phenotype in *rlk c rlk b* was due to the defective egg apparatus. In

addition, some populations of wild-type pollen tubes were able to enter *rlk c rlk b* ovules and seeds were formed, indicating that fertilization did not affect the double mutant. However, guidance phenotype could not be observed when *rlk c rlk b* pollen grains were pollinated on wild-type pistil. The *rlk c rlk b* pollen tubes were able to accurately target to wild-type ovules, indicating normal pollen tube attraction. In Arabidopsis, it has been shown that the guidance mutants are defective in development of the female gametophyte. For example, the *bel1* mutant has defective female gametophyte development (Brambilla et al., 2007). In *maa* mutant, the pollen tubes fail to target the female gametophyte because the formation of a central cell is disrupted (Shimizu et al., 2008). In this study, the sporophytic tissues of *rlk c rlk b* ovules appeared normal, compared to those of wild-type. However, the female gametophyte of *rlk c rlk b* was arrested post-meitotically. It is likely that the interaction between sporophytic tissues, such as nucellus, and gametophytic tissues is essential for female gametogenesis. In Chapter 2, we reported that the synergid and egg cells were aberrantly specified, which were indicated by a synergid- and egg-specific marker (Figure 2.11). We demonstrated that defective in synergid and egg specifications failed the female gametophyte function. We support that the micropylar guidance requires communication between the synergids and the pollen tubes.

RLK C and _RLK D_ Play Essential Role in Male Fertility

We demonstrate that *RLK C* and *RLK D* function redundantly to regulate fertility of the pollen. The knockout of *RLK D* gene did not show apparent reproductive phenotype while *rlk c* showed a slight decrease of viable pollen grains, indicating partial

male sterility in the *rlk c* mutant. In previous chapter, we showed that *RLK C* promoter expression was very weak in mature pollen grains and pollen tubes (Figure 2.4D-F). This is consistent with a subtle disstortion of RLK C gene transmission through the male gametophyte (Table 2.1) and a mild defect in pollen viability (Figure 2.9E) in *rlk c.* However, the *rlk c rlk d-2* double mutant displayed more severe male sterility, indicating that *RLK C* and *RLK D* probably function redundantly. It is most likely that the major contribution for male fertility originates from *RLK C* because pollen viability in the *rlk d* mutant appeared normal. The *rlk c rlk d-2* anthers developed normally; however, only defect in the mature pollen grain was observed, indicated by a decrease of pollen viability and an increase of abnormal vacuole accumulation (Figure 3.8D). Some RLKs have been shown to be involved in male fertility. Most of the male-sterile *RLK* mutants were defective in the development of sporophytic tissues, which are required for normal pollen development (Albrecht et al., 2005; Colcombet et al., 2005; Hord et al., 2006). For example, EXCESS MICROSPOROCYTES1/ EXTRA SPOROGENOUS CELL (EMS1/EXS) is an LRR RLK. Lack of *EMS/EXS* activity caused no formation of the tapetum (Canales et al., 2002; Zhao et al., 2002). However, we did not observe any sporophytic phenotypes. To clarify which stage of pollen development affects the partial sterility of *rlk c rlk d-2*, more experiments are required, such as ultrastructures of microspores and mature pollen grains by scanning electron microscope (SEM) and transmission electron microscope (TEM).

A Potential Signaling Role of LRR- RLK C, -RLK B and -RLK D in Sexual Reproduction

LRR-RLKs have the LRR domain located outside the plasma membrane, suggesting their functions in signal transduction. We propose that RLK C and RLK B function redundantly to elicit a signal transduction pathway involved in development of the female gametophyte. The accurate specifications and developments of synergid and egg are required for pollen tube guidance and fertilization. In mature synergids, the guidance signal is distributed outside to lead the pollen tube to the micropyle. Other receptors on the plasma membrane of the pollen tube are required to perceive the guidance cue from the synergids. We also demonstrate that male fertility requires overlapping *RLK C* and *RLK D* signaling pathways. In both cases, it is likely that the major contribution for male and female fertility is from *RLK C* signaling due to no apparent phenotype in the *rlk b* and *rlk d.* In wild-type scenario, RLK C interacts with other partners and might share the ligands and the signaling components with those. To regulate gamete fertility, the signaling pathway of RLK C and others are required. In the *rlk c* mutant, the activity of *RLK C* is lost. However, the *rlk c* mutant displayed subtle defective in pollen fertility and seed production. This suggests that other signaling networks, such as RLK B and RLK D, is also required for sexual reproduction. Similar to other known RLKs, the putative ligands for these LRR-RLKs are still unknown. Evidence has shown that RLKs interact with ROP GTPases, the key player to mediate multiple extracellular signals. This suggests that RLKs might act as potential upstream regulators for ROPs. For example, FERONIA, an LRR-RLK, activates ROP2 GTPase to

regulate NADPH oxidase-derived reactive oxygen species (ROS)-mediated root hair development (Duan et. al., 2010).

REFERENCES

Albrecht, C., Russinova, E., Hecht, V., Baaijens, E. and de Vries, S. (2005). The *Arabidopsis thaliana* somatic embryogenesis receptor-like kinases 1 and 2 control male sporogenesis. Plant Cell, 17: 3337-3349.

Alonso, J. M., Stepanova, A. N., Leisse, T. J., et al. (2003). Genome-wide insertional mutagenesis of *Arabidopsis thaliana*. Science, 301: 653–657.

Brambilla, V., Battaglia, R., Colombo, M., Masiero, S., Bencivenga, S., Kater, M.M., and Colombo, L. (2007). Genetic and molecular interactions between BELL1 and MADS box factors support ovule development in Arabidopsis. Plant Cell, 19: 2544-2556.

Canales, C., Bhatt, A.M., Scott, R. and Dickinson, H. (2002). EXS, a putative LRR receptor kinase, regulates male germline cell number and tapetal identity and promotes seed development in Arabidopsis. Current Biology, 12: 1718–1727.

Colcombet, J., Boisson-Dernier, A., Ros-Palau, R., Vera, C. E. and Schroeder, J. I. (2005). Arabidopsis somatic embryogenesis receptor kinases 1 and 2 are essential for tapetum development and microspore maturation. Plant Cell, 17: 3350-3361.

Dietrich, R. A., Delaney, T. P., Uknes, S. J., Ward, E. R., Ryals, J. A., Dangl, J. L. (1994). Arabidopsis mutants simulating disease resistance response. Cell, 77:565-577.

Duan, Q., Kita, D., Li, C., Cheung, A.Y., Wu, H. (2010). FERONIA receptor-like kinase regulates RHO GTPase signaling of root hair development. Proc Natl Acad Sci USA, 107: 17821–17826.

Germain, H., Gray-Mitsumune, M., LaXeur, E., Matton, D.P. (2008). ScORK17, a transmembrane receptor-like kinase predominantly expressed in ovules is involved in seed development. Planta, 228: 851–862.

Heslop-Harrison, J. (1987). Pollen germination and pollen tube growth. International Review of Cytology 107: 1-78.

Higashiyama, T., Yabe, S., Sasaki, N., Nishimura, Y., Miyagishima, S., Kuroiwa, H., Kuroiwa, T. (2001). Pollen tube attraction by the synergid cell. Science, 293: 1480-1483

Honys, D., Twell, D. (2003). Comparative analysis of the Arabidopsis pollen transcriptome. Plant Physiol **132:** 640-652.

Hord, C.L.H., Chen, C., DeYoung, B.J., Clark, S.E., Ma, H. (2006). The BAM1/BAM2 receptor-like kinases are important regulators of Arabidopsis early anther development. Plant Cell, 18: 1667–1680.

Miyazaki, S., Murata, T., Sakurai-Ozato, N., Kubo, M., Demura, T., Fukudo, H. (2009). ANXUR1 and 2, sister genes to FERONIA/SIRENE, are male factors for co-ordinated fertilization. Current Biology, 19: 1327-1331.

Mittler, R., Shulaev, V., Lam, E. (1995). Coordinated activation of programmed cell death and defense mechanisms in transgenic tobacco plants expressing a bacterial proton pump. Plant Cell, 7: 29-42.

Mori, T., Kuroiwa, H., Higashiyama, T., and Kuroiwa, T. (2006). Generative Cell Specific 1 is essential for angiosperm fertilization. Nature Cell Biology, 8: 64-71.

Muschietti, J., Eyal, Y., McCormick, S. (1998). Pollen tube localization implies a role in pollen-pistil interactions for the tomato receptor-like protein kinases LePRK1 and LePRK2. Plant Cell, 10: 319-330.

Palanivelu, R., Preuss, D. (2006). Distinct short-range ovule signals attract or repel *Arabidopsis thaliana* pollen tubes in vitro. BMC Plant Biology, 6: 7.

Ruzin, S.E. (1999). Plant microtechnique and microscopy. Cambridge, Oxford University Press.

Sessions, A., Burke, E., Presting, G., Aux, G., McElver, J., Patton, D., Dietrich, B., Ho, P., Bacwaden, J., Ko, C., Clarke, J. D., Cotton, D., Bullis, D., Snell, J., Miguel, T., Hutchison, D., Kimmerly, B., Mitzel, T., Katagiri, F., Glazebrook, J., Law, M., Goff, S.A. (2002). A high-throughput Arabidopsis reverse genetics system. Plant Cell, 14: 2985- 94.

Shimizu, K.K., Ito, T., Ishiguro, S. and Okada, K. (2008). *MAA3* (*MAGATAMA3*) helicase gene is required for female gametophyte development and pollen tube guidance in *Arabidopsis thaliana*. Plant and Cell Physiology, 49: 1478-1483.

Vinagre, F., Vargas, C., Schwarcz. K., Cavalcante J., Nogueira E.M., Baldani J.I., Ferreira, P.C.G., Hemerly, A.S. (2006). SHR5: a novel plant receptor kinase involved in plant–N2-fixing endophytic bacteria association. Journal of Experimental Botany, 57: 559–569.

Zhao, D.Z., Wang, G.F., Speal, B., Ma, H. (2002). The EXCESS MICROSPOROCYTES1 gene encodes a putative leucine-rich repeat receptor protein kinase that controls somatic and reproductive cell fates in the Arabidopsis anther. Genes Development, 16: 2021–2031.

Figure 3.1 Gene expression levels in wild-type and T-DNA insertion lines of LRR-RLK B and LRR-RLK D. (A and B) Tissue-specific expressions of Arabidopsis *RLK B* and *RLK D*, respectively revealed by semi-quantitative RT-PCR. *ACTIN3*, Actin gene-specific primer set was used for PCR as the control. (C and D) Genomic structures of *RLK B* and *RLK D*. Exons are represented by boxes and introns by lines. (C) Diagram showing a T-DNA insertion site in the first intron of *RLK B* (SALK_111226). (D) Diagram showing two T-DNA insertion sites in the first exon (SALK_039722) and in the eight intron (SAIL_1160_G06.V) of *RLK D*. (E) RT-PCR analysis of Arabidopsis *RLK B* transcript levels in wild-type and *rlk b* using RLK B gene-specific primer set. (F) RT-PCR analysis of 4 mutant backgrounds. *rlk c*, *rlk b* and *rlk d-1/2* plants did not have detectable levels of *RLK C*, *RLK B* and *RLK D* mRNA, respectively. None of these null mutations affected trancript levels of other members of LRR-RLK. *ACTIN3*, Actin gene-specific primer set was used for PCR as the control.

Figure 3.1

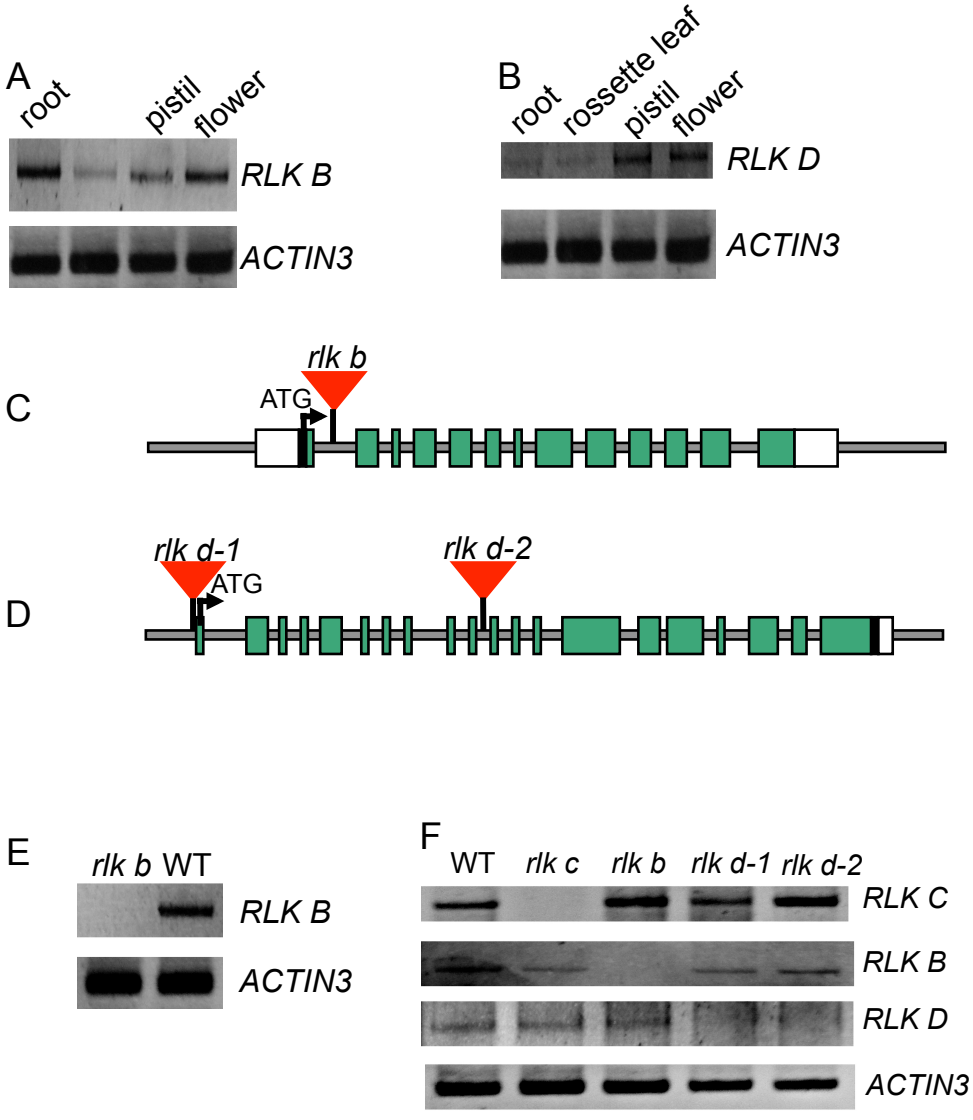
A
root
pistil
flower
RLK B
ACTIN3
B
root
rossette leaf
pistil
flower
RLK D
ACTIN3
C
rlk b
ATG
D
rlk d-1
ATG
rlk d-2
E
rlk b WT
RLK B
ACTIN3
F
WT
rlk c
rlk b
rlk d-1
rlk d-2
RLK C
RLK B
RLK D
ACTIN3

Figure 3.2 Characterization of the *rlk b* and *rlk d1/2* mutants. (A-D) Seed set analysis of wild-type (A), *rlk b* (B), *rlk d-1* (C) and *rlk d-2* (D). (E) Quantitative analysis of seed production in wild-type, *rlk b, rlk d-1* and *rlk d*-2. (F) Quantitative analysis of *in vivo* pollen tube guidance in wild-type, *rlk b, rlk d-1* and *rlk d*-2. (G-H) Analysis of *in vivo* pollen tube growth and guidance in wild-type (G) and *rlk b* (H) by aniline blue staining. (I-L) Analysis of *in vivo* pollen tube guidance by GUS staining. Pollen from LAT52p-GUS (I and K) and *rlk d-2* (J and L) plants was pollinated onto wild-type pistils. (K) An enlarged view of I. (L) An enlarged view of J. (M) Quantitative analysis of double fertilization in wild-type, *rlk b, rlk d-1* and *rlk d*-2.

Figure 3.2

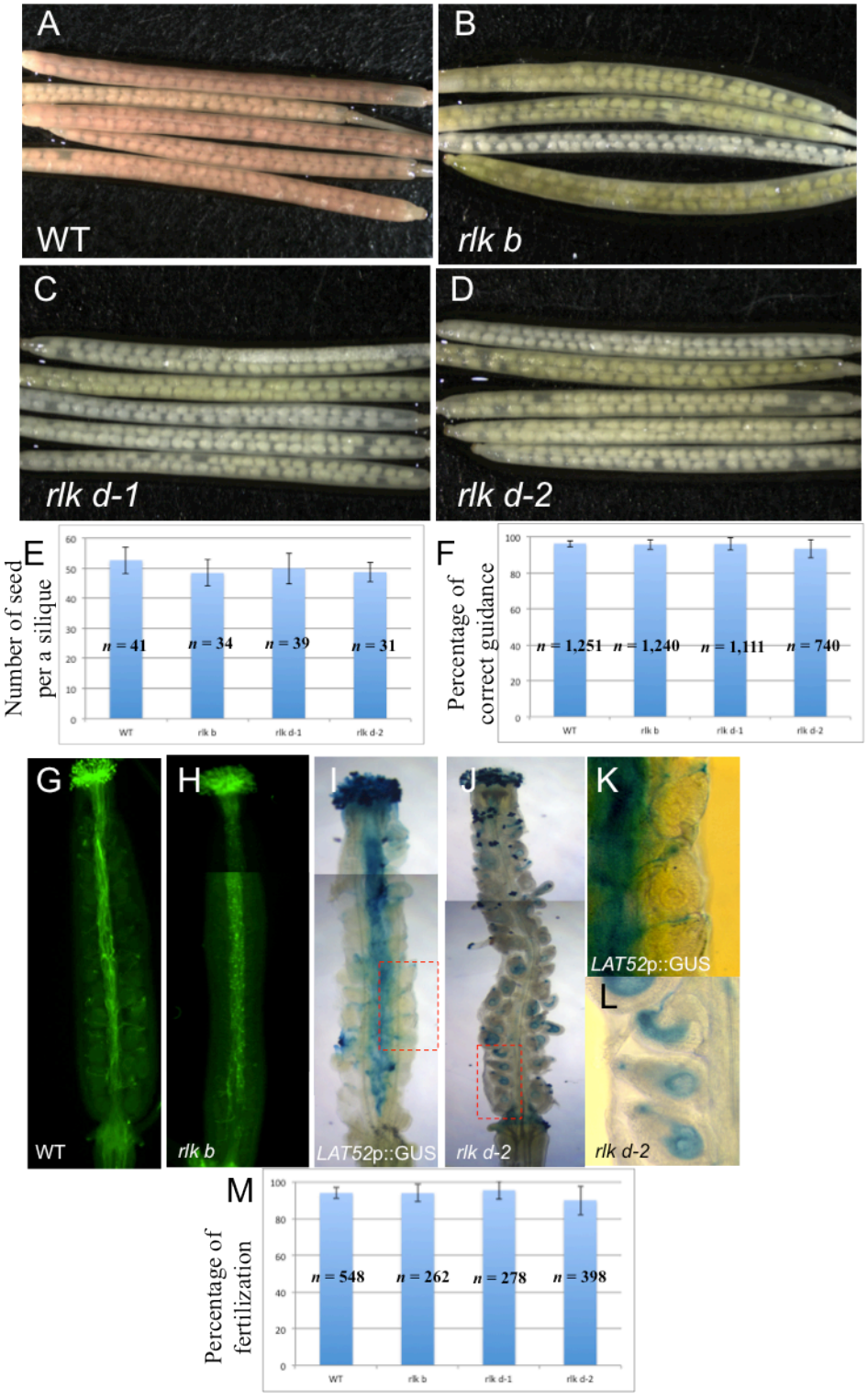
A
WT
B
rlk b
C
rlk d-1
D
rlk d-2
E
Number of seed per a silique
n = 41
n = 34
n = 39
n = 31
WT
rlk b
rlk d-1
rlk d-2
F
Percentage of correct guidance
n = 1,251
n = 1,240
n = 1,111
n = 740
G
WT
H
rlk b
I
LAT52p::GUS
J
rlk d-2
K
LAT52p::GUS
L
rlk d-2
M
Percentage of fertilization
n = 548
n = 262
n = 278
n = 398

Figure 3.3 Analysis of fertilization and pollination in *RLK* double mutants. Mature siliques of wild-type (A), *rlk c rlk b* (B), *rlk c rlk d-2* (C) and *rlk b rlk d-2* (D) were dissected to examine the number of seed per a silique. Arrows indicate gaps found in siliques of *rlk c rlk b and rlk c rlk d-2* plants. (E) Quantitative analysis of seed production in wild-type and *RLK* double mutants. (F-I) Pollen tube guidance analysis in wild-type (F), *rlk c rlk d-2* (G) and *rlk c rlk b* (H). (I) An enlarged view of H (red box). Red stars indicate untargeted and unfertilized ovules. (J) Quantitative analysis of *in vivo* pollen tube guidance in wild-type and double mutants after aniline blue staining. The number of ovules receiving pollen tube was counted and shown in a percentage (± S.D.). (K) RT-PCR analysis of Arabidopsis *RLK* transcript levels in wild-type and double mutants using RLK gene-specific primer set. *ACTIN3*, Actin gene-specific primer set was used for PCR as the control.

Figure 3.3

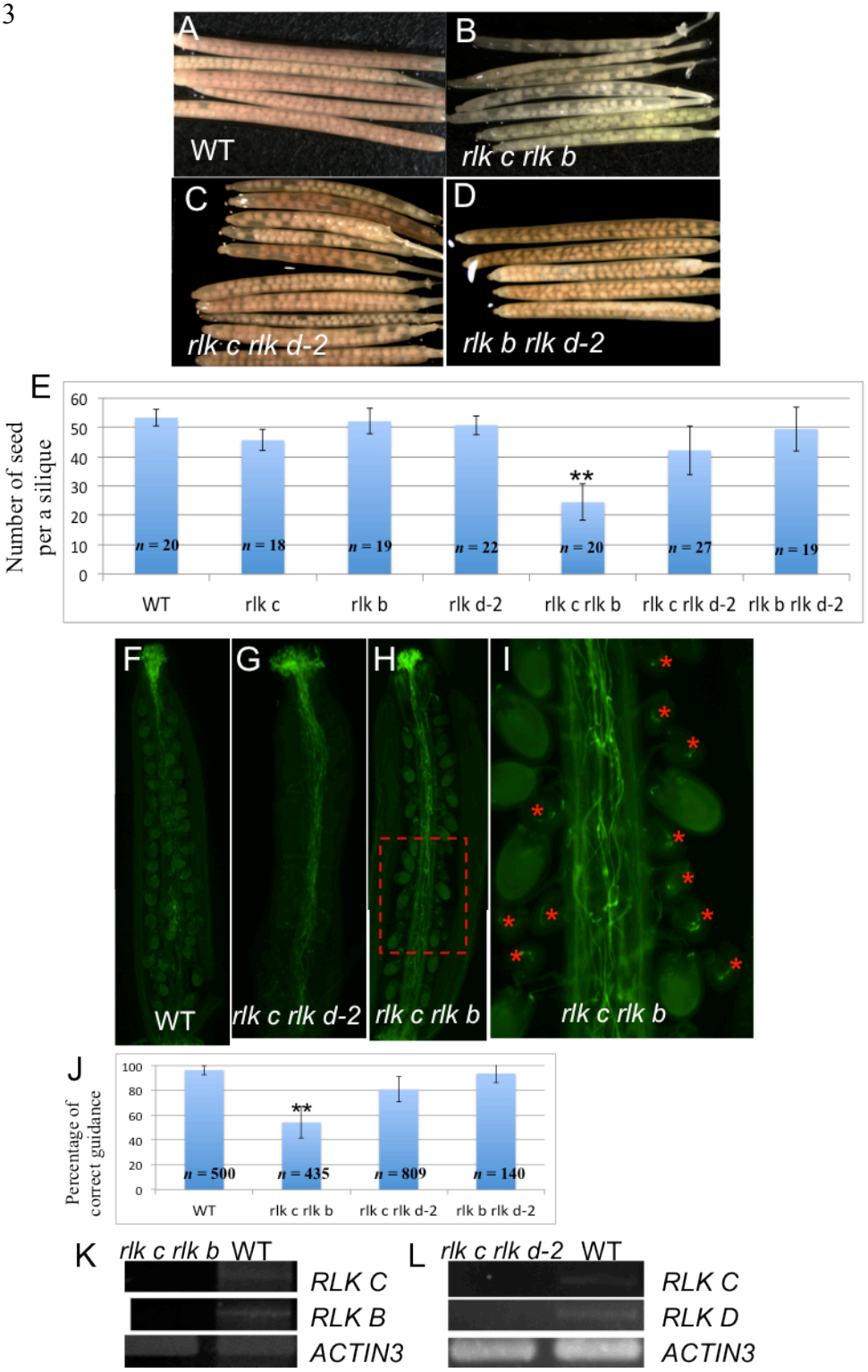
A
WT
B
rlk c rlk b
C
rlk c rlk d-2
D
rlk b rlk d-2
E
Number of seed per a silique
60
50
40
30
20
10
0
n = 20
n = 18
n = 19
n = 22
**
n = 20
n = 27
n = 19
WT
rlk c
rlk b
rlk d-2
rlk c rlk b
rlk c rlk d-2
rlk b rlk d-2
F
WT
G
rlk c rlk d-2
H
rlk c rlk b
I
rlk c rlk b
J
Percentage of correct guidance
100
80
60
40
20
0
**
n = 500
n = 435
n = 809
n = 140
WT
rlk c rlk b
rlk c rlk d-2
rlk b rlk d-2
K
rlk c rlk b
WT
RLK C
RLK B
ACTIN3
L
rlk c rlk d-2
WT
RLK C
RLK D
ACTIN3

Figure 3.4 Reciprocal cross analysis between wild-type and *rlk c rlk b*. (A-D) *In vivo* pollen tube growth and guidance was visualized by aniline blue staining in each cross. (A and C) *rlk c rlk b* pollen grains were pollinated on wild-type pistil. (C) An enlarged view of A (red box). (B and D) Wild-type pollen grains were pollinated on *rlk c rlk b* pistil. (D) An enlarged view of B (red box). Stars indicate untargeted ovules. (E-H) *In vivo* pollen tube guidance was observed in wild-type and *rlk c rlk b* by GUS staining. (E and G) *LAT52*p::GUS pollen grains were pollinated on wild-type pistil. (G) An enlarged view of E (red box). (F and H) *LAT52*p::GUS pollen grains were pollinated on *rlk c rlk b* pistil. (H) An enlarged view of F (red box). Stars indicate untargeted ovules. (I) Quantitative analysis of *in vivo* pollen tube guidance in reciprocal cross between wild-type and *rlk c rlk b* after aniline blue staining. The number of ovules receiving pollen tube, indicating correct guidance was counted and shown in the percentage (± S.D.).

Figure 3.4

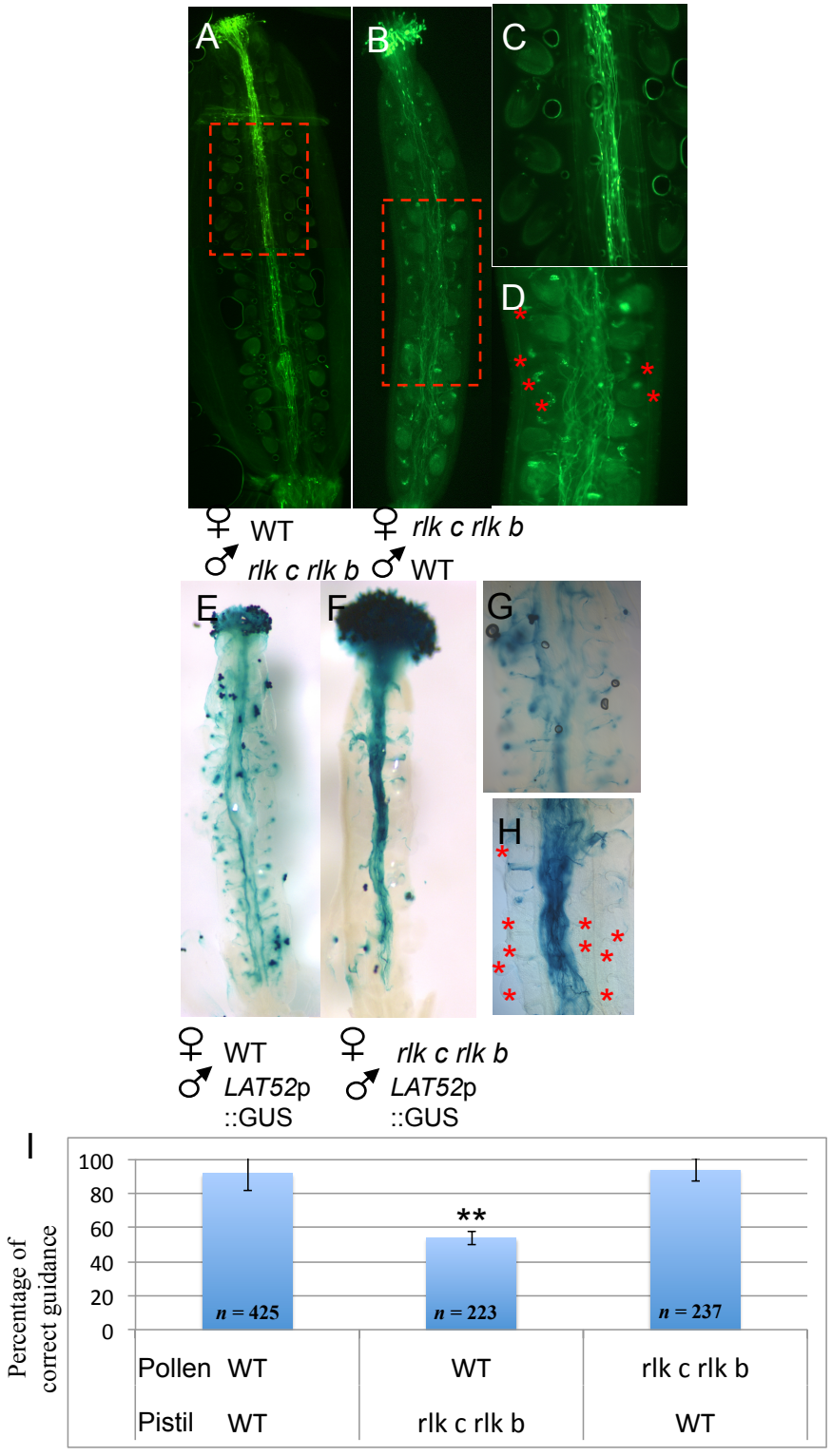
A
B
C
D
♀ WT
♂ rlk c rlk b
♀ rlk c rlk b
♂ WT
E
F
G
H
♀ WT
♂ LAT52p ::GUS
♀ rlk c rlk b
♂ LAT52p ::GUS
I
Percentage of correct guidance
100
80
60
40
20
0
**
n = 425
n = 223
n = 237
Pollen WT
Pistil WT
WT
rlk c rlk b
rlk c rlk b
WT

Figure 3.5 Semi-*in vivo* analysis of *rlk c rlk b* ovules. Wild-type pollen tubes germinated on sigma of wild-type (A) and *rlk c rlk b* (C). Arrows indicate positions of pollen tubes. (B) Pollen tubes were correctly guided to the micropyle of wild-type ovules. (D-G) Pollen tubes missed their targets to *rlk c rlk b* ovules. (H) Quantitative analysis of semi-*in vivo* pollen tube guidance between wild-type and *rlk c rlk b* ovules. The number of ovules receiving pollen tube, indicating accurate guidance was counted and shown in the percentage (± S.D.).

Figure 3.5

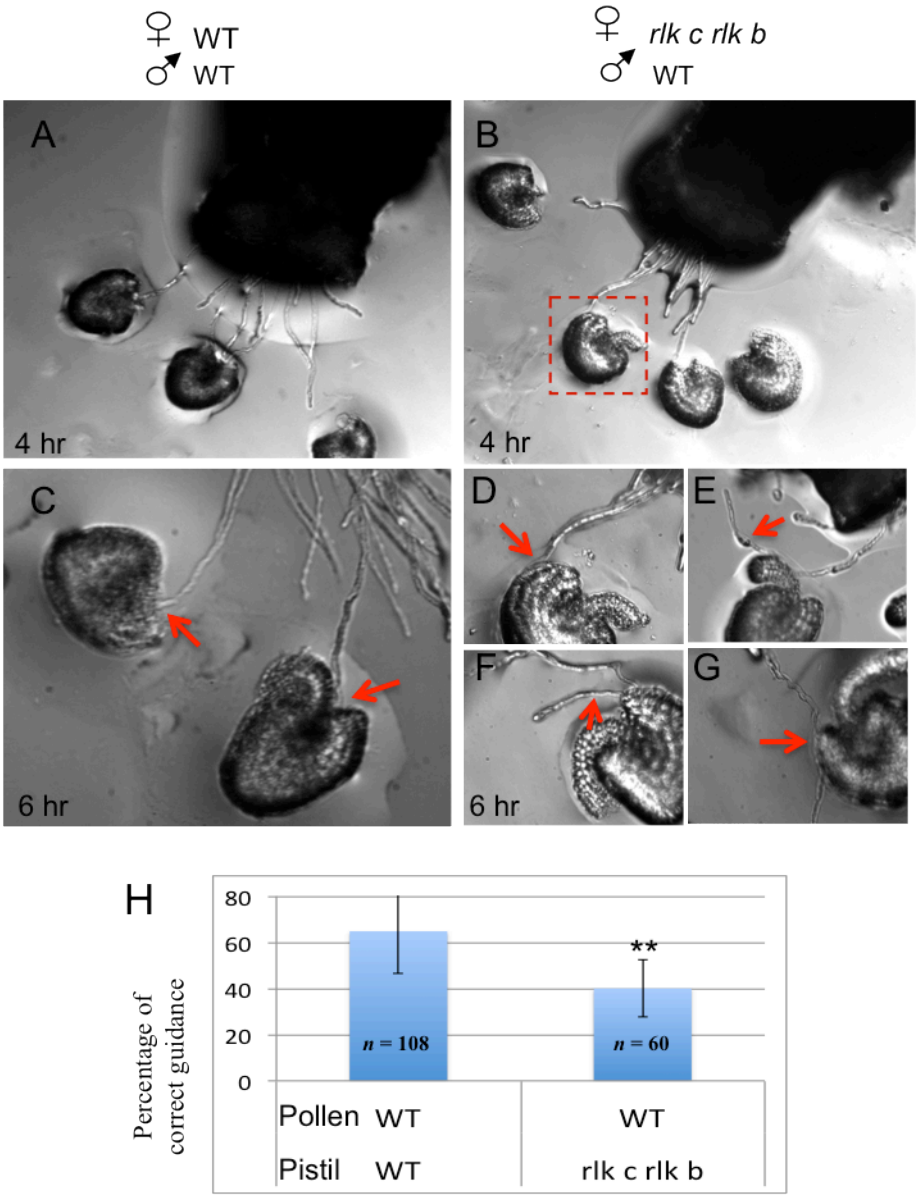
♀ WT
♂ WT
♀ rlk c rlk b
♂ WT
A
4 hr
B
4 hr
C
6 hr
D
E
F
6 hr
G
H
Percentage of correct guidance
80
60
40
20
0
n = 108
n = 60
**
Pollen WT
Pistil WT
WT
rlk c rlk b

Figure 3.6 Analysis of mature female gametophyte of the *rlk c rlk c* double mutant. (A and B) *rlk c rlk b* ovules developed normally. (C-F) Pistils were stained with aniline blue staining for callose. Stars indicate ovules showing high intensity of fluorescence (C and D) In wild-type, most ovules displayed no fluorescent signal. (E-G) Many ovules from *rlk c rlk b* pistils exhibited strong fluorescence indicating programmed cell death (PCD). Arrow in F indicates strong fluorescence in the embryo sac. (G) Bright-field image of ovule from F. (H) Quantitative analysis of early PCD found in pistils at anthesis stage (after aniline blue staining). The number of viable pollen was examined and shown in the percentage (± S.D.). (I-K) *rlk c rlk b* pistils produced normal female gametophytes (I and J) and arrested female gametophytes (K). (L-N) Aniline blue staining of young *rlk c rlk b* pistil. (L and M) Evidence of programmed cell death (PCD) of 3 megaspores at the micropylar region. (N) An enlarged view of L.

Figure 3.6

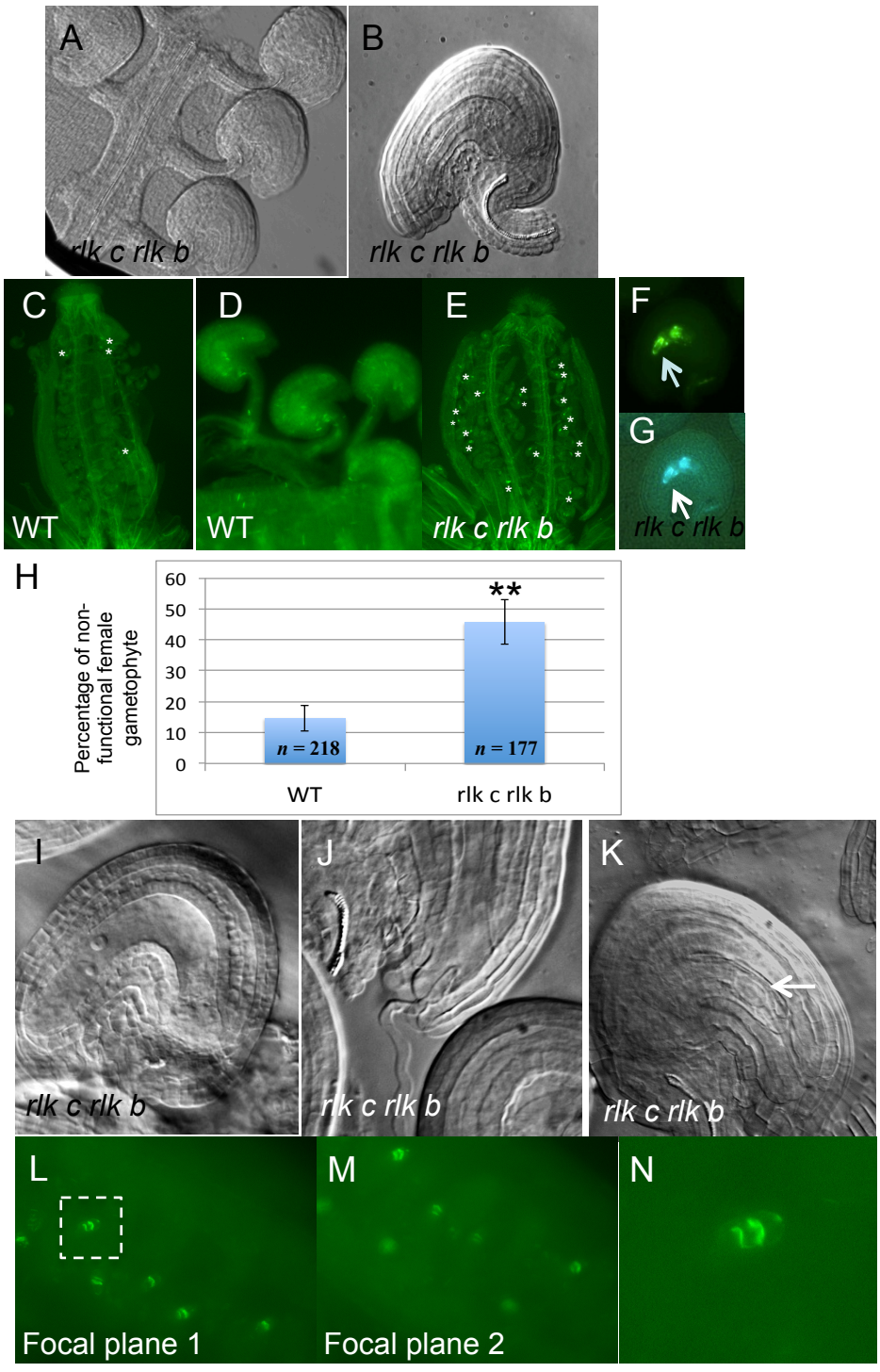
A
rlk c rlk b
B
rlk c rlk b
C
WT
D
WT
E
rlk c rlk b
F
G
rlk c rlk b
H
Percentage of non-functional female gametophyte
60
50
40
30
20
10
0
**
n = 218
n = 177
WT
rlk c rlk b
I
rlk c rlk b
J
rlk c rlk b
K
rlk c rlk b
L
Focal plane 1
M
Focal plane 2
N

Figure 3.7 Pollen viability of *rlk c rlk d-2*. Fluorescence microscopy of FDA-stained pollen derived from wild-type (A), *rlk c* (B), *rlk b* (C), *rlk d-2* (D) and *rlk c rlk d-2* (E) plants. FDA stains live pollen grains in bright-green. (E and F) Non-viable pollen grains (arrowhead) were not observed under fluorescent microscope. (G) Quantitative analysis of pollen viability in *rlk c rlk d-2* after FDA staining. The number of viable pollen was counted and shown in a percentage (± S.D.).

Figure 3.7

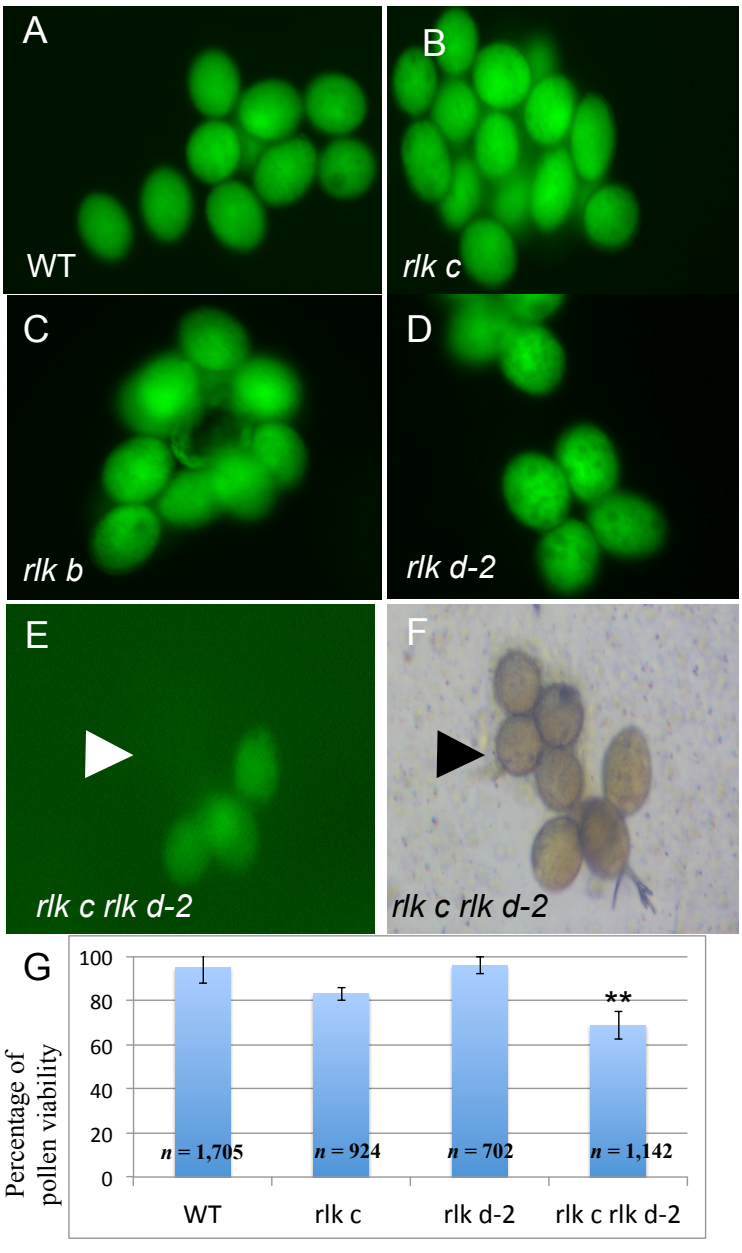
A
WT
B
rlk c
C
rlk b
D
rlk d-2
E
rlk c rlk d-2
F
rlk c rlk d-2
G
Percentage of pollen viability
100
80
60
40
20
0
n = 1,705
n = 924
n = 702
n = 1,142
**
WT
rlk c
rlk d-2
rlk c rlk d-2

Figure 3.8 Staining of vacuoles in wild-type and *rlk c rlk d-2* pollen grains. Neutral red used to stain vacuoles in mature pollen grains appears red under bright-field microscope. Neutral red-stained pollen grains derived from wild-type (A) and *rlk c rlk d-2* plants (B and C). Arrowheads indicate pollen grains showing abnormal neutral red pattern. (D) Quantitative analysis of vacuole accumulation in wild-type, *rlk c* and *rlk c rlk d-2* mature pollen grains. The number of pollen showing abnormal vacuole accumulation was counted after neutral red staining and shown in the percentage ± S.D.

Figure 3.8

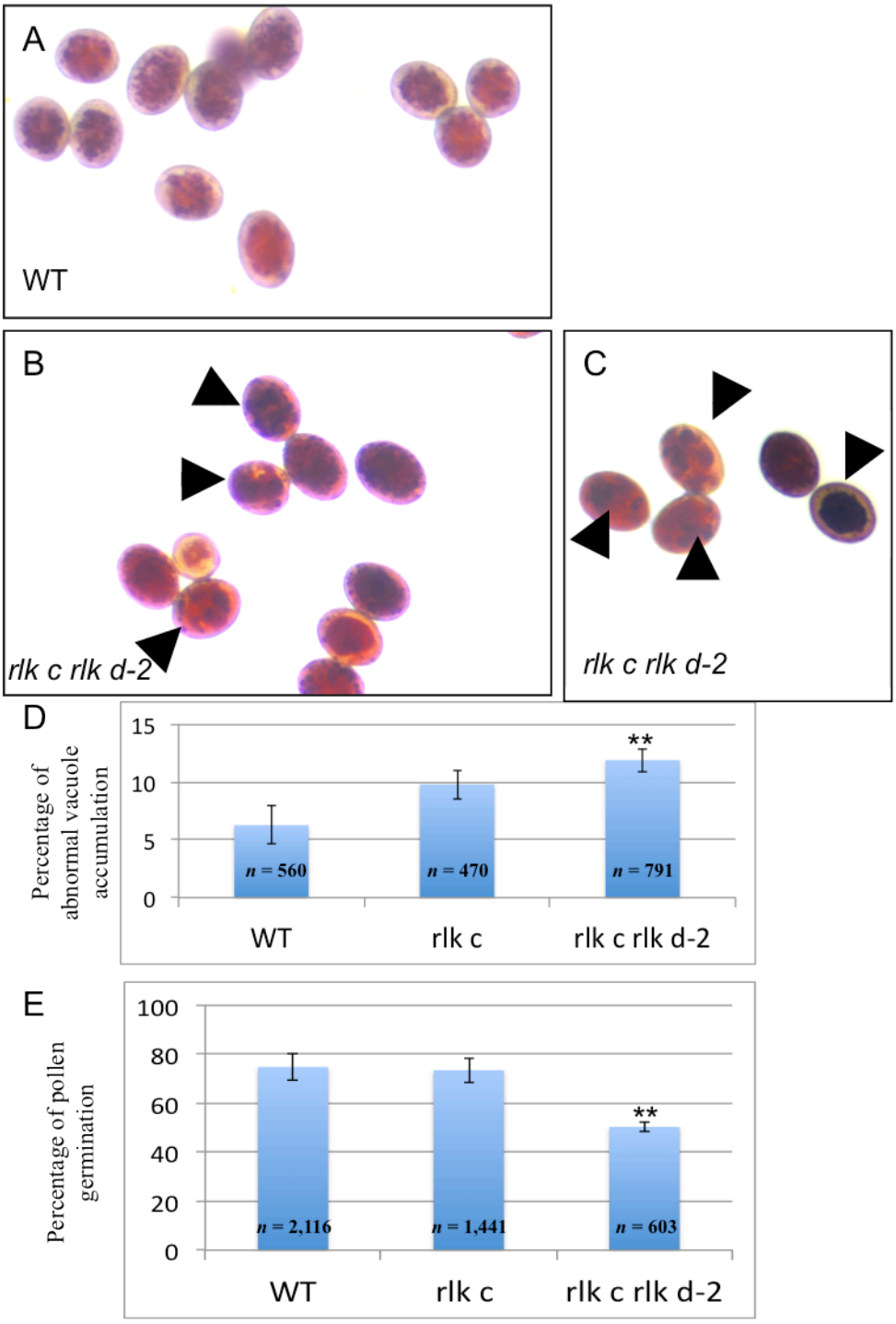
A
WT
B
rlk c rlk d-2
C
rlk c rlk d-2
D
Percentage of abnormal vacuole accumulation
15
10
5
0
n = 560
n = 470
n = 791
**
WT
rlk c
rlk c rlk d-2
E
Percentage of pollen germination
100
80
60
40
20
0
n = 2,116
n = 1,441
n = 603
**
WT
rlk c
rlk c rlk d-2

Figure 3.9 Analysis of pollen development in *rlk c rlk d-2*. Pollen development was determined in wild-type (A, C, E and G) and *rlk c rlk d-2* (B, D, F and H) anthers. (A and B) Pollen mother cells (PMCs) or meiocytes were observed in each anther locule. (C and D) Tetrads were formed after meiosis of PMCs. Microspores were enclosed in the callose wall. (E) Wild-type microspores were released into the locule. The callose was no longer observed. (F) In *rlk c rlk d-2*, microspores still contacted with each other, which is similar to *rlk d-2* pollen. (G) Wild-type mature pollen grains were developed. (H) Aborted pollen grains were detected in *rlk c rlk d-2* anther. Arrows indicate aborted pollen grains.

Figure 3.9

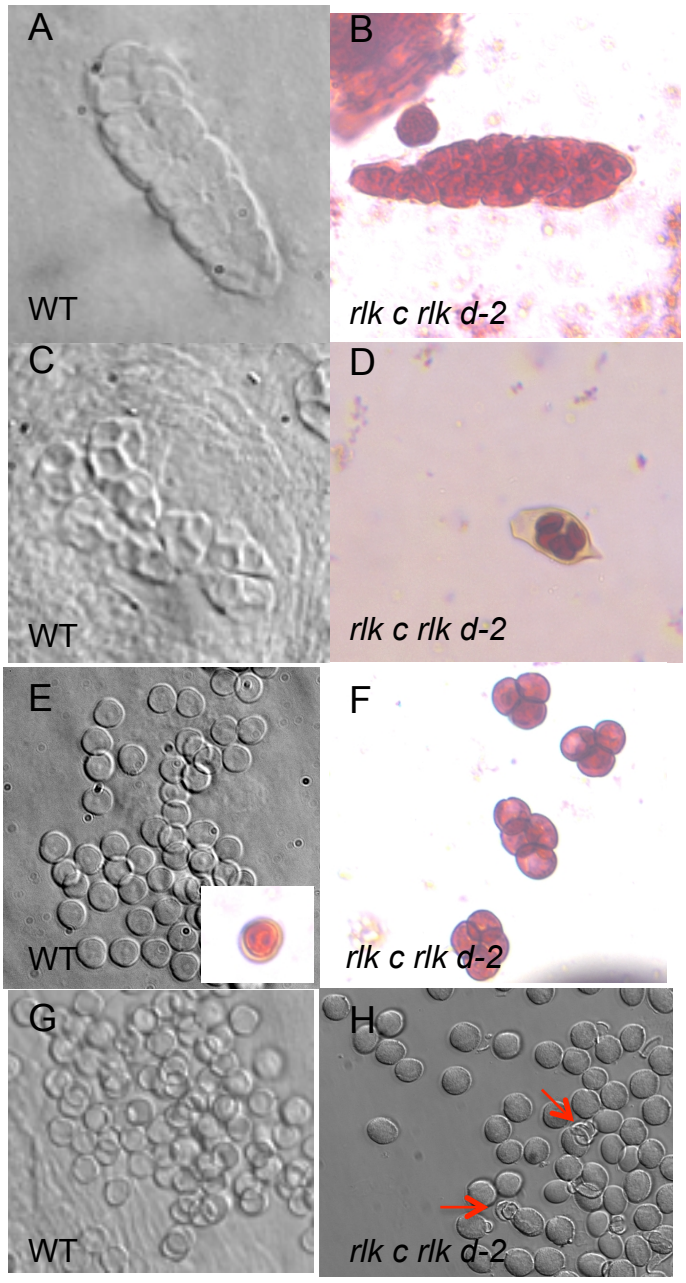
A
WT
B
rlk c rlk d-2
C
WT
D
rlk c rlk d-2
E
WT
F
rlk c rlk d-2
G
WT
H
rlk c rlk d-2

Table 3.1 Segregation analysis for the *rlk b* mutant

Parent (F0)		Segregation in F1 plants	Expected ratio	Observed ratio
Pollen donor	Pistil donor			
WT $^{(+/+)}$	*rlk b* $^{(+/-)}$	WT $^{(+/+)}$: *rlk b* $^{(+/-)}$	1 : 1	1 : 0.98 ^{ns} (n = 117)
rlk b $^{(+/-)}$	WT $^{(+/+)}$	WT $^{(+/+)}$: *rlk b* $^{(+/-)}$	1 : 1	1 : 0.96 ^{ns} (n = 109)

^{ns} Not significantly different from the expected ratio (χ^2, $P < 0.05$)

Table 3.2 Segregation analysis for the *rlk d-1* mutant

Parent (F0)		Segregation in F1 plants	Expected ratio	Observed ratio
Pollen donor	Pistil donor			
WT $^{(+/+)}$	*rlk d-1* $^{(+/-)}$	WT $^{(+/+)}$: *rlk d-1* $^{(+/-)}$	1 : 1	1 : 0.90 ^{ns} (n = 180)
rlk d-1 $^{(+/-)}$	WT $^{(+/+)}$	WT $^{(+/+)}$: *rlk d-1* $^{(+/-)}$	1 : 1	1 : 0.92 ^{ns} (n = 94)

^{ns} Not significantly different from the expected ratio (χ^2 , $p < 0.05$)

Table 3.3 Segregation analysis for the *rlk d-2* mutant

Parent (F0)		Segregation in F1 plants	Expected ratio	Observed ratio
Pollen donor	Pistil donor			
WT $^{(+/+)}$	*rlk d-2* $^{(+/-)}$	WT $^{(+/+)}$: *rlk d-2* $^{(+/-)}$	1 : 1	1 : 0.96 ^{ns} (n = 273)
rlk d-2 $^{(+/-)}$	WT $^{(+/+)}$	WT $^{(+/+)}$: *rlk d-2* $^{(+/-)}$	1 : 1	1 : 0.94 ^{ns} (n = 92)

^{ns} Not significantly different from the expected ratio (χ^2 , $P < 0.05$)

Table 3.4 Segregation of F1 progeny for the *rlk c rlk b* double mutant

Parent (F0)		Segregation in F1 plants	Expected ratio	Observed ratio
Pollen donor	Pistil donor			
rlk c $^{(+/-)}$ *rlk b* $^{(+/-)}$	WT $^{(+/+)}$	WT $^{(+/+)}$: *rlk c* $^{(+/+)}$ *rlk b* $^{(+/-)}$: *rlk c* $^{(+/-)}$ *rlk b* $^{(+/+)}$: *rlk c* $^{(+/-)}$ *rlk b* $^{(+/-)}$	1:1:1:1	1:0.54:0.15:0.08 ** (n = 76)
WT $^{(+/+)}$	*rlk c* $^{(+/-)}$, *rlk b* $^{(+/-)}$	WT $^{(+/+)}$: *rlk c* $^{(+/+)}$ *rlk b* $^{(+/-)}$: *rlk c* $^{(+/-)}$ *rlk b* $^{(+/+)}$: *rlk c* $^{(+/-)}$ *rlk b* $^{(+/-)}$	1:1:1:1	1:0.30:0.40:0.30 ** (n = 80)

^{ns} Not significantly different from the expected ratio (χ^2 , $P < 0.05$)

** Significantly different from the expected ratio (χ^2 , $P < 0.01$)

Table 3.5 Segregation of F1 progeny for the *rlk c rlk d-2* double mutant

Parent (F0)		Segregation in F1 plants	Expected ratio	Observed ratio
Pollen donor	Pistil donor			
rlk c $^{(+/-)}$ *rlk d-2* $^{(+/-)}$	WT $^{(+/+)}$	WT $^{(+/+)}$: *rlk c* $^{(+/+)}$ *rlk d-2* $^{(+/-)}$: *rlk c* $^{(+/-)}$ *rlk d-2* $^{(+/+)}$: *rlk c* $^{(+/-)}$ *rlk d-2* $^{(+/-)}$	1:1:1:1	1:0.66:0.64:0.68 ** (n = 312)
WT $^{(+/+)}$	*rlk c* $^{(+/-)}$ *rlk d-2* $^{(+/-)}$	WT $^{(+/+)}$: *rlk c* $^{(+/+)}$ *rlk d-2* $^{(+/-)}$: *rlk c* $^{(+/-)}$ *rlk d-2* $^{(+/+)}$: *rlk c* $^{(+/-)}$ *rlk d-2* $^{(+/-)}$	1:1:1:1	1:0.70:0.70:0.68 * (n = 176)

* Significantly different from the expected ratio (χ^2 , $P < 0.05$)

** Significantly different from the expected ratio (χ^2 , $P < 0.01$)

CHAPTER 4

Dominant Negative Approach to Study the Functions of Leucine Rich Repeat Receptor-Like Kinases (LRR-RLKs) in Arabidopsis Sexual Reproduction.

ABSTRACT

In this chapter, dominant negative (DN) approach was used to study RLK functions in pollen aspects, such as pollen development, pollen tube growth and guidance. DN-RLK transgenic plants containing mutated RLKs from three LRR-RLK genes; RLK C, RLK B and RLK D, were generated using a pollen-specific promoter (LAT52). Phenotypic characterizations were performed including the silique analysis, the pollen tube growth and guidance analyses. Based on the study, we demonstrate that the dominant negative RLK C receptor lacking the kinase enhances defect in pollen fertility and seed production in the *rlk c* mutant. According to reciprocal crosses, the *LAT52*p::DN-RLK C pollen did not show pollen tube guidance defect. This supports that *RLK C* plays a role in the regulation of pollen fertility during the reproductive stage. However, the *LAT52*p::DN-RLK B and *LAT52*p::DN-RLK D transgenes do not cause a phenotype in their null mutants. Here, we show that the DN approach used in this study could overcome the functional redundancy of the RLK C signaling pathway.

INTRODUCTION

Dominant-Negative Approach to Study RLK Signal Transduction

Loss-of-function mutation is the primary tool to discover function of a particular gene. Due to the large family of *RLK* gene containing over 600 members, it is difficult to dissect their functions by this type of mutation. In addition, RLKs are known to form oligomers through their extracellular domains. Thus, the T-DNA insertion probably causes no apparent phenotype. For example, if one gene is knockout, another gene might compensate the function of the former gene. The possible solution for this difficulty is to generate multiple knockout plants containing more than one gene knockout, as described in Chapter 3. However, generating the multiple mutations is time-consuming, therefore the dominant negative (DN) approach has been pursued to characterize the potential gene functions. DN is a mutation whose gene product adversely affects the normal, wild-type gene product within the same cell. The benefit of the DN approach is to solve the problem of functional redundancy of genes in a large family, such as RLKs. Accordingly, the functions of genes in the whole subfamily will be revealed. Lines of evidence have shown that the DN approach has been effectively used to study gene functions in both animal and plant (Freeman, 1996; Amaya et al., 1991); Shpak et al., 2003).

In *Arabidopsis*, an LRR-RLK called ERECTA is involved in organ shape regulation. Using its own promoter, a truncated ERECTA lacking the kinase domain caused dominant negative effects, including compact inflorescences and short siliques (Shpak et al, 2003). Though the *erecta* mutant displayed no apparent phenotype indicating the functional redundancy in ERECTA signal transduction. Another effort to

elucidate RLK roles was performed under the control of the constitutive CaMV *35S* promoter to drive the expression of the DN-RLK constructs in the vegetative tissues of wild-type. The result shows that SRF6 and SRF7 play role in cellulose synthesis (unpublished data). Taken together, these suggest that the DN approach is an applicable tool to uncover RLK signaling cascade in *Arabidopsis*.

The objective of the study in this chapter is to reveal the putative functions of three unknown LRR-RLKs in sexual reproduction of *Arabidopsis* by the DN approach. To elucidate roles of pollen RLKs, the transgenic plants containing mutated RLKs will be generated. Principally, the DN version of RLK proteins, lacking their kinases, were generated. Hypothetically, the truncated RLKs act as DN receptors by forming an inactive complex with the native RLKs (Figure 4.1A) and by blocking the normal activity of the kinase of the native RLKs. Then, they were over-expressed by a pollen specific promoter of *LAT52* in *Arabidopsis* (Col-0) and their loss-of-function mutants (*rlk c*, *rlk b* and *rlk d-2*). *LAT52* is expressed in pollen grains after meiosis until mature stage. Consequently, the DN-RLKs should be expressed only in the pollen and not in other plant tissues. Later, the pollen phenotypes were characterized from homozygous transgenic plants.

MATERIALS AND METHODS

Plant Materials and Plant Growth Condition

Arabidopsis thaliana accession Columbia-0 (Col-0) plants used in this study were grown in the growth room and chamber at the University of California, Riverside. To surface clean Arabidopsis seeds, 70% ethanol and the sterilization solution (20% bleach,

0.05% tween 20 and double-distilled water) were added to the seeds for 5 minutes. Seeds were washed thoroughly 3-5 times with sterile water to remove the bleach residue and seeds were immediately planted on petri dishes containing plant growth medium: one-half strength Murashige and Skoog (MS) salts (Sigma), 0.5% sucrose, 0.8% phyto agar (Research Products International Corp.), 1xB5 (1,000x in distilled water: 10% myo-inositol, 0.1% nicotinic acid and 0.1% pyroxidine HCI) and 1xThiamin (2,000x in distilled water: 0.2% thiamin HCI) pH5.8 with 1M KOH. Seeds were kept at 4°C for 3-4 days to break dormancy. After the cold treatment, the petri dish was placed in the growth room. Seven to ten day-old seedlings were transferred to soil (Sunshine Mix#1, Sun Gro Horticulture) at 22°C under a 16 light/ 8 dark-hour photoperiod with 200 μEm-2s-1 illumination.

Construction of DN-RLKs and Generation of Transgenic Plants

To generate transgenic plants expressing DN-RLK constructs, a pair of specific primers for each *RLK* was designed to amplify DNA sequence that encodes the extracellular and the transmembrane domains but not the kinase. Polymerase chain reaction (PCR) was performed to amplify the required DNA sequences from wild-type flower cDNA as DNA template using the following primers (for RLK C, 5'-ATGGAAGCTTTGAGGATTTATCTATGG-3' and 5'-ACCTCAAGATCAAAAGAGT AGTTACATCC -3'; for RLK B, 5'-ATGAGATCGAAGTATTTTTGTTCGTTA-3' and 5'- CGAAACATCCTTCAGCATTTCA-3'; for RLK D, 5'-ATGGTTTTGACGGA AGAAGGTG-3' and 5'- ATTGTCTGTAGCCAGAGCCAACTC-3'). To clone DN-RLK segments between pDONR and LpGWB2, a Gateway Technology (Invitrogen) was

used. LpGWB2, the destination vector, with *LAT52* promoter was used to drive DN-RLK expression in the pollen. pDONR and LpGWB2 vectors contain zeocin (100 μg/ml) and hygromycin (30 μg/ml) resistant gene, respectively, which were used as selectable markers. The sequences of all fragments created by PCR were confirmed after bacteria transformation. The DN-RLK constructs were introduced into *Agrobacterium tumefaciens* strain GV3103 by electroporation. Finally, floral dipping (Clough and Bent, 1998) was performed to introduce the *LAT52*p::DN-RLK constructs into wild-type, *rlk c* (SALK_005132), *rlk b* (SALK_111226) and *rlk d-2* (CS842841) mutants. For each DN-RLK construct, 5-6 independent transgenic lines were generated. The primary transformants (T_0) were allowed to set seeds. These seeds were collected and selected on 0.5X Murashige and Skoog (1962) solid medium containing 30 μg/ml hygromycin and 100 μg/ml carbenicillin. Only T_1 seedlings with hygromycin resistant gene were able to survive on the plate. After ten days, transformed seedlings were selected based on their normal morphology, which are green seedlings with long well established roots. Then, the seedlings were transferred to soil.

RT-PCR Analysis

The expression levels of the *LAT52*p::DN-RLK in T_2 plants were determined by RT-PCR. Total RNAs isolated from open flowers (Qiagen's RNeasy Kit) were used in a reverse transcriptase (Invitrogen) reaction. The cDNAs were used as templates in RT-PCR using gene specific primers for *RLK*s (for *RLK C*, 5'-ATGGAAGCTTTGAGGAT TTATCTATGG-3' and 5'-AACAGTCAACACAAACGCCAAAG-3'; for *RLK B*, 5'-T GTTCGTTAGCTCTTGTTCTTGGTCTC-3' and 5'-AGCCAAATCTGCAACCTCTCT

CTG-3'; for *RLK D*, 5'-TTGACGGAAGAAGGTGGTGAAGTT-3' and 5'-TATAGGT CCACACAATCGAAGCAGATT-3'; for *ACTIN3,* 5'-GGAACAGTGTGACTCACACC ATC-3' and 5'-AAGCTGTTCTTTCCCTCTACGC- 3' as amplification control).

Analysis of Seed Set in Mature Siliques

Homozygous plants from T_2 and T_3 generations were used for phenotypic characterization. *LAT52*p::DN-RLK transgenic plants were examined for seed production. Mature siliques were incubated in 100% ethanol over night and the number of seeds and unfertilized ovules per a silique were counted.

Analysis of *in vivo* Pollen Tube Growth and Guidance

Aniline blue staining was performed to observe the growth of *LAT52*p::DN-RLK pollen. The anthers from wild-type floral buds (stage 12) were emasculated and plants were kept in the growth room for 24 hours. Plants used as pollen donor were taken from the growth room and kept at room temperature for an hour before pollination. Self and reciprocal-cross pollination were carried out. Fresh pollen grains from mature flowers (stage 13) were used to manually apply on the stigma of the emasculated pistil. The pollinated pistils were harvested after pollination for 18-24 hours. Pistils were fixed in the fixative solution (3:1 v/v ethanol and acetic acid) for 2 hours at room temperature. The pistils were dehydrated using the following concentrations of ethanol series: 95%, 70%, 50% and 30% (15 minutes for each change at room temperature). The pistils were softened in 8M NaOH overnight, washed with distilled water to remove the NaOH residue and stained with decolorized aniline blue (DAP) for 2 hours as previously described (Mori et al., 2006). Pollen tube growth behavior inside the female tissues was

observed under a fluorescence microscope (Nikon Microphot FXA, Nikon) and images were captured with a Spot Insight Camera (Diagnostic Instruments Inc.).

Pollen Analysis

(A) Pollen Viability Test by FDA Staining

The viability of DN-RLK pollen grains was assessed by FDA staining (Heslop-Harrison and Heslop-Harrison, 1970). Pollen grains were collected from freshly dehisced anthers and immersed in the pollen growth liquid media and incubated at 28°C for 30 minutes. A drop of 0.5 μg/mL FDA (fluoreacein diacetate) was added to the pollen growth media and observed immediately with a Nikon ECLIPSE microscope (Nikon Instruments) equipped with epifluorescence and fluorescein isothiocyanate (FITC) filter.

(B) *In Vitro* Pollen Germination Test

The *in vitro* assay was used to determine pollen tube germination and pollen tube growth. DN-RLK plants were incubated at room temperature for an hour, the anthers were brushed on the pollen growth solid medium (18% sucrose, 0.01% Boric acid, 1mM $CaCl_2$, 1mM Ca $(NO_3)_2$, 1mM $MgSo_4$ pH 7.0 and 0.5% Select agar). The plates were incubated at 28°C for 4 hours before the analyses. Pollen tube growth was observed with a Nikon ECLIPSE microscope (Nikon Instruments) and images were captured with a Hamamatsu Digital Camera (Hamamatsu Photomics).

RESULTS

*LAT52*p::DN-RLK C Plant Exhibited More Severe Seed Production than *rlk c*

To determine the expression levels of three DN-RLK mutants, DN-RLK primer sets were used. RT-PCR analysis revealed that the transcript levels in the *LAT52*p::DN-RLKs plants used in this study were higher than those of their loss-of-function mutants (Figure 4.2A and 3A), suggesting that the DN constructs were successfully transformed. Analysis of seed production was performed after self-pollination of each *LAT52*p::DN-RLK mutant. The data indicated a significant decrease of seed production only for self-pollinated *LAT52*p::DN-RLK C (37.25 ± 11.05 ; $n = 52$; $p < 0.01$; Figure 4.2D and E), as compared to *rlk c* (44.80 ± 3.62 ; $n = 50$) and wild-type (52.90 ± 4.53 ; $n = 52$). The mature siliques from *LAT52*p::DN-RLK C plants exhibited more gaps, suggesting a defect in pollination and fertilization (Figure 4.2D). However, self-pollination of *LAT52*p::DN-RLK B and *LAT52*p::DN-RLK D plants appeared normal (Figure 4.3D). The average seed number per a silique of *LAT52*p::DN-RLK B and *rlk b* plants were 48.72 ± 5.74 ($n = 29$) and 48.41 ± 4.36 ($n = 34$), respectively (Figure 4.3E). The average seed number per a silique of *LAT52*p::DN-RLK D and *rlk d-2* plants were 54.55 ± 3.87 ($n = 25$) and 54.18 ± 3.38 ($n = 17$), respectively (Figure 4.3F). No aborted seed in the siliques was observed in both *LAT52*p::DN-RLK B (Figure 4.3C) and *LAT52*p::DN-RLK D (Figure 4.3D) transgenic plants, indicating normal pollination and fertilization.

To examine pollen tube behavior, the *LAT52*p::DN-RLK C pollen grains were pollinated on wild-type pistils and aniline blue staining was performed. The result showed normal pollen tube growth toward the base of wild-type pistils in all

*LAT52*p::DN-RLKs mutants. As expected, a significant decrease of correct micropylar guidance was observed for only *LAT52*p::DN-RLK C (93.61% ± 2.75%; n = 563; p < 0.05), compared to wild-type (97.03% ± 2.71%; n = 202),. However, this number was not statistically different compared with *rlk c*. The percentage of ovules that could correctly attract the pollen tubes in *LAT52*p::DN-RLK B and *LAT52*p::DN-RLK D were 95.13% ± 4.27% (n = 800) and 95.13% ± 4.27% (n = 468). This result was not statistically different compared with wild-type in which 95.65% ± 2.69% of ovules recruited the pollen tubes (n = 600; Figure 4.3F).

_LAT52_p::DN-RLK C Transgene Enhances Male Sterility in _rlk c_

To analyze pollen phenotypes in *LAT52*p::DN-RLKs, pollen viability was assessed by fluorescein diacetate. Only *LAT52*p::DN-RLK C pollen grains displayed decreased viability more severe than that of their loss-of-function mutants. Approximately 72.45% (n = 1,693; p < 0.01) of the *LAT52*p::DN-RLK C pollen grains were viable (Figure 4.4B and C), compared with pollen grains from wild-type plants (95.06%; n = 810; Figure 4.4A) and *rlk c* plants (83.01%; n = 924), respectively. The viability of *LAT52*p::DN-RLK B (84.27%; n = 1,634) and *LAT52*p::DN–RLK D (84.64%; n = 703) pollen appeared normal, as compared to wild-type and their loss-of-function mutants.

DISCUSSION

In this chapter, we report that the dominant negative RLK C receptor lacking the kinase enhances a defect in pollen development resulting in reduced male fertility and seed production in the *rlk c* mutant. This supports that RLK C functions during the reproductive stage. However, the *LAT52*p::DN-RLK B and *LAT52*p::DN-RLK D transgenes do not cause phenotype in their null mutants. According to reciprocal crosses, the *LAT52*p::DN-RLK C pollen did not show pollen tube guidance defect. Indeed, pollen tubes of *LAT52*p::DN-RLK C grew and correctly targeted to wild-type ovules (Figure 4.2F). However, the viability of the *LAT52*p::DN-RLK C pollen appeared significantly decreased, compared to that of wild-type and the *rlk c* mutant (Figure 4.3E). We demonstrate that *RLK C* plays a role in the regulation of pollen fertility. These findings confirm that the functional redundancy in RLK C signaling pathway is essential to regulate male fertility. As mentioned, the *LAT52*p::DN-RLK C transgene enhanced the *rlk c* mutant phenotype. This suggests the overlapping and redundancy in the RLK C signaling pathway. In the ERECTA signaling, overexpression of the DN transgene driven by *ERECTA* promoter also enhanced the phenotypes in the *erecta* mutant, indicating the redundancy in ERECTA signaling pathway (Shpak et al., 2003). However, in CLV1 and rice XA21 signaling pathways, the CLV1 and XA21 act in linear and homodimeric manner. Therefore, the DN transgene driven by their native promoters did not cause more phenotypes in their null mutants. In the *rlk c* mutant expressing the *LAT52*p::DN-RLK C transgene, it is likely that the DN-RLK acts in dominant negative manner to interact with

the ligands and the signaling components for RLK C. Thus, the inactive DN-RLK C receptor interferes other signaling pathways and enhances the *rlk c* phenotype.

Our working hypothesis is that the overexpression of DN-RLK would act as a receptor to bind the putative ligands at the extracellular domain. However, in absence of the kinase, the DN receptor could not be active to phosphorylate the downstream regulators. Thus, the signal could not be able to amplify in this signaling cascade (Figure 4.1). Furthermore, it is likely that the DN receptor can homo/heterodimerize with other related members. In Chapter 3, we report that RLK C and RLK D function redundantly to regulate pollen development. Here, we show that the DN approach used in this study could overcome the functional redundancy of the RLK C signaling pathway. This study supports that the DN approach is a powerful tool to study the RLK functions in *Arabidopsis*. However, the possibility of non-specific binding of ligands to the extracellular domain of the DN-RLK could not be eliminated in this study. In addition, overexpression of the DN-RLK transgene probably interferes the activity of other genes, resulted in more severe phenotype in the mutant. Furthermore, protein studies will be useful to confirm our findings in the post-transcriptional level, including quantifying the increase amount and stability of the truncated DN-RLK proteins in the transgenic plants, compared to the endogenous RLK proteins.

REFERENCES

Amaya, E., Musci, T.J., Kirschner, M.W. (1991). Expression of a dominant negative mutant of the FGF receptor disrupts mesoderm formation in the *Xenopus* embryos. Cell, 66: 257–270.

Clough, S.J. and Bent, A.F. (1998). Floral dip: a simplified method for Agrobacterium-mediated transformation of Arabidopsis thaliana. Plant Journal, 16:735-43.

Freeman, M. (1996). Reiterative use of the EGF receptor triggers differentiation of all cell types in the Drosophila eye. Cell, 87: 651–660.

Heslop-Harrison, J. and Heslop-Harrison, Y. (1970). Evaluation of pollen viability by enzymatically induced fluorescence; intracellular hydrolysis of fluorescein diacetate. Stain Technology, 45: 115-120.

Mori, T., Kuroiwa, H., Higashiyama, T., and Kuroiwa, T. (2006). Generative Cell Specific 1 is essential for angiosperm fertilization. Nature Cell Biology, 8: 64-71.

Shpak, E.D., Lakeman, M.B. and Torii, K.U. (2003). Dominant-negative receptor uncovers redundancy in the Arabidopsis ERECTA leucine-rich repeat receptor-like kinase signaling pathway that regulates organ shape. Plant Cell, 15: 1095-1110.

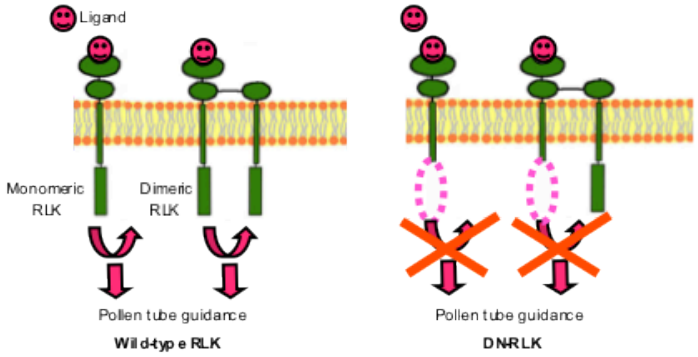

Figure 4.1 Diagram showing native wild-type RLK (left) and dominant negative (DN)-RLK lacking the kinase domains (right).

Figure 4.2 Gene expression levels and defects in seed production in dominant-negative (DN)-RLK C plants. (A) Semi-quantitative RT-PCR analysis of *LAT52*p::DN-RLK C transcripts in open flowers of wild-type and two *LAT52*p::DN-RLK C lines (C1 and C2). The top gel indicates the transcript levels of *LAT52*p::DN-RLK C in each independent line and wild-type. The middle gel indicates endogenous RLK C and *LAT52*p::DN-RLK C transcripts using primers that amplify both *LAT52*p::DN-RLK C and endogenous RLK C. *TUBULIN*, tubulin gene-specific primer set was used for PCR as the control. (B and C) Mature siliques from wild-type (B) and *LAT52*p::DN-RLK C (C) plants were examined for seed production analysis. Arrows indicate gaps observed in *LAT52*p::DN-RLK C siliques. (D) Quantitative analysis of seed production in wild-type, *rlk c* and *LAT52*p::DN-RLK C lines. Mature siliques were dissected to examine the number of seed per a silique. (E) Quantitative analysis of *in vivo* pollen tube growth and guidance in wild-type and *LAT52*p::DN-RLK C lines by reciprocal cross. After aniline blue staining, the number of ovules receiving pollen tube was counted and shown in a percentage (± S.D.).

Figure 4.2

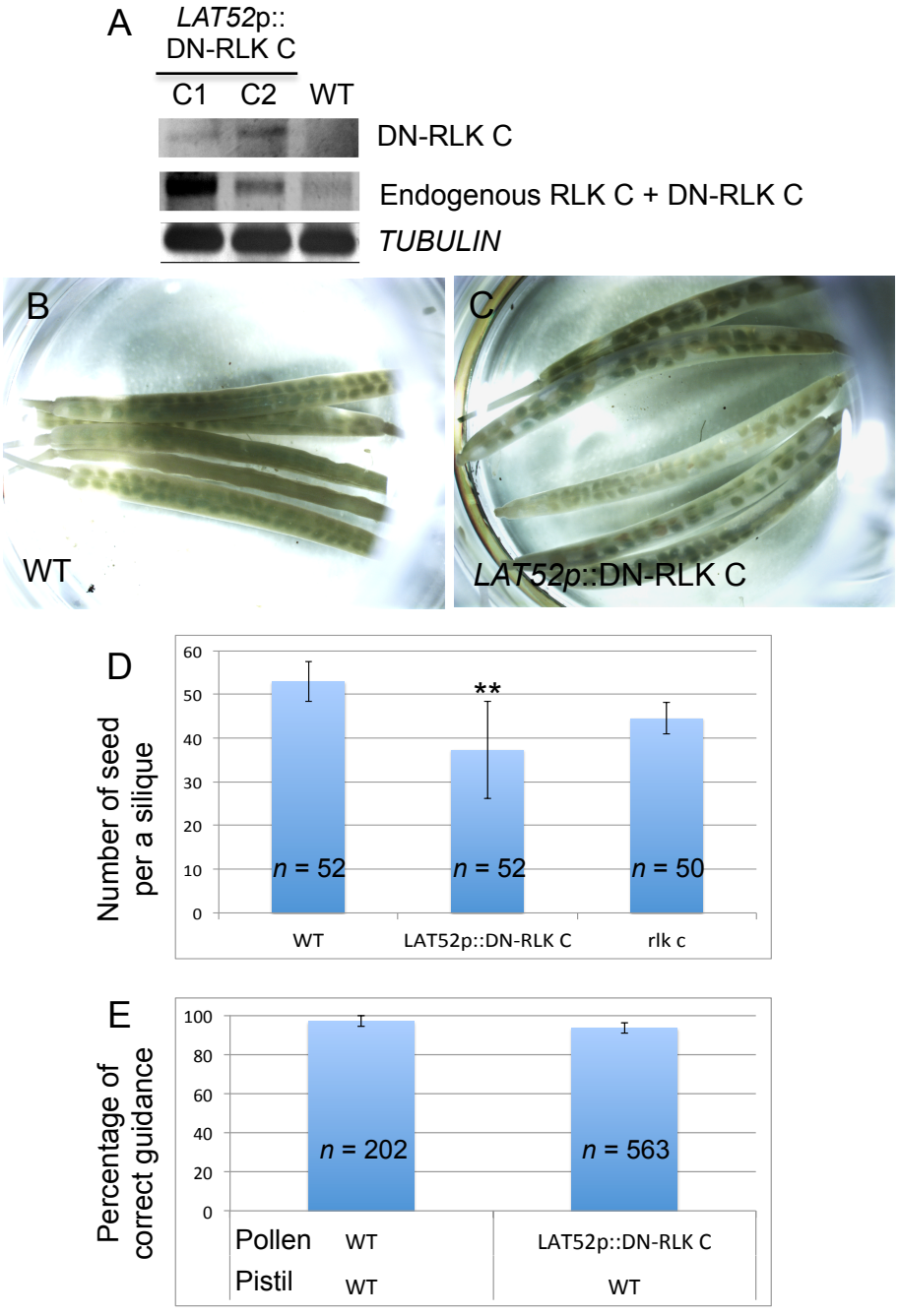
A
LAT52p::
DN-RLK C
C1
C2
WT
DN-RLK C
Endogenous RLK C + DN-RLK C
TUBULIN
B
WT
C
LAT52p::DN-RLK C
D
Number of seed per a silique
60
50
40
30
20
10
0
**
n = 52
n = 52
n = 50
WT
LAT52p::DN-RLK C
rlk c
E
Percentage of correct guidance
100
80
60
40
20
0
n = 202
n = 563
Pollen
Pistil
WT
WT
LAT52p::DN-RLK C
WT

Figure 4.3. Gene expression levels and analysis of pollination and fertilization of dominant-negative (DN)-RLK B and –RLK D plants. (A) Semi-quantitative RT-PCR analysis of *LAT52*p::DN-RLK B transcripts in open flowers of wild-type and three *LAT52*p::DN-RLK B lines (B1, B2 and B3). The top gel indicates the transcript levels of *LAT52*p::DN-RLK B in each independent line, *rlk b* and wild-type. The middle gel indicates endogenous RLK B and *LAT52*p::DN-RLK B transcripts using primers that amplify both *LAT52*p::DN-RLK B and endogenous RLK B. *ACTIN3*, actin gene-specific primer set was used for PCR as the control. (B-D) Mature siliques from wild-type (B), *LAT52*p::DN-RLK B (C) and *LAT52*p::DN-RLK D (D) plants were examined for seed production analysis. (E) Quantitative analysis of seed production in wild-type, *LAT52*p::DN-RLK B and *LAT52*p::DN-RLK D lines. Mature siliques were dissected to examine the number of seed per a silique. (F) Quantitative analysis of *in vivo* pollen tube growth and guidance in wild-type, *LAT52*p::DN-RLK B and *LAT52*p::DN-RLK D lines after aniline blue staining. The number of ovules receiving pollen tube was counted and shown in a percentage (± S.D.).

Figure 4.3

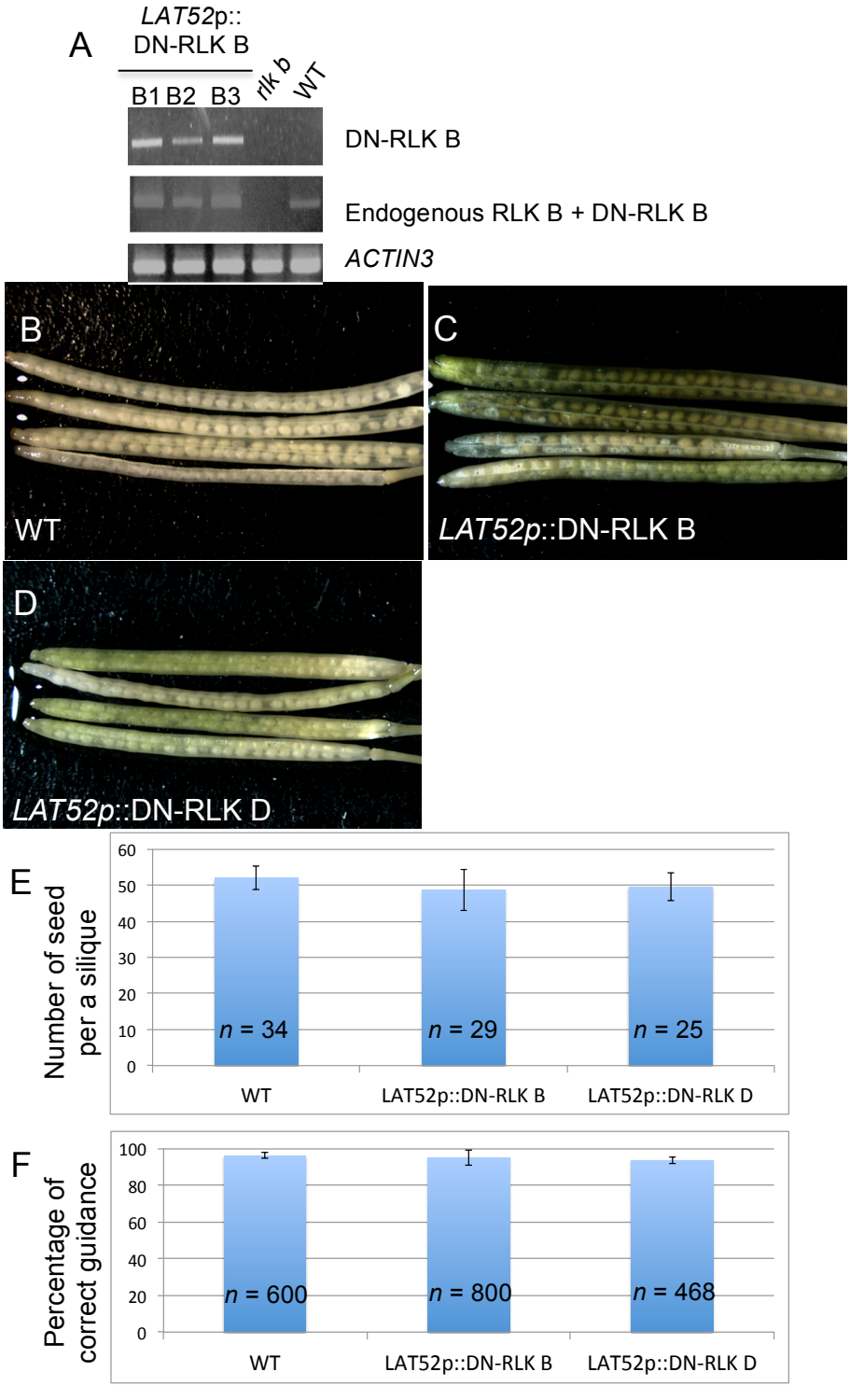
A
LAT52p::
DN-RLK B
B1 B2 B3
rlk b
WT
DN-RLK B
Endogenous RLK B + DN-RLK B
ACTIN3
B
WT
C
LAT52p::DN-RLK B
D
LAT52p::DN-RLK D
E
Number of seed per a silique
60
50
40
30
20
10
0
n = 34
n = 29
n = 25
WT
LAT52p::DN-RLK B
LAT52p::DN-RLK D
F
Percentage of correct guidance
100
80
60
40
20
0
n = 600
n = 800
n = 468
WT
LAT52p::DN-RLK B
LAT52p::DN-RLK D

Figure 4.4 Pollen viability of *LAT52*p::DN-RLK C. Fluorescence microscopy of FDA-stained pollen derived from wild-type (A) and *LAT52*p::DN-RLK C (B) plants. FDA stains live pollen grains in bright-green. (B) Non-viable pollen grains (white arrows) were not observed under fluorescent microscope. (C) Quantitative analysis of pollen viability in *LAT52*p::DN-RLK C plants after FDA staining. The number of viable pollen was counted and shown in the percentage (± S.D.).

Figure 4.4

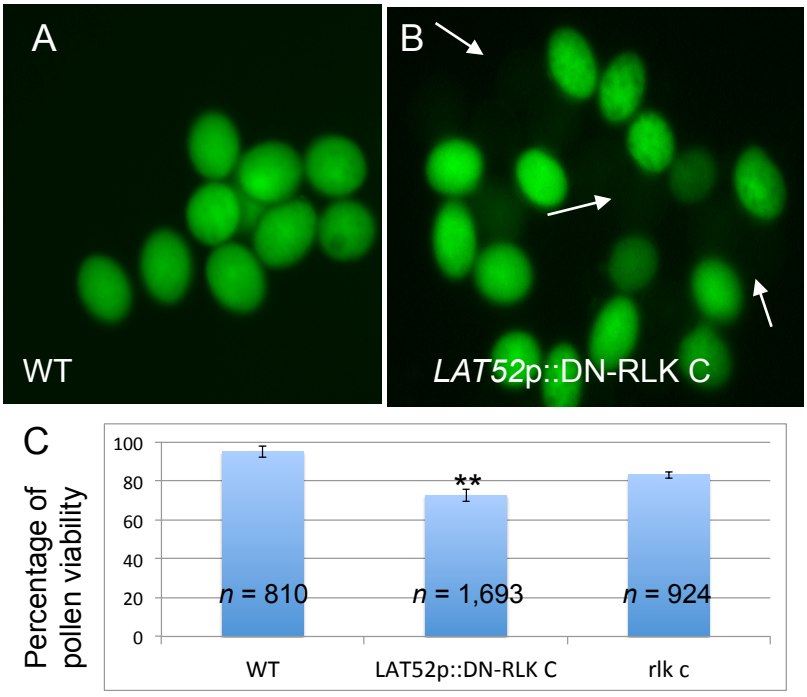
A
WT
B
LAT52p::DN-RLK C
C
Percentage of pollen viability
100
80
60
40
20
0
**
n = 810
n = 1,693
n = 924
WT
LAT52p::DN-RLK C
rlk c

CONCLUSIONS

In Arabidopsis, some of LRR-RLK genes have been characterized. However, functions of most of them are still unknown. LRR-RLKs have the LRR domain located outside the plasma membrane, suggesting their functions in signal transduction. It has been demonstrated that LRR-RLKs function in different aspects of plant growth and development, such as organ shape and inflorescence architecture. According to the phenotypic characterization of *rlk c*, *rlk c rlk d-2*, *rlk c rlk b* mutants and analysis of the *LAT52*p::DN-RLK C transgenic plants, we propose that the overlapping RLKs signaling pathways are required for full male and female fertilities.

In Chapter 2, we demonstrated that LRR-RLK C plays role in fertility of female gametophyte. Ovule development of *rlk c* appeared normal; however, the synergid and the egg cells were not specified in some embryo sacs, suggesting abberent identity. RLK C belongs to LRR III-type of the LRR-RLK subfamily. Among 47 members in LRR III, none have a known function in reproduction. The loss-of-function mutant of *RLK C* exhibited subtle defects in seed production and pollen tube guidance. Based on transmission analysis, both female and male transmission efficiencies were distorted. However, defect in the male gametophyte was not observed. Using the transgenic reporter *Arabidopsis* plants expressing the β-glucuronidase (GUS) gene under the control of *RLK C* promoter revealed that *RLK C* was predominantly active at the micropylar regios of the unfertilized embryo sac. We propose that the RLK C signaling pathway is required for female gametophytic development resulting in accurate pollen tube guidance in *Arabidopsis thaliana*. However, RLK C is expressed throughout the vegetative tissues,

such as secondary roots and leaves. Thus, it is possible that function of RLK C is not restricted to the reproductive stage.

In Chapter 3, we demonstrated that RLK C functions redundantly with others and regulates sexual reproduction. Two more LRR-RLK genes (RLK B and RLK D) were identified: RLK B and RLK D belong to LRR VI and LRR VIII type of the LRR-RLK subfamily, respectively. The results suggest that the interaction between sporophytic and gametophytic tissues is essential for gametogenesis. The loss-of-function mutants of *RLK B* and *RLK D* did not display apparent reproductive phenotypes and their transmission efficiencies appeared normal. Mutations in RLK B and RLK D could enhance phenotype in *rlk c* in different ways. Loss-of-function mutations in *RLK C* and *RLK B* loci exhibited severe aberrant pollen tube guidance and seed production. It is most likely that RLK C and RLK B function redundantly to control specification of the female gametophyte resulting in accurate pollen tube guidance. We propose that RLK C and RLK B function redundantly to elicit a signal transduction pathway involved in female gametophyte development. The function of *RLK C and RLK B* is required for the initiation of female gametogenesis. By contrast, loss-of-function mutations in *RLK C* and *RLK D* loci caused a great decrease of pollen fertility. The *rlk c rlk d-2* double mutant displayed more severe male sterility, indicated by a decrease of pollen viability and an increase of abnormal vacuole accumulation. In both cases, it is likely that the major contribution to male and female fertility comes from *RLK C* signaling due to no apparent phenotype in the *rlk b* and *rlk d.* However, mutations in *RLK B* and *RLK D* did not show a phenotype, indicating their unique roles in sexual reproduction. Taken together, we provide evidence that RLK

C, RLK B and RLK D function to achieve full fertility in pollen and female gametophyte. In wild-type scenario, RLK C interacts with other partners and might share the ligands and the signaling components with those. To regulate gamete fertility, the signaling pathway of RLK C and others are required. In the *rlk c* mutant, the activity of RLK C gene is lost. However, the *rlk c* mutant displayed subtle defect in pollen fertility and seed production. This suggests that other signaling networks, such as RLK B and RLK D, are also required for sexual reproduction.

In Chapter 4, based on our study of dominant-negative (DN) RLK C, it is likely that multiple RLKs are required for proper function in sexual plant reproduction. We show that the DN-RLK C receptor lacking the kinase domain greatly enhances defects in pollen viability and seed production in the *rlk c* mutant. This confirms that the functional redundancy in the RLK C signaling pathway is essential to regulate male fertility. In the *rlk c* mutant carrying the *LAT52*p::DN-RLK C transgene, it is likely that the DN-RLK C acts in dominant negative manner to interact with the ligands and the signaling components for RLK C. Thus, the inactive DN-RLK C receptor interferes with other signaling pathways and enhances the *rlk c* phenotype. Here, we show that the DN approach could overcome the functional redundancy of the RLK C signaling pathway and supports that the DN approach is a powerful tool to study the RLK functions in Arabidopsis.

The approaches described in this study aimed to elucidate the potential functions and mechanisms of RLK signaling pathways in sexual plant reproduction. An understanding of key events in pollination and fertilization, such as gametophyte fertility and pollen tube guidance, are required for productive agricultural manipulation and ecological management.